الجمهورية الجزائرية الديمقراطية الشعبية
People's Democratic Republic of Algeria
وزارة التعليم العالي والبحث العلمي
Ministry of Higher Education and Scientific Research

جامعة زيان عاشور بالجلفة
Ziane Achour University of Djelfa

كلية العلوم و التكنولوجيا
Faculty of Science and Technology

Department: Mechanical Engineering

Order N° : . …. / 2022

Defense authorization N° ……/2022

DOCTORAL THESIS

3rd Cycle Doctoral (D-LMD)

Presented by

Youcef Abdellah Ayoub LAOUID

With a view to obtaining the doctoral diploma in 3rd Cycle Doctoral (D-LMD)

Branch: Mechanics

Specialty: Energetics

Topic

Thermo-economic optimization of organic Rankine cycle for waste heat recovery

Supported, on 06/07/ 2022, before the jury composed of:

Last and first name	Grade	Institution of affiliation	Designation
Mr Farid MESSELMI	Professor	University of Djelfa	President
Mr Cheikh KEZRANE	MCA	University of Djelfa	Supervisor
Mr Yahia LASBET	Professor	University of Djelfa	Co-Supervisor
Mr Lakhdar AIDAOUI	Professor	University of Djelfa	Examiner
Mr Ameur HOUARI	Professor	University Centre Of Naama	Examiner
Mr Khatir NAIMA	MCA	University Centre Of Naama	Examiner

Djelfa University, FST - 2022

ملخص

يتم إنشاء قدر كبير من الحرارة المهدرة كمنتج ثانوي في العمليات الصناعية. ومع ذلك، فإن معظم الحرارة المهدرة منخفضة الدرجة يتم التخلص منها مباشرة في البيئة دون استخدامها. مع فوائد كفاءة استخدام الطاقة، والقدرة على توليد الطاقة والصداقة البيئية، تمثل دورة رانكين العضوية نهجًا فعالًا لاستعادة الطاقة من الحرارة الضائعة منخفضة الدرجة. أولاً، يتم تقديم لمحة عامة عن النمو التاريخي والحالة التكنولوجية والتطبيقية الحالية لدورة رانكين العضوية. ثانيًا، يتم التحقيق في مفهوم دورة رانكين العضوية مع اعادة تسخين البخار. وبشكل أكثر تحديدًا، تم تصميم نموذج إعادة تسخين البخار، باستخدام أنواع سوائل عمل مختلفة. تم استخدام الخوارزمية الجينية لحساب القيم المثلى لضغط التبخر، بالإضافة إلى ضغط إعادة التسخين ودرجة حرارة التحميص ودرجة حرارة نقطة الضغط من أجل تعظيم كفاءة الإكسرجي وتقليل التوصيل الحراري الكلي. تشير النتائج إلى أن السوائل الرطبة تنتج طاقة أكبر مقارنة بالسوائل الجافة و الإيزونتروبيا. في حالة السوائل الرطبة، يكون لحرارة التحميص تأثير إيجابي على كفاءة الطاقة، ومع ذلك، بالنسبة للسوائل الجافة و الإيزونتروبيا ، فإن زيادة درجة حرارة التحميص تقلل من إنتاج الطاقة. علاوة على ذلك، فإن درجة حرارة التحميص المثلى تقترب من الحد الأعلى للسوائل الرطبة. تكشف النتائج أنه يمكن تحقيق أقصى قدر من الكفاءة البالغة 49.1٪ من خلال إضافة المبادل الحراري الداخلي إلى النظام، والذي يتوافق مع تحسن بنسبة 13.6٪ مقارنةً بالدورة الاساسية. المبخر والمكثف هما المكونان اللذان يحتويان على أعلى مساهمة في الإكسرجي المدمر، على التوالي. تمثل دورة رانكين العضوية مع مبادل حراري داخلي التدمير الأقل للطاقة للمبخر والعنفة. يرجع هذا النقص في الإكسرجي المدمر بشكل أساسي إلى وجود المبادل الحراري. تظهر هذه النتائج أنه يجب تصميم المبخر والمكثف بشكل أفضل لتقليل الإكسرجي المدمر في هذه المكونات. علاوة على ذلك، تم إجراء تحسين اقتصادي حراري لأنظمة استرداد الحرارة المهدرة باستخدام تكوينات مختلفة من دورات رانكين العضوية. تشير النتائج إلى أن اختيار تكلفة إنتاج الكهرباء وصافي العمل كدوال استمثال يمكن أن يكون أكثر جاذبية لتكوينات دورة رانكين العضوية، بسبب الاستخدام الكامل للحرارة وانخفاض تكلفة إنتاج الكهرباء لجميع سوائل العمل. بمقارنة تكوينات الدورة، تظهر دورة رانيكن العضوية مع مبادل حراري داخلي ما يقرب من 0.4–5٪ و 2.53–8.78٪ أعلى من صافي العمل مقارنةً بدورة رانكين مع مسترجع والدورة الأساسية، على التوالي. ومع ذلك، فإن دورة رانكين مع مسترجع مناسبة في الغالب للسوائل الرطبة. علاوة على ذلك، يحتوي التكوين الأساسي على أدنى تكلفة إنتاج الكهرباء، يليه التكوين مع المسترجع، بينما يحتوي التكوين مع مبادل حراري داخلي على أعلى تكلفة إنتاج الكهرباء؛ تتأثر تكلفة إنتاج الكهرباء بشدة بتكوين الدورة، بغض النظر عن نوع سائل العمل. على وجه الخصوص، وجد أن سوائل العمل التي تصل إلى الأداء الأمثل هي تلك التي لديها درجة حرارة تبخر مثالية لدرجة حرارة مدخل مصدر الحرارة بين 0.68–0.75 و 0.66–0.73 و 0.64–0.73 لـ للتكوين الاساسي والتكوين مع مبادل حراري داخلي والتكوين المعدل، على التوالي.

كلمات مفتاحية:

دورة رانكين العضوية، استرداد الحرارة المهدرة، سائل العمل، تكوين الدورة، تحسين الاقتصاد الحراري.

Abstract

A significant amount of waste heat is generated as a by-product in industrial processes. However, most of the low-grade waste heat is directly dismissed into the environment without being used. With the benefits of energy efficient, power generation capabilities and environmentally-friendliness, the Organic Rankine Cycle (ORC) represents an effective approach to recover energy from low-grade waste heat. Firstly, an overview of the historical growth and current technological and application status of the ORC technology is presented. Secondly, the concept of reheat ORC is investigated. More specifically, a reheat ORC is modelled, using different working fluids types. The genetic algorithm was used to calculate the optimal values of the evaporation pressures of the reheat ORC, as well as, reheat pressure, superheat degree and pinch point temperature in order to maximize the exergy efficiency and minimise total thermal conductance. The results indicate that wet fluids produce more power output compared to dry and isentropic fluids. In the case of wet fluids, superheat has a positive impact on exergy efficiency, however, for dry and isentropic fluids the increase of superheat degree decreases the power output. Moreover, the optimal superheat degree approaches its upper bound for wet fluids. The results reveal that a maximum of 49.1% exergetic efficiency can be achieved by the addition of Internal Heat Exchanger (IHE) to the system, which corresponds to a 13.6% improvement compared to the ORC without IHE. The evaporator and condenser are the components with the highest exergy destruction contribution, respectively. The ORCs with IHE represent the lower exergy destruction of evaporator and expander. This exergy reduction is mainly due to the presence of the IHE. These results show that evaporator and condenser must be better designed to decrease the exergy destructions in these components. Furthermore, a thermo-economic optimization of waste heat recovery systems using different ORC configurations has been performed. Results indicate that, the selection of electricity production cost (EPC) and net power output as objectives can be more attractive for ORC configurations, due to the full utilization of the possible heat in the exhaust gas and to the low EPC for all working fluids. Comparing the cycle configurations, ORC with IHE exhibits approximately 0.4-5% and 2.53-8.78% higher net power output compared to regenerative ORC and basic ORC, respectively. However, regenerative ORC is mostly suitable for wet fluids. Moreover, the basic ORC configuration has the lowest EPC, followed by the regenerative configuration, while ORC-IHE has the highest EPC; the EPC is highly affected by the cycle configuration, regardless of the working fluid type. In particular, it is found that, the working fluids reaching the optimal performance are those that have an optimal evaporation temperature to inlet temperature of the heat source ratio between 0.68-0.75, 0.66-0.73 and 0.64-0.73 for basic-ORC, ORC-IHE and regenerative ORC, respectively.

Keywords:

Organic Rankine cycle, waste heat recovery, working fluid, cycle configuration, thermo-economic optimization

Résume

Une quantité importante de chaleur résiduelle est générée comme sous-produit dans les processus industriels. Cependant, la majorité de cette chaleur résiduelle de faible qualité est directement rejetée dans l'environnement sans être utilisée. Avec ses avantages en termes d'efficacité énergétique, de capacité de production d'énergie et de respect de l'environnement, le cycle organique de Rankine représente une méthode efficace pour récupérer l'énergie de la chaleur résiduelle de faible qualité. Tout d'abord, une vue d'ensemble de la croissance historique et de l'état de l'art des cycles ORC est présentée. Ensuite, le concept d'ORC avec resurchauffe est étudié. Plus précisément, un ORC avec resurchauffe est modélisé, en utilisant différents types de fluides de travail. L'algorithme génétique a été utilisé pour calculer les valeurs optimales des pressions d'évaporation, ainsi que la pression de resurchauffe, le degré de surchauffe et la température du point de pincement du cycle, afin de maximiser l'efficacité éxergétique et de minimiser la conductance thermique totale. Les résultats indiquent que les fluides humides produisent plus de puissance par rapport aux fluides secs et isentropiques. Dans le cas des fluides humides, la surchauffe a un impact positif sur l'efficacité éxergétique, cependant, pour les fluides secs et isentropiques, l'augmentation du degré de surchauffe diminue la puissance produite. De plus, le degré de surchauffe optimal se rapproche de sa limite supérieure pour les fluides humides. Les résultats révèlent qu'un rendement éxergétique maximal de 49,1 % peut être atteint par l'ajout d'un récupérateur au système, ce qui correspond à une amélioration de 13,6 % par rapport à l'ORC sans récupérateur. L'évaporateur et le condenseur sont les éléments qui contribuent le plus à la destruction d'éxergie, respectivement. Les ORC avec récupérateur représentent la plus faible destruction d'exergie de l'évaporateur et du détendeur. Cette réduction d'exergie est principalement due à la présence du récupérateur. Ces résultats montrent que l'évaporateur et le condenseur doivent être mieux conçus pour diminuer la destruction d'exergie dans ces éléments. De plus, une optimisation thermoéconomique des systèmes de récupération de chaleur résiduelle utilisant différentes configurations ORC a été réalisée. Les résultats indiquent que la sélection des objectifs de coût de production d'électricité et de puissance nette peut être plus intéressante pour les configurations ORC, en raison de l'utilisation complète de la chaleur possible dans les gaz d'échappement et du faible coût de production d'électricité pour tous les fluides de travail. En comparant les configurations de cycle, l'ORC avec récupérateur présente une puissance nette supérieure d'environ 0,4-5 % et 2,53-8,78 % par rapport à l'ORC régénératif et l'ORC de base, respectivement. Cependant, l'ORC régénératif est surtout adapté aux fluides humides. Par ailleurs, la configuration ORC de base présente le coût de production d'électricité le plus faible, suivie par la configuration régénérative, tandis que l'ORC avec récupérateur présente le coût de production d'électricité le plus élevé ; le coût de production d'électricité est fortement affecté par la configuration du cycle, indépendamment du type de fluide de travail. En particulier, il est constaté que les fluides de travail atteignant la performance optimale sont ceux qui ont un rapport optimal entre la température d'évaporation et la température d'entrée de la source de chaleur entre 0,68 -0,75, 0,66-0,73 et 0,64-0,73 pour l'ORC de base, l'ORC avec récupérateur et l'ORC régénératif, respectivement.

Mots clés :

Cycles organiques de Rankine (ORC), valorisation de rejets thermiques, fluide de travail, configuration du cycle, optimisation thermoéconomique.

ACKNOWLEDGEMENTS

First and foremost, praises and thanks to ALLAH almighty who has been giving me everything to accomplish this study.

I am very grateful to Dr Cheikh KEZRANE for his support during the whole period of this work. I would like to thank him for the guiding and all valuable discussions we had. Special thank goes to Pr Yahia LASBET for his support and guidance during this work.

I would like to present my warm thanks to Pr Farid MESSELMI for having accepted to chair the jury, to Pr Lakhdar AIDAOUI, Pr Ameur HOUARI and Dr Khatir NAIMA for having taken the time to read this work and for their comments.

My special thanks and appreciation goes to members of the laboratory of development in mechanics and materials.

Furthermore, I would like to thank my parents, my family and friends for their encouragement, support, love and care.

Dedicate to

My parents

My family

All who knows me.

Journal Publications

Kezrane, C., Laouid, Y. A., Lasbet, Y., & Habib, S. H. (2018). Comparison of different Organic Rankine Cycle for power generation using waste heat. European Journal of Electrical Engineering–n, 151, 169.

Laouid, Y. A. A., Kezrane, C., Lasbet, Y., & Pesyridis, A. (2021). Towards improvement of waste heat recovery systems: A multi-objective optimization of different Organic Rankine cycle configurations. *International Journal of Thermofluids*, *11*, 100100.

Laouid, Y. A. A., Kezrane, C., Lasbet, Y., & Pesyridis, A. (2021). Performance analysis and optimisation of a reheat organic Rankine cycle. *International Journal of Sustainable Energy*, 1-23.

Conferences Presentations

Laouid, Y. A. A., Kezrane, C., & Lasbet, Y. (2018). The Performance of Reheat Organic Rankine Cycle using Wet Fluids. Naâma, 17-18 Décembre 2018, Congrès National sur les Energies et Matériaux (CNEM 2018).

Laouid, Y. A. A., Kezrane, C., & Lasbet, Y. (2019). Effects of the population size on the performance of genetic algorithms in case of organic Rankine cycle modelling. Djelfa, Algeria, 10 April 2019, Journée Académique sur les Mathématiques Appliquées (JAMA'19).

Laouid, Y. A. A., Kezrane, C., & Lasbet, Y. (2019). Waste Heat Recovery Using Organic Rankine Cycles with Low Fluid Environmental Impacts. Istanbul, 17-18 June 2019 4th Eurasian Conference on Civil and Environmental Engineering.

Laouid, Y. A. A., Kezrane, C., & Lasbet, Y. (2019). Exergy analysis and multi-objective optimization of regenerative Organic Rankine Cycle for waste heat recovery. Djelfa, 29-30 June 2019 The First International Conference on Materials, Environment, Mechanical and Industrial Systems ICMEMIS'19.

Laouid, Y. A. A., Kezrane, C., & Lasbet, Y & L. NORD. (2019). Wet working fluids for regenerative ORC with varying heat source temperature. Västerås, Sweden, Aug 12-15, 2019, International Conference on Applied Energy 2019 (ICAE 19).

Laouid, Y. A. A., Kezrane, C., & Lasbet, Y. (2020). Thermodynamic performance and multi-objective optimization of regenerative organic Rankine cycle for low temperature waste heat recovery. El Oued, January 20-21, 2020, International Symposium on Materials, Energy and Environment (MEE 20).

Laouid, Y. A. A., Kezrane, C., & Lasbet, Y. (2020). Thermo-economic optimization of Organic Rankine Cycle using low-grade heat source. Naâma February 11-12, 2020, National conference On Applied Energetics (NCAE 20).

Table of contents

Nomenclature

Variables

A	Heat transfer area, (m^2)
B, C, K, F	Factors of the investment model, (-)
C_{BM}	Bare module cost, ($)
C_h	Heat capacity rate, ($kJ.s^{-1}.K^{-1}$)
C_{OM}	Maintenance and operation costs, ($)
c_p	Specific heat capacity, ($kJ.kg^{-1}.K^{-1}$)
C_p	Purchased cost, ($)
C_{tot}	Total investment, ($)
EPC	Electricity production cost, ($\$.kW^{-1}.h^{-1}$)
$\dot{E}x$	Exergy flow, (kW)
F_{BM}	Bare module factor, (-)
F_M	Material factor, (-)
F_p	Pressure factor, (-)
h	Specific enthalpy, ($kJ.kg^{-1}$)
H	Pump head, (m)
$h_{full-load}$	Full load operation hours, (h)
i	Interest rate, (%)
$\dot{m}$	Mass flow rate, ($Kg.s^{-1}$)
M	Molar mass, ($Kg.mol^{-1}$)
P	Pressure, (bar)
$\dot{Q}$	Heat, (kW)
ΔT	Temperature difference, (K)
T	Temperature, (K)
U	Overall heat transfer coefficient, ($kW.m^{-2}.K^{-1}$)
UA	Thermal conductance, ($kW.\ K^{-1}$)

W	Power, (kW)

Greek symbols

Δ	Difference
η	Efficiency, (%)
ε	Effectiveness, (%)

Subscripts

1-8	State points in the cycle
con	Condenser
CP	Circulating pump
cr	Critical
cw	Cold water
eco	Economizer
eva	Evaporator (two phase evaporator)
Evap	Evaporator
ex	Exergy
FH	Feed heater
g	Gas
gen	Generator
H	Hot
hot	Inlet heat source temperature
in	Inlet
L	Low
m	Mean
net	Net
Out	Outlet
PP	Pinch point
P	Pump
Reh	Reheater
sat	Saturation

Sup	Superheater
T	Turbine
th	Thermal
tot	Total
Wf	Working fluid
int	Intermediate

Acronyms

CFC	Chlorofluorocarbon
HC	Hydrocarbons
HCFC	Hydrochlorofluorocarbons
HFC	Hydrofluorocarbons
HFE	Hydrofluoroethers
GA	Genetic algorithm
IEO	International Energy Outlook
GHG	Greenhouse gas
GWP	Global warming potential
HP	High pressure
LP	Low pressure
HTE	High Temperature Evaporator
LTE	Low Temperature Evaporator
IHE	Internal heat Exchanger
LMTD	Logarithmic mean temperature difference
NSGA-II	Non-dominated sorting genetic algorithm-II
OTEC	Ocean Thermal Energy Conversion
ODP	Ozone depletion potential
ORC	Organic Rankine cycle
PFC	Perfluorocarbons
PPTD	Pinch point temperature difference
TOPSIS	Technique for order preference by similarity to an ideal solution

List of figures

List of figures

List of tables

1. Introduction

1.1. Background

The United States energy information administration said in its latest International Energy Outlook 2021 (IEO2021) that, global energy demand and energy-related carbon emissions will continue to rise through 2050, with oil remaining the largest energy source just ahead of surging renewables [1]. IEO2021 forecast that world energy consumption will grow by 47% in the next 30 years, driven by population and economic growth, particularly in developing Asian countries. This growth in demand leads to various environmental and economic challenges, as fossil fuel usage has numerous major impacts such as acid precipitation, ozone layer damage, resource depletion, and global warming [2].

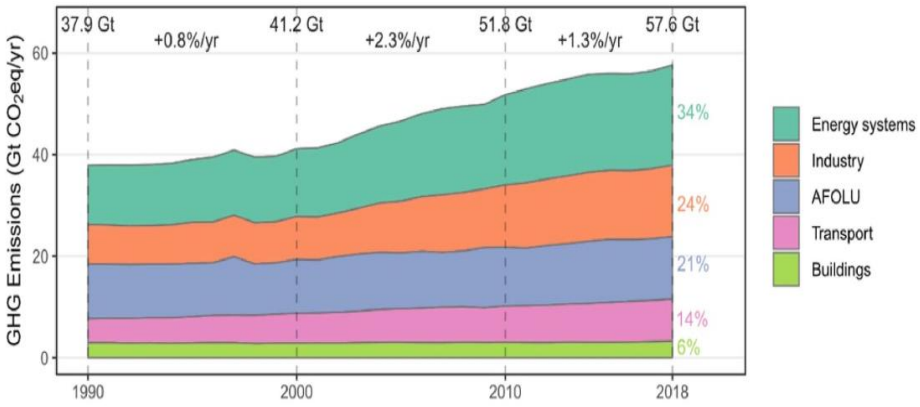

Figure 1.1 *Total global anthropogenic GHG emissions [3].*

As shown in **figure 1.1**, global greenhouse gas emissions continued to rise between 1990 and 2018, although the rate of emissions growth has slowed since 2010. Greenhouse Gas (GHG) emissions reached the peak in human history in 2018, reaching 58 GtCO2eq. The highest share of emissions in 2018 was from the energy systems sector (34%), followed by industry (24%), AFOLU (agriculture forestry and other land uses) (21%), transportation (14%), and building operations (6%). The estimates are based on the direct emissions generated in each sector. GHG emissions in 2018 were about 11% higher than 2010 GHG emission levels. One-third of this increase in GHG emissions between 2010 and 2018 came from energy systems, followed by industry (30% of the increase), transportation (20%), AFOLU (12%) and buildings (4%).

In an effort to limit climate change to a low level, many countries make an effort to decouple the effects of growth of their gross domestic product and their GHG emissions. United Nations Framework Convention on Climate Change in 1992 ratified by 50 states, through the Kyoto Protocol in 1997 signed by 84 governments to the recent agreement at the Paris Climate Conference (COP 21) in December 2015 involving 195 nations. It is therefore clear that the energy sector must play a key role in reducing global emissions. The COP 21 agreement in Paris sent a strong signal to the world that a low-carbon future has been chosen as humanity's common path. There were two main approaches for overcoming the environmental problems;

the first is to develop and enhance the use of renewable energy sources like solar [4], wind [5], biomass [6], and geothermal [7]. The second approach is to find a way for enhancement of energy conversion systems so that the system efficiently uses the energy that can be received from a source. The international energy agency reported that efficiency improvements made since 2000 prevented 12% additional energy use in 2017. Efficiency gains also prevented 12% more greenhouse gas emissions and 20% more fossil fuel imports, including over USD 30 billion (United States dollars) in avoided oil imports in international energy agency countries [8]. As shown in **Figure 1.1**, the industrial sector has a share of the GHG emitted: 24% of the total GHG emitted in 2018 are attributed to industry. The worldwide total final energy consumption which is used in form of heat represents 50 % [9] ;(in which, industrial heat makes up two-thirds of industrial energy demand and almost one-fifth of global energy consumption) [10]. Thus, it seems logical that a large part of the aforementioned increases in energy efficiency should be made in the industrial sector.

Another way of increasing the use of the fuel input into an industrial process is to convert waste heat into additional products, such as electricity. It was estimated that 20-50 % of all energy input of industrial processes leave the process in form of waste heat [11]. The potential for waste heat conversion is therefore very large. Electricity and heat represent 31.9 % of the world CO_2 emissions [12]. The electricity production from waste heat can therefore have an important impact on CO_2 emissions if it substitutes power production from the existing power plants.

1.2. Waste heat

Industrial waste heat is, by definition, the energy produced during industrial processes and that is not used in the process (wasted energy or released into the environment). It is inevitable that most industrial processes generate waste heat due largely to thermodynamic limitations and equipment inefficiencies, but the waste heat varies considerably from process to process. Waste heat streams are characterized by the following parameters: temperature, flow rate, composition. The same parameters of the available cooling stream are also required to determine the recoverable heat potential for producing mechanical power. The grade or quality describes the amount of thermal energy that can be recovered from a heat source. While waste heat temperatures vary considerably by source, cooling streams tend to vary less. The waste heat potential has been generally classified according to the waste heat stream temperature. High grade heat: temperature is higher than 480 °C, medium-grade heat: temperature ranges between 240-480 °C , low-grade heat: temperature is lower than 240 °C [13]. Forman et al. [14] estimated the global waste heat potential at 245 PJ, with 63% of this energy below 100 °C and 79% below 200 °C. From this, it is clear that low temperature waste heat could be a significant source of energy if it can be effectively exploited.

High-grade waste heat is available from industrial processes like metal smelting, hydrogen plants and fume incinerators. These waste heat sources are typically solid or gaseous. Recovering heat from these environments can be challenging due to the high temperatures. Medium-grade waste heat sources are most typically found in power generation applications from steam or gas turbine exhaust, as well as in heating applications such as cement kilns, drying ovens, and internal combustion engines. Medium-grade waste heat sources are generally gaseous and can be used directly as heat sources. The majority of the available waste heat is considered of low quality. Examples of common sources of low-grade waste heat are: cooling

water from furnaces or power cycles and refrigeration cycles. **Table 1-1** lists the waste heat sites and thermal levels.

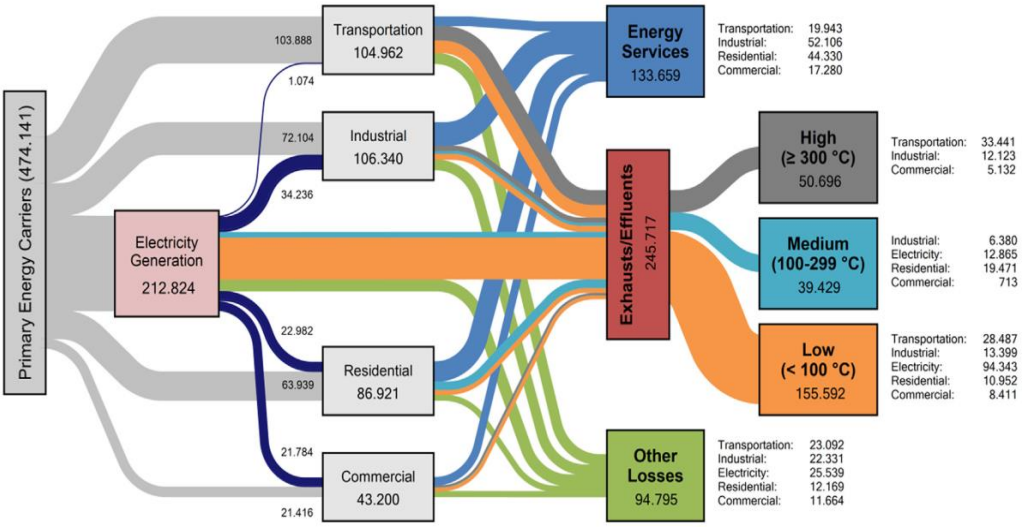

Figure 1.2 *Estimated global waste heat distribution of 2012 in Peta J [14].*

Table 1-1 *Waste heat sources and temperature range [15]*

Categories	**Heat sources**	**Temperature (◦C)**	**Suggested recovery technology**
High temperature (>650 ◦C)	Solid waste	650–1000	Air preheating Steam Rankine cycle Steam generation (Heating) Heat exchanger (preheating) Thermoelectric Thermal PV
	Fume incinerators	650–1450	
	Nickel refining furnace	1370–1650	
	Glass melting furnace	1000–1550	
	Aluminium refining furnaces	650–760	
	Copper reverberatory furnace	900–1100	
	Copper refining furnace	760–815	
	Zinc refining furnace	760–110	
	Cement kiln	620–730	
	Hydrogen plants	650–1000	
Medium temperature (230–650 ◦C)	Steam boiler exhaust	230–480	Steam Rankine cycle Organic Rankine cycle Heat exchangers (pre-heating process) Air pre-heating Thermoelectric Thermal PV
	Gas turbine exhaust	370–540	
	Drying and baking ovens	230–600	
	Catalytic crackers	425–650	
	Reciprocating engine exhausts	315–600	
	Catalytic crackers	425–650	
	Annealing furnace cooling systems	425–650	
Low temperature (<230 ◦C)	Process steam condensate	50–90	Space heating Domestic water heating Heat pump Organic Rankine Cycle Heat exchangers Absorption/adsorption cooling Kalina cycle Piezoelectric
	Cooling water from:		
	Internal combustion engines	66–120	
	Hot processed liquids and solids	32–232	
	Annealing furnaces	66–230	
	Drying, baking and curing ovens	93–230	
	Welding and injection molding machines	32–88	
	Bearings	32–88	
	Air compressors	27–50	

1.3. Waste heat recovery technologies

Captured and reused waste heat is a zero-emission alternative to costly purchased fuels or electricity. Several techniques are available to transfer waste heat to a productive end-use. Three basic components (**Figure 1.3**) are necessary for waste heat recovery: 1) an accessible source of waste heat, 2) a recovery technology, and 3) the use of the recovered energy.

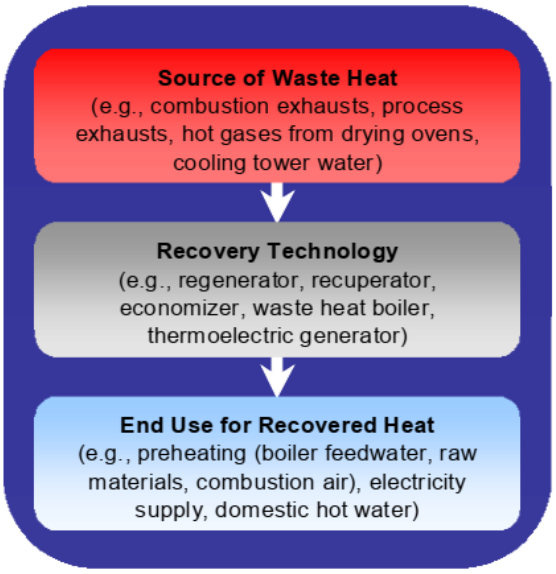

Figure 1.3 *Three essential components are required for waste heat recovery.*

In order to exploit the energy from waste heat streams, technologies capable of recovering this energy into a usable form of energy are required. Technologies used to recover waste heat from industry can be categorized depending on how the waste heat is reused: it can be used directly (at the same or at a lower temperature level), or it can be transformed to another form of energy or to a higher temperature. Four categories of technologies used to recover waste heat can be identified [16]:

- Waste heat to heat: the waste heat recovered is used to produce thermal energy at a higher temperature level (heat pumps, mechanical vapour compression, etc.).
- Waste heat to cold: technologies that utilize the waste heat recovered to produce cooling energy (absorption and adsorption chiller, etc.).
- Waste heat to power: technologies that convert the waste heat recovered to electricity (organic Rankine cycles (ORCs), Kalina cycles, etc.).
- Direct use as heat: the waste heat recovered is used directly at the same or a lower temperature. Heat exchangers are the dominant technologies of this category.

Recovering energy from high-grade heat sources tends to be used directly as heat or in steam power cycles, which are both mature and well-known technologies. The obstacles to extracting high-grade waste heat are due to the challenges of operating the equipment at high temperatures, and thus quite different from those of low to medium-grade heat sources. Commonly, high-grade heat recovery results in additional low and medium grade waste heat, which can be utilized by the techniques described below, in what is known as a cascade. **Figure 1.4** shows the subdivision into categories of the waste heat recovery technologies.

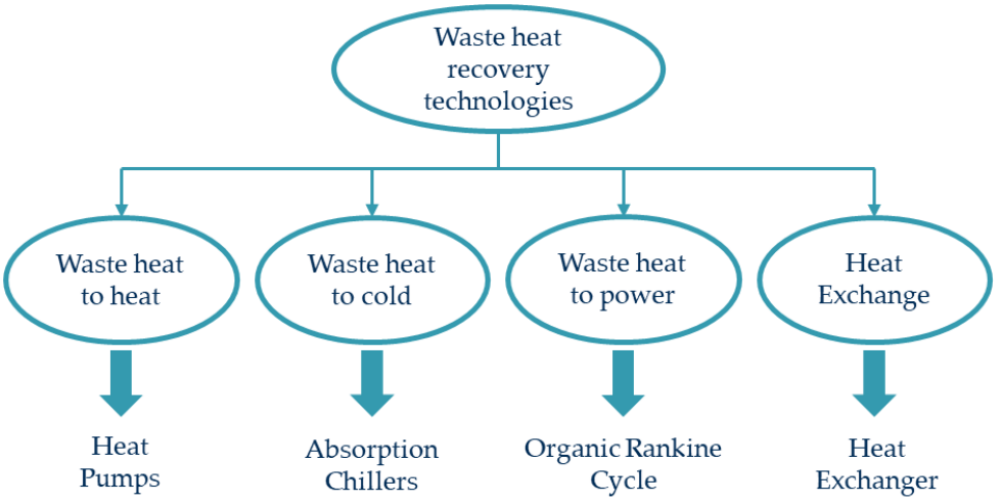

Figure 1.4 *Categorization of waste heat recovery technologies [17].*

1.3.1. Waste heat to heat

In scenarios where a local heat demand is needed but the quality of the available waste heat source is too low to satisfy this demand, heat upgrade technologies, such as the vapour compression cycles (also known as a heat pump cycle) , can be used to utilize the available waste heat and meet the heat demand. In these situations, heat exchangers are employed to recover heat from a working medium that then goes through a thermodynamic cycle to produce a higher grade heat stream. A heat pump has four major components: the evaporator, compressor, condenser and expansion valve. **Figure 1.5** shows a vapour compression cycle, the cycle operates as follows: in the evaporator, the working fluid vaporizes by absorbing thermal energy from a low temperature waste heat source. The compressor increases the pressure of the working fluid causing it to become a superheated vapour. In the condenser, the heat is rejected from the working fluid to the cooling stream, at higher temperature than was absorbed from the heat source. Finally, the condensed vapour is expanded through an expansion valve whereby it returns to its original state, allowing the cycle to repeat. Thus, the waste heat is upgraded by the mechanical work added in the compressor. Commonly, vapour compression cycles work at low-grade heat streams, around -20 to 100°C, and are capable of providing temperature rises of 20 to 50°C. This can make them suitable for providing domestic hot water. Heat pumps are most feasible for low-temperature product streams in process industries, including chemicals, petroleum refining, pulp and paper, and food processing [15].

1.3.2. Waste heat to cold

Absorption and adsorption systems are very similar to vapour compression cycle but the mechanical compression stage is replaced by a chemical process as shown in **Figure 1.5**. In the absorption cycle, it is an absorbent liquid, while the adsorption cycle uses a solid medium for compression stage. Both the absorption and adsorption cycles require an additional heat source and sink, and thus have many possible configurations. For example, if the waste heat is provided to the generator, the system can supply cooling and extract heat from the working fluid via the evaporator. The heat source is diverse, ranging from hydrocarbon fuels, solar energy, geothermal energy, district heating network or waste heat [18]. Absorption and adsorption cycles are quite complex; however they have several advantages over mechanical compression cycles. For example, the absence of moving parts without a mechanical

compressor, the use of environmentally friendly refrigerants as working fluids, and the ability to use high temperature heat sources, as a result there are many commercially available systems.

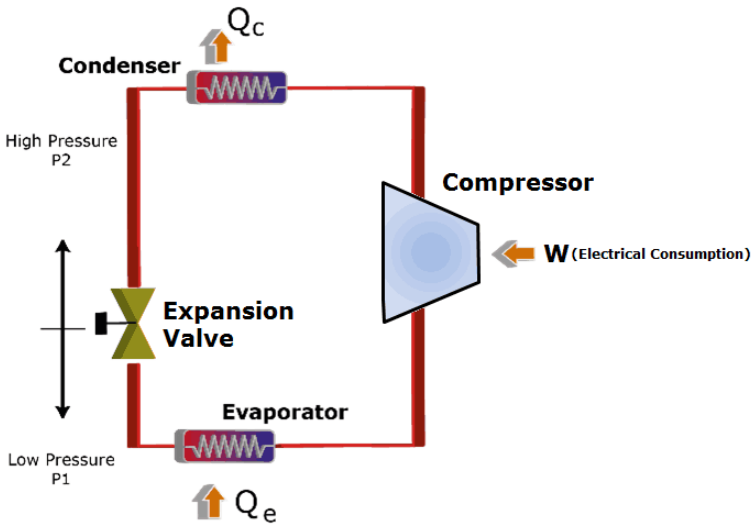

Figure 1.5 Vapour compression cycle.

1.3.3. Waste heat to power

The most popular heat recovery techniques convert waste heat into mechanical work; this work can then be used or converted into electricity via a generator. Examples of such technologies are thermodynamic cycles and thermoelectric power generation. Thermodynamic cycles converting heat into mechanical energy. In binary cycles, heat is captured from the heat source via a heat exchanger and transferred to a secondary fluid, called the working fluid. There are many types of thermodynamic cycles that produce mechanical work, and the most common in waste heat recovery technologies are the Rankine and Kalina cycles [19].

The Rankine cycle using water as a working fluid is generally used in large thermal power plants, this cycle is illustrated in **figure 1.6**.

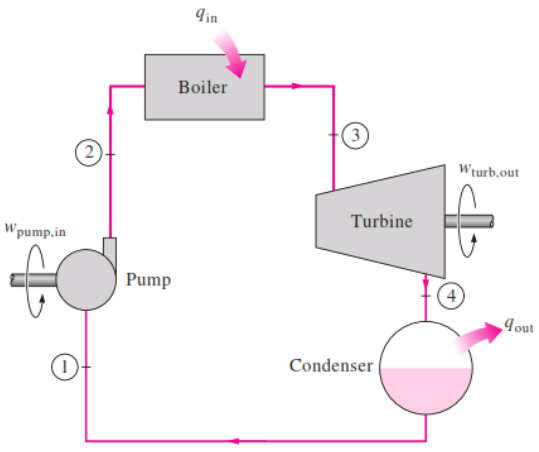

Figure 1.6 Diagram of the basic Rankine cycle.

In a Rankine cycle, the water (at condensation pressure) is pumped to a higher pressure (isentropic work addition). It is preheated, evaporated and superheated by a heat source at constant pressure (isobaric heat addition). The steam then is expanded through a turbine or

(isentropic work extraction). To close the cycle, the steam exiting the expander is condensed to water at constant pressure before it enters the pump again (isobaric heat rejection). The work that is used to drive a generator is recovered from the turbine. Water is a suitable working fluid for Rankine cycle because of its high thermal and chemical stability. Its low viscosity and high heat capacity. It is non-toxic and non-flammable, and has a low cost and high abundance. Nevertheless, water is only suitable for use in Rankine cycles with heat source temperatures above 350 ° C [15], below this temperature, the cycle is unlikely to be economical, because low pressure steam requires larger heat exchangers and the cycle is less efficient . At temperatures less than 300°C (low and medium quality heat), the ORC [20] or the Kalina cycle [21] can be used.

The ORC is a Rankine cycle that uses organic working fluids with low boiling points, instead of steam, to recover heat from a lower temperature heat source. The wide range of possible working fluids that may be used within the ORC leads to applicability over a wide temperature range and thus facilitates adaptation to different heat sources. The typical sizes of ORCs for industrial applications vary from 0.5 to 20 MW [22]. Sources of thermal energy for the ORC include geothermal, solar and biomass energy, and industrial waste heat. ORC technology is not particularly new; at least 30 commercial plants worldwide were employing the cycle before 1984 [15]. The largest margin for growth has been forecast in the field of industrial waste heat recovery. Among all of the thermodynamic cycles for low-grade heat-to-power conversion, ORC is so far the most commercially developed one. Both M-watts and k-watts scales can be found in operation. The ORCs are favoured for their simplicity in configuration; more details about the ORC will be given next chapter.

The Kalina cycle is an innovative bottoming cycle developed by Alexander Kalina in the late 1970s and early 1980s, which a working fluid comprised of at least two different components, typically water and ammonia [23]. This is more complex than the Rankine cycle, see **Figure 1.7**, but the same four key processes of the Rankine cycle are employed evaporation, expansion, condensation and compression, with the addition of a generator and absorber.

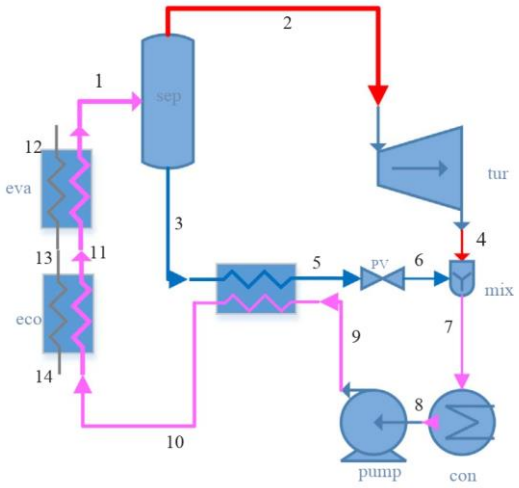

Figure 1.7 *Schematic diagram of the Kalina cycle [24].*

The main difference between single-fluid cycles and cycles using mixed fluids is the temperature profile during boiling and condensation. The generator and absorber control the ratio of water to ammonia so the ratio of components varies in different parts of the system to decrease thermodynamic irreversibility and therefore increase the overall thermodynamic

efficiency. For single fluid cycles (e.g., steam or organic Rankine), the temperature stays constant during boiling. When heat is transferred to the working medium, the temperature of the working medium slowly increases to its boiling temperature, at which point the temperature remains constant until all the water has evaporated. In contrast, a binary mixture of water and ammonia (each with a different boiling point) will increase its temperature during evaporation. This results in better thermal compatibility with the waste heat source and the coolant in the condenser. Thus, these systems achieve a significantly higher energy efficiency. The first power plant based on the Kalina cycle was constructed in Canoga Park, California in 1991, which is a 3MW demonstration plant and put into operation in 1996 [25]. Studies predict the Kalina cycle could perform up to 30 - 50 % more efficient than the ORC but experimental results show much smaller improvements in system efficiency of just 3 % [26]. The Kalina cycle is favoured for better temperature matching between heat carrier and mixed working fluid compared to pure fluids. However, the architecture of the Kalina cycle is more complex and the high cycle pressure, results in high capital costs.

Traditional power cycles involve using heat to create mechanical energy and ultimately electrical energy, new technologies are being developed that can generate electricity directly from heat. Therefore, direct electrical conversion methods have the potential to be simpler and require lower maintenance than traditional power generation.

Thermoelectric systems are semiconductor solids that allow direct generation of electricity when subject to a temperature differential. Thermoelectric systems use the Seebeck effect, when two different semiconductor materials are subject to a heat source and heat sink, the thermal gradient causes a heat flux and charge carriers flow from the hot to cold regions, creating a potential difference [27]. Thermoelectric systems are available for variable temperatures of over 1000°C and have no moving or complex parts, making them maintenance free and silent in operation [28]. Unfortunately, the thermoelectric systems available today are not only expensive, but also have relatively low yields. At a temperature of more than 1000 °C [29], the yield remains below 20% and at 400 °C it does not reach 10% [29–31].

Piezoelectric power generation is a process of converting low temperature waste heat (100-150°C) to electricity [15]. Piezoelectric devices are made out of thin-film membranes and they work by converting mechanical energy in the form of ambient vibrations such as oscillatory gas expansion into electricity (usually in the nW–mW range) [32–34]. There are several technical challenges and disadvantages associated with these devices that limit their use for heat recovery, namely, low efficiency, high internal impedance, complex oscillatory fluid dynamics within the liquid/vapour chamber, the need for long-term durability and very high cost[15]. Having mentioned that the main issue with the use of piezoelectric devices are associated with the high cost of manufacturing these devices as well as the way the systems must be designed to enable power generation [35].

Thermionic energy converter is a heat engine that produces electricity directly using heat as its source of energy and electron as its working fluid. Thermionic devices operate similar to thermoelectric devices; however, they operate through thermionic emission [36]. In this technology, a temperature difference drives the flow of electrons through a vacuum from a metal to a metal oxide surface to generate electricity [37]. The functionality of this technology is shown to be limited to high temperature applications (above 1000°C) and be inefficient. However, several efforts have been made to improve their efficiency and enable their use for low temperature applications (100-300°C) [15].

1.3.4. Direct use as heat

The most direct use of a waste heat source is to recover the heat using a heat exchanger and use it to satisfy the heat demand. Heat exchangers are a well-established technology and several types have been developed for common waste heat applications. They are widely used to transfer heat from the combustion exhaust gases to the combustion air entering the furnace. As the preheated combustion air enters the furnace at a higher temperature, lower energy must be supplied by the fuel. Typical technologies used for air preheating include recuperators, furnace regenerators and burner regenerators. Other heat exchanger systems used to recover heat are: economizers, regenerators, and waste heat boilers [37]. The feasibility of these technologies is limited by having a waste heat stream that can help meet a local heat demand. Heat streams can be transported over short distances via thermally insulated heat pipes to a heat requirement, called heat networks. However, over long distances (several kilometres), the cost of the pipes makes the transporting of the heat stream expensive.

1.4. Scope and structure of the present thesis

This chapter highlights current challenges in meeting energy demand. Using waste heat to fulfil part of the energy demand decreases carbon emissions, enhances fuel economy, and further secures energy supply by generating more electricity for the same amount of fuel. Thus, there is a strong incentive to use waste heat sources. Several sources of waste heat are identified in Section 1.2, which offer a significant unused energy resource. Global waste heat represents approximately 245 PJ of untapped energy, with 63% of this energy below 100°C and 79% below 200°C [14]. Finally, in the previous section, waste heat recovery technologies were identified and discussed. The existing heat recovery technologies are given in **Table 1-1**. The applicability of these technologies is determined by further factors such as cost, size, etc.

ORC is increasingly becoming a principal effective solution in producing energy from low-grade heat sources due to its simplicity, component availability, maintainability and high efficiency compared to other cycles [38]. The aim of this thesis is to model and perform the thermo-economic optimization of ORCs for the recovery of low grade waste heat sources. The organisation of the work in this thesis is presented in **Figure 1.8**. The influence of the choice of the working fluids and the cycle configurations will be studied and the different combinations will be compared. Every chapter is outlined as follows:

Chapter 2 presents an introductory review on ORC systems, with an overview of their history, a review of the ORC application, a review of the ORC main component selections.

Chapter 3 focuses on the thermodynamic performance of the reheat ORC with different working fluid types. The relationship of the main operating parameters, such as evaporation pressure, reheat pressure and superheat degree to the performance of the reheat ORC system is discussed. Moreover, the present chapter also considers the possible presence of an internal heat exchanger within the ORC and its influence on overall system performance.

Chapter 4 deals with the thermo-economic optimization of different ORC configurations. In order to produce cost-effective cycle designs capable of achieving increased economic profitability, it is necessary to take into account not only the theoretical thermodynamic performance of ORCs but also the technological limitations and costs of the employed equipment components.

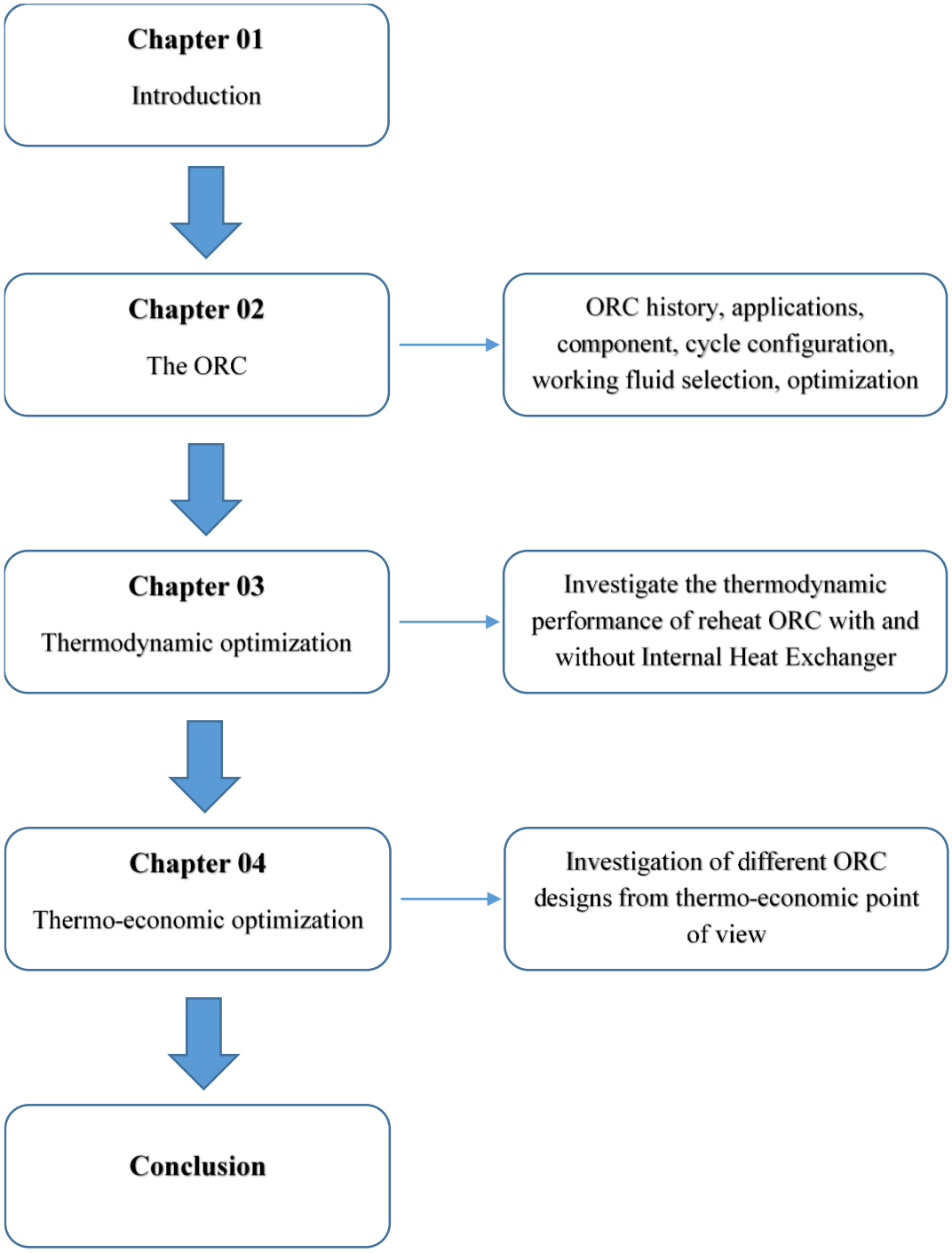

Figure 1.8 *Organization of the work in this thesis.*

2. The Organic Rankine Cycle

2.1. Introduction

The ORC is a thermodynamic power cycle suitable for the exploitation of several different energy sources (geothermal, solar, waste heat sources, etc.) and is particularly appropriate for medium-low temperature heat sources [39–42]. The ORC finds its origins in the conventional steam Rankine cycle, the configuration of the ORC is somewhat simpler than that of the steam Rankine cycle: there is no water-steam drum connected to the boiler and one single heat exchanger can be used to perform the three evaporation phases (preheating, vaporization and superheating). The main difference between the organic and the conventional Rankine cycle is the working fluid used in the cycle. The boiling point of working fluid in the ORC is much inferior to steam; thus, there is no requirement to achieve high temperatures to generate vapour for running a micro-turbine or expander. The ORC is characterised by a simple structure, good flexibility, availability of components, requires less maintenance and for these reasons it is currently considered the most promising technology for exploiting medium and low temperature heat sources. [43]. **Figure 2.1** presents the schematic and *T-S* diagram of a typical ORC.

A typical ORC has four main components: the evaporator, expansion machine, pump and condenser. The working fluid is compressed in the pump. Next, the liquid is heated and vaporized in the evaporator, which changes the liquid from liquid to vapour. Subsequently, the vapour is expanded in an expander which extracts energy from the superheated working fluid to generate power. Finally, the vapour condenses in a condenser which changes the state from vapour to liquid again, and the cycle repeats.

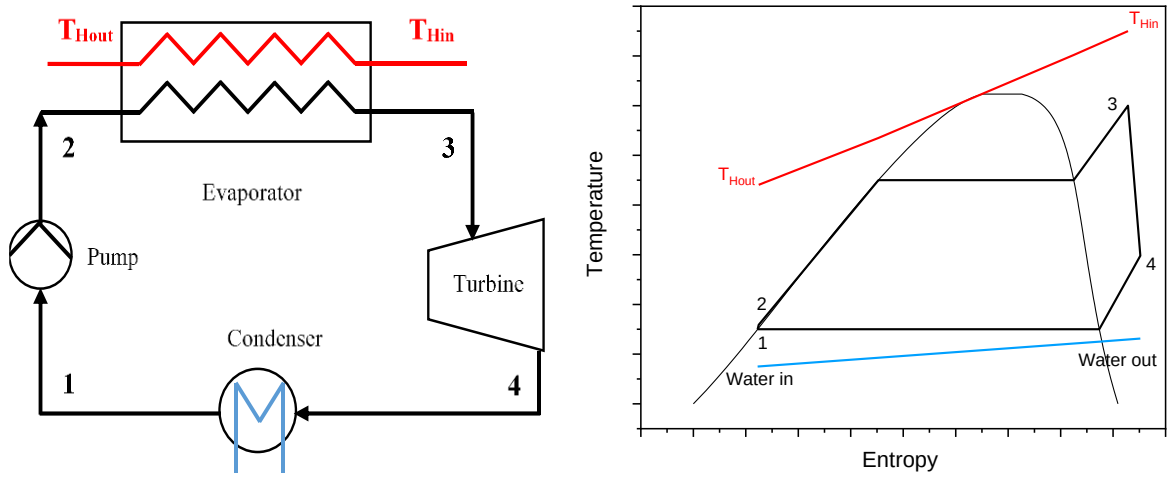

Figure 2.1 *Schematic and T-S diagram of a typical ORC.*

Due to the thermal stability limit of organic working fluids, an upper temperature bound in ORC applications is specified, which is typically considered to be 400 °C. Biomass and

geothermal ORCs are generally considered for larger capacities that typically range from one to several MW, while the lower temperature limits are about 200 °C and below 100 °C respectively. Meanwhile, the global lower temperature bound is between 200 °C and 300 °C for micro-mini combined heat and power systems at a scale of 0.1 to a few kW and waste heat recovery applications at a scale of a few kW to hundreds of kW. For solar rural electrification within the same scale, the lower temperature limit is 150 °C. **Figure 2.2** shows a range of ORC applications grouped by energy source, power output and heat source temperature.

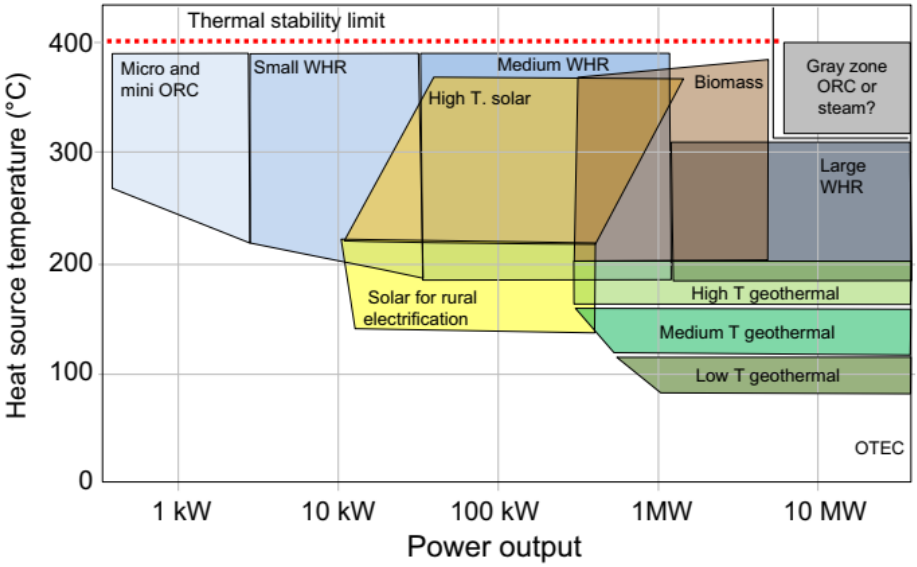

Figure 2.2 *Overview of ORC applications grouped by energy source, power output and heat source temperature [6].*

2.2. Organic Rankine cycle history

The history of ORC systems is pretty long, starting in the first half of the 19th century, until ORC power systems became a significant niche market in the 21st century power industry. A brief history of ORC cycles was presented, citing the important events in the development of this technology. The salient points are outlined below:

1823. Humphrey Davy suggested the ORC cycle as an alternative to the steam engine. He suggested the use of liquids that could be vaporized at a lower temperature in a boiler heated by a condenser and employing the vapour produced in another engine, and could thus generate more power. This is called a bottoming cycle [44], [45].

1824 In his work published in 1824, Sadi Carnot already proposed the use of other substances to replace water [46].

1825 Thomas Howard patented the concept of an engine using alcohol or ether as working fluid [47].

1829 Ainger suggested cascade cycles of liquids of different boiling points, the boiler of each liquid operating as a condenser for the next higher fluid in the series, the external heat source being required only for vaporizing the highest boiling point liquid [48].

1853 The French engineer Du Trembley created a binary heat engine with steam for the high temperature engine and ether for the low temperature engine. After

evaporating in the boiler and expanding in the cylinders, the steam has released its thermal energy of condensation to the second engine, causing the ether to evaporate and expand into another cylinder, producing more work. In this way, the engine is the first commercial application of an organic fluid [48].

1883 Frank W. Ofeldt patented a naphtha engine, which was essentially a closed cycle vapour engine using naphtha instead of water as the working fluid. Naphtha was used as working fluid, lubricant and as fuel for the evaporation of the working fluid. The engine was developed by the Gas Engine and Power Company, which announced in 1890 that it had sold 500 ORC engines based on Ofeldt's design [49].

1904 Willsie built two solar ORC engines using sulphur dioxide, one of 6 horsepower (4.5 kW), and the other of 15 horsepower (11 kW) [48].

1907 Shuman built a solar ORC engine, using a flat solar collector of 110 m^2 to boil ether at temperatures around 120 °C and drive a 3.5 HP (2.6 kW) engine [49].

1923 In Italy, Romagnoli used water at 55 °C to boil ethyl chloride and run a 1.5 kW engine [49,50].

1935 Luigi D'Amelio, a professor at the University of Naples in Italy, was the first to use an organic fluid in a real turbine system. He made detailed studies of a solar power plant based on an ORC engine using monochloroethane as working fluid. The vapour expansion was ensured by an impulse single-stage turbine, the evaporation and condensation temperatures were 40°C and 23°C respectively, with a turbine power of about 4 kW. The estimated thermal conversion efficiency was of approximately 3.6% [22,49].

1939-1940 D'Amelio's work led to the realization of a 2.6 kW prototype for the conversion of low-grade geothermal energy in 1939. Based on this prototype, he built an 11 kW geothermal ORC pilot power plant on the island of Ischia, Italy in 1940, using ethylene as a working fluid. The plant operated for a few years and was decommissioned in the early 1950s [48,49].

1952 The first commercially operated geothermal power plant was in Kiabukwa, Democratic Republic of Congo, in 1952. The plant was supplied with hot water at a temperature of 91°C and a mass flow rate of 40 kg/s from a geothermal spring. It featured a power capacity of 200 kW, and supplied electric power to a mining company for a number of years [49,51].

1958- 1961 Tabor and Bronicki established the criteria for the selection of suitable organic fluids to optimize the efficiency of the cycle, in a small engine project, as part of a program to harness solar energy. The physical properties of the working fluid were selected according to criteria that related to the characteristics of the heat source and heat sink, as well as the power output [49,52].

1961-1962 Tabor and Bronicki designed, built, and tested several small solar ORC units 2-10 kW with monochlorobenzene as the working fluid at 140–150 °C. Some of these plants are reported to have operated for 12 years without repairs [52].

1967 The second oldest geothermal ORC power plant was commissioned at Paratunka in the Kamchatka peninsula in 1967. It was a pilot plant exploiting geothermal

water at 80 °C, rated at 680 kW, and using refrigerant R12 as the working fluid. It served a small village and some farms with both electricity and heat for use in greenhouses [49,53].

1975 In 1975, Barber built a 1 kW ORC using R113 coupled to a solar flat-plate collectors, the evaporation and condensation temperatures were equal to 93 °C and 35 °C, the efficiency of the ORC module was approximately 7% [49].

1976-1978 In 1976, Agelino, Macchi and Gaia built a 4 kW ORC using perchloroethylene as working fluid in a saturated cycle.
A medium temperature ORC followed in 1978 by the same group, with an output of 35 kW, the heat source was thermal oil at 280 °C from a parabolic trough, the cold sink was water at (25-32 °C), in recuperated cycle [48].

1979 In 1979, McCabe built a commercial 12.5 MW ORC using a dual-fluid cycle in which two different working fluids (isopentane and isobutene) were used on two interconnected ORC power plants, one a subcritical cycle and one a supercritical cycle [51].

1981 By 1981, there were 2150 Rankine engines with 16 different working fluids, built by about 20 different engine manufacturers [22].

1985 Barber built a geothermal plant of two 700 kW units using evaporative condensers cooling and a turbine of his design and manufacture in Susanville. As of 2015 the plant is still in operation [48].

1990s Many of the ORC system manufacturers and component providers are available. Research continues in the field and new technologies are emerging.

Although the above history of the ORC is only brief, it can give us an overview of the development history of the ORC cycle.

2.3. Organic Rankine cycle application

ORCs can be used to generate electricity in smaller capacities (starting from only a few kW) compared to steam cycles and from lower-temperature heat sources (from 90 °C onwards) [54,55]. ORCs can be applied in many different sectors such as in geothermal energy [56], in biomass [42], with solar energy [40] and for internal combustion engines [57] which are forms of waste heat recovery or even in Ocean Thermal Energy Conversion (OTEC) [58].

2.3.1. Geothermal energy

The earth is increasingly warmer the deeper one goes. This underground energy originating from the centre of the earth, usually referred to as geothermal energy, can be used to generate electricity and/or for heating processes. Geothermal heat sources are available over a broad range of temperatures, from a few tens of degrees up to 300 °C. Among the advantages of geothermal energy over other renewable sources, such as solar, wind and biomass, are its enormous potential, free of harmful emissions and carbon as well as climate neutral and its Independency from weather and seasonal conditions [59,60]. Geothermal energy is generally classified as renewable, and the validity of this definition is subject to the rate of extraction: only if the rate of extraction from the reservoir does not exceed the reservoir replenishment rate [61]. The technological lower bound for power generation is about 80 °C (as previously shown in **Figure 2.2**). Below this limit, the conversion efficiency becomes very low and

geothermal plants are not economical [62]. The geothermal energy can be recovered by drilling deep boreholes (several thousand metres deep depending on the geological formation) and pumping the hot brine to the surface through a production well. The hot brine can transfer its heat directly to an organic fluid via the evaporator or to a secondary working fluid through a second heat exchanger, which increases safety but reduces efficiency. The brine is then returned to the injection well at a lower temperature. At higher temperatures (>150 °C), geothermal heat sources enable combined heat and power generation: the condensing temperature is fixed at a higher temperature (e.g. 60 °C), which allows the cooling water to be used for district heating. In this way, the overall energy is increased, but at the expense of a lower electrical efficiency and power production [62]. As the end of 2020, the total capacity of ORC plants was 4.1 GW, distributed over 2845 ORC units. Geothermal energy attracts most applications, with an installed capacity corresponding to 77.4 %% of the total. Although in terms of the number of plants this share is smaller, with geothermal systems tending to have a higher power output than other applications [63]. **Figure 2.3** shows a schematic of a geothermal ORC binary power cycle. The hot geothermal brine can either transfer its heat directly to an organic working fluid via an evaporator or to a secondary working fluid through a second heat exchanger, increasing safety but diminishing efficiency. Next, the geothermal brine is returned to the injection well at a lower temperature. The working fluid is heated, evaporated, expanded and passed through the recuperator or Internal Heat Exchanger (IHE) and condenser before pumped to the evaporator again, and the cycle repeats.

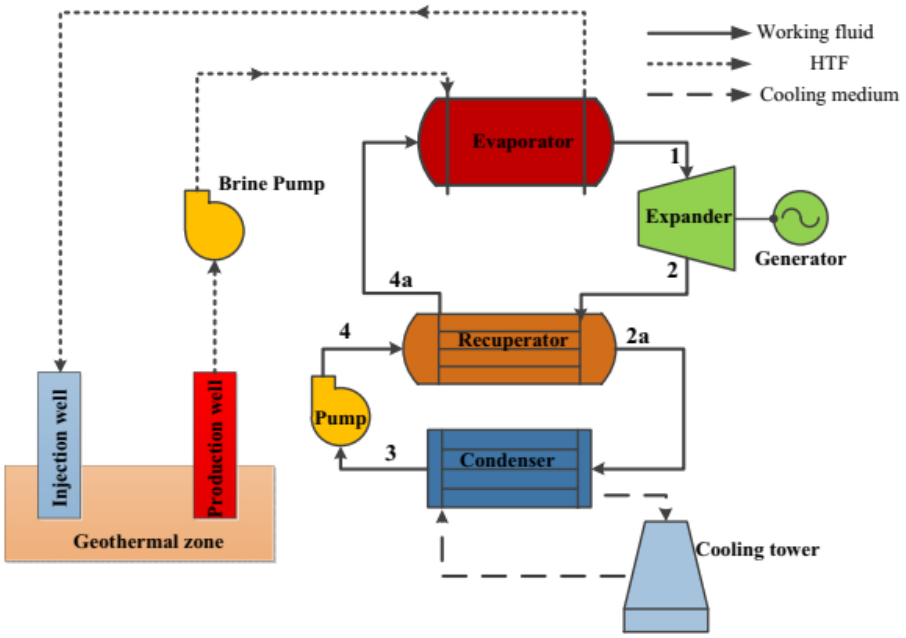

Figure 2.3 *Schematic of a geothermal ORC binary power cycle [64].*

2.3.2. Biomass

Biomass is an energy source, which allows power production with a limited carbon dioxide emission to the atmosphere. More than 400 ORC units of this type are in operation [63]. Most often these plants are installed into wood manufacturing sites, and feature the combined heat and power arrangement, whereby the heat released by the ORC unit, at temperatures below 100 °C, is used for process purposes (e.g., wood drying), or district heating [49] . Biomass boilers generally operate with synthetic oil as heat transfer fluid rather than a direct heat transfer to the working fluid. The use of heat transfer fluid (synthetic oil) has some advantages such as low pressure in the evaporator, insensitivity to the load changes, this makes the control and the operation of the cycle safer and simpler. For small biomass units, the electricity production cost is still not competitive and a combination of heat and power production is needed to assure the profitability of the investment. As a result, to achieve high energy conversion efficiency, biomass combined heat and power are often driven by heat demand rather than electricity demand. In most cases, biomass Combined Heat and Power (CHP) unit are limited to 6-10 MW thermal power, which is equivalent to 1-2 MW electrical power, due to the difficulty of transferring the heat over long distances [62]. The rated net electrical efficiency is generally between 15 and 20 %, while the total energy efficiency can reach 90% [49]. Most of the ORC biomass systems are binary cycles as shown in **Figure 2.4**. The heat from the biomass feed-burner is transferred via the flue gases to the heat transfer fluid (thermal oil), at a temperature varying between 150 and 320 °C. Then the hot thermal oil is directed to the ORC evaporator to evaporate the working fluid. Then, the evaporated fluid is expanded, passes through an IHE and is finally condensed. The condenser is used for hot water generation.

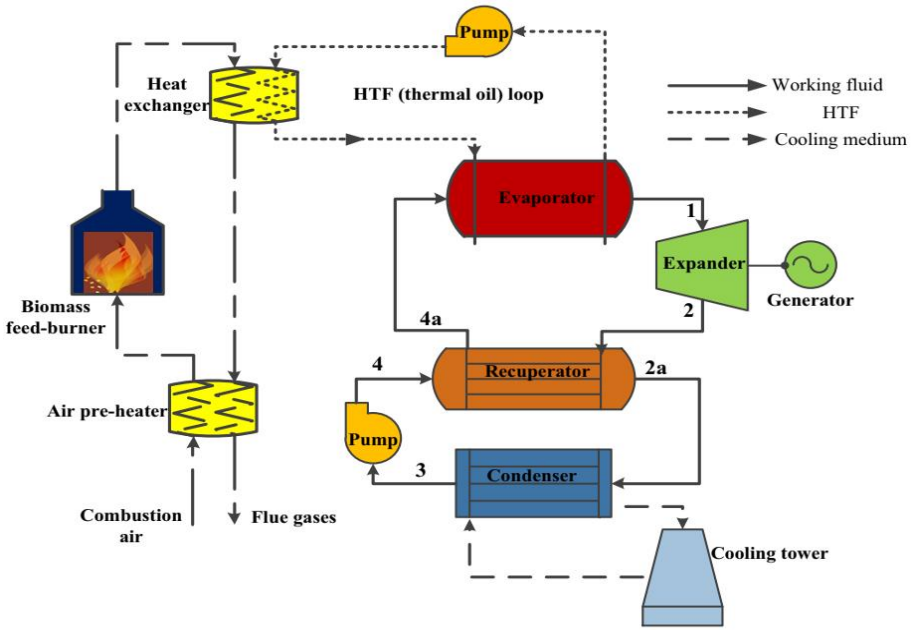

Figure 2.4 Schematic of a biomass combined heat and power ORC system [64].

2.3.3. Solar

With an estimated 3.4×10^6 exajoule of energy reaching the Earth's surface each year, solar energy is the most abundant source of energy [65]. Concentrating solar power is a proven technology in which the radiation emitted by the sun is concentrated by a solar collector and transferred to a high temperature fluid. This heat is then used in the ORC cycle to generate electricity. A suitable heat transfer fluid, usually a synthetic oil or molten salt, is used in the solar collectors. The hot fluid finally transfers heat to the working fluid driving the ORC. Two possibilities for the design of solar power plants in terms of maximum working fluid temperature can be distinguished. High temperature entails increased conversion efficiency, but calls for high-cost collectors and large thermal storage. In smaller scale installations instead, ORCs become competitive with steam cycles. In these plants, a lower maximum plant temperature is chosen, which allows simpler technological solutions, but leads to a lower conversion efficiency compared to the first option. The disadvantage of solar energy is its intermittent nature, which causes an imbalance between consumer demand and the availability of the heat source. To avoid this, the addition of thermal energy storage is considered to shift the excess energy from periods of high-insolation to night-time periods or to periods of unfavourable conditions. These solutions increase the efficiency, reliability and flexibility of the system. An interesting application of ORCs combined with solar power is the stand-alone configuration in remote regions, for end-users not connected to the electricity grid. The implementation of this system has recently been proposed by STG International for a rural clinic in Lesotho, using built-in-site parabolic trough collectors, monoethylene glycol as the heat transfer fluid and a R245fa based ORC with a 3kWe power output [66]. This configuration is intended to replace or supplement diesel generators in off-grid areas of developing countries, generating clean energy at low cost. **Figure 2.5** shows the schematic of the solar ORC power cycle.

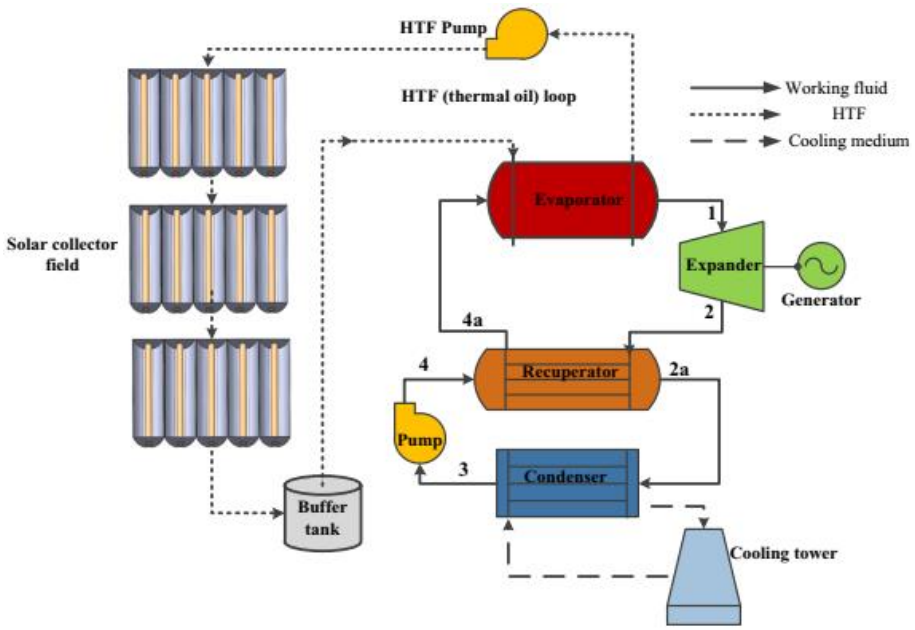

Figure 2.5 Schematic of a solar ORC system [64].

2.3.4. Waste heat recovery

In many industrial processes, a large amount of energy is discharged into the environment in the form of hot gases or liquid streams. It is increasingly important to recover this waste heat to achieve huge energy savings and minimize environmental impact by improving industrial energy efficiency. Statistical studies indicate that about 50% of the energy used to generate power is being wasted due to the limitation of the energy conversion process and a lack of execution of reliable recovery technologies [67,68]. Most of the thermal energy is wasted at temperatures between 60 and 400°C, with capacity increasing monotonically to huge amounts at lower temperatures [49]. Generally, waste heat can be found at temperatures of 300-400°C in industries such as glass, iron and steel, non-ferrous metals, bricks and ceramics processing. Medium temperature waste heat at 150°C is found in industries such as food, chemicals, refining and building utilities. Waste heat at low temperatures is easily found in almost all areas of industry. In [69], the authors present a comparison of ORC with other waste heat recovery technologies, such as the Stirling engine, thermoelectricity and the Brighton reverse cycle. The results revealed that ORC is the best performing technology for heat recovery and power generation using heat sources at temperatures ranging from 200°C to 400°C. In the temperature range (300-400°C), the ORC has to compete with small steam Rankine cycles which are commonly proposed for these applications.

The cement plants are an example of industrial processes appropriate for the application of ORCs and some commercial installation are already under operation. In a typical modern kiln, approximately 23% of the heat input to the system is lost due to waste gases, with the cooler excess gas and by radiation throughout the entire surface of the system [70]. Moreira et al. [71] carried out a thermo-economic assessment of ORC system for waste heat recovery in cement plants. The proposed ORCs were able to produce around (4000–9000) kW and thus eliminating the production of 221 kgCO_2/year). In addition, they pointed that, that the proposed ORCs for cement industry waste heat recovery are environmentally interesting and extremely competitive in terms of their financial and technical properties. The ORC for waste heat recovery in cement plants is illustrated in **Figure 2.6**. The working fluid receives heat from the exhaust gas in the evaporation unit at constant pressure. Next, the working fluid experiences isentropic expansion in the turbine. Heat is then transferred from the working fluid to the cooling water in the condenser at constant pressure and isentropic compression of the working fluid occurs in the pump. Finally, the working fluid returns to the evaporation unit, and a new cycle begins.

As an energy-intensive industry, the steel energy consumption accounting for 15-20% of the total industrial energy consumption of China [72]. About 68% of the energy is lost as waste heat via flue gases and steam discharged from sintering machines blast furnaces, converters, and reheating furnaces in steel production [73]. The flue gas temperature varies in the range of 200-450°C that contains a large quantity of middle and high quality waste energy. In addition, the temperature of the pressurized cooling water exiting the furnace is typically 90°C to 150°C. This hot water is another suitable source of heat recovery. It can be used to heat offices and buildings or to preheat any other process if required. Also, this moderate temperature hot water can also be used to generate electricity.

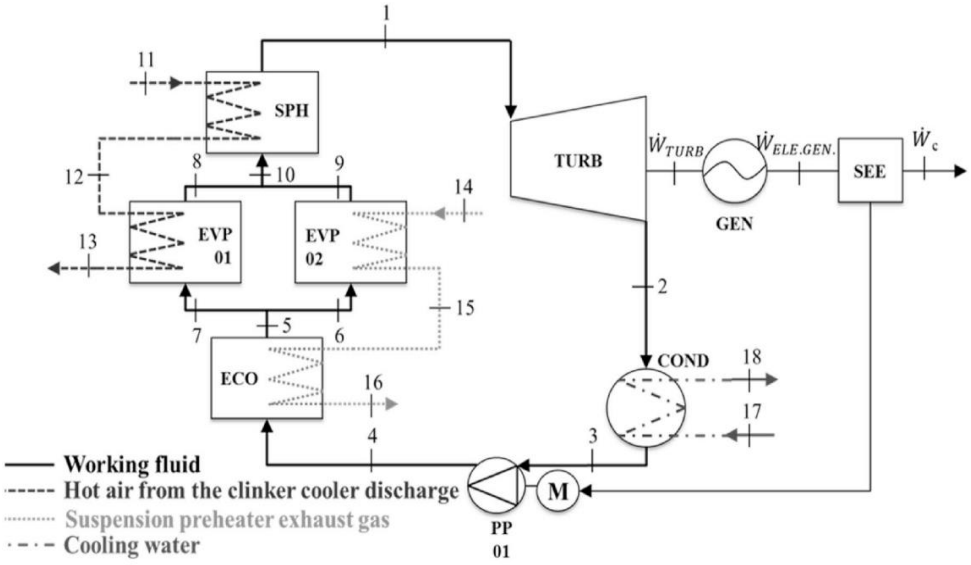

Figure 2.6 Schematic of an ORC for waste heat recovery in cement industry [71].

On average, about one third of energy generated from the fuel is wasted by exhaust gases for typical internal combustion engine. For instance, for a typical 2L gasoline engine used on passenger cars, 21% of the released energy is wasted through the exhaust at the most common load and speed condition. This rises to 44% at the peak power point [74]. The integration of the ORC with the internal combustion engine to improve the overall efficiency of the system is a common commercial practice, and almost all ORC producers offer this solution in their catalogues. The use of this solution, results in increase of the power output by 3% if the heat is simply recovered from water jacket and by 10% if the heat from the high-temperature flue gases is utilized [75].

The glass industry is another area of possible application of ORC technology. An intermediate heat transfer loop can collect thermal energy from the hot gas exiting the oven that melts and refines the raw materials. Heat can be recovered at temperatures of (400 - 500 °C) down to 200°C [76]. This source is characterized by stable temperature profile and a constant mass flow rate of the exhaust gases.

2.3.5. Ocean Thermal Energy Conversion

Ocean Thermal Energy Conversion (OTEC) is one of the most typical clean and sustainable energy technologies which can utilize the temperature difference between warm surface seawater and cool deep seawater to generate power via ORC. The OTEC concept has been studied for a long time, though no commercial application exists. It suffers from the problems of low thermal efficiency and high investment cost and the failures and damaging of the deep tube [49,75]. In fact, it is necessary to pump a huge deep water flow rate with flexible pipes which are subjected to relevant stress due to the action of ocean streams and tidal currents. Experimental research has recently resumed and pilot plants have been built, using ammonia as the working fluid in a saturated cycle configuration [49]. Technical problems related to deep-water pipes and pumps can now be solved thanks to advancements in off-shore technology. Economic viability might be achieved in the future, depending on energy value and policy,

arguably only with large installations. Some innovative aspects related to OTEC power plants are presented in literature, an example is the study on the hybridization of an OTEC power plant with the addition of solar concentrators, and the utilization of complex configuration (multiple pressure level) for maximum efficiency [77]. **Figure 2.7** shows the schematic of the OTEC system employing ORC for power generation. The organic fluid is pressurized by the ORC pump to the evaporator, where it is heated by warm seawater and turns to saturated or superheated vapour. Next, the saturated vapour expands in the expansion machine to generate power until it becomes low-pressure vapour, which will further condenses to saturated liquid through the condenser. At last, the saturated liquid working fluid will be pumped back to the evaporator to finish an entire cycle.

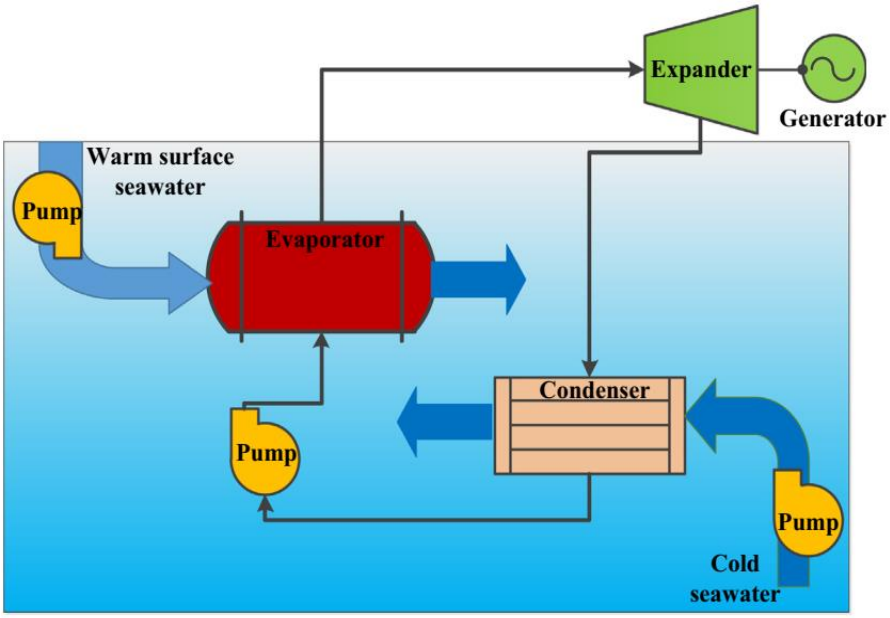

Figure 2.7 schematic of the OTEC system employing ORC for power generation [64].

2.3.6. Other applications

Other applications attracted some research efforts because the use of an ORC power system implies several advantages. Even if their use is nowadays confined to niche markets, the potential upside of these fields is impressive due to high number of possible installations.

An example is the micro-scale ORCs for domestic combined heat and power applications, which produced by the UK based FlowEnergy Limited [78]. The system, launched in January 2015, is powered by natural gas and operates with pentane (working fluid) at a cycle temperature of 150 °C, while it produces hot water for an exterior storage tank. It can produce up to 1 kWe of electrical power, using a scroll expander connected to a generator, and a thermal power ranging from 7,4 kW to 14,1 kW [78].

Another filed acquiring more and more attention in recent years is the use of ORC coupled with heavy-duty diesel engines. The road transport sector, mostly powered by heavy-duty diesel engines, has been estimated to contribute for 14% to the world global greenhouse gases emissions in 2014 [79]. They release to the environment large amount of heat since the efficiency of these devices generally ranges between 40-45% and the thermal power can be

recovered from different streams having different thermal levels. In particular, heat is available at low temperature from the charge air cooler and from the coolant and the lube oil and at high temperature from exhaust gas recirculation. Recovering exhaust gas recirculation heat (as well as engine cooling jacket water heat) is helpful in particular for the vehicle cooling circuit, as the heat that should be rejected to the coolant, and then to the ambient through the cooling pack, is used to produce additional useful power.

Another important advantage of ORC technology is the possibility of producing small amounts of power in remote areas, like arctic areas or offshore and on shore platforms. In remote areas, the conversion of solar energy in electricity could be an important option to enhance the development of rural communities. Compared to the main competitive technology, the photovoltaic collector, Solar ORCs have the advantage of being more flexible and allow the production of hot water as a by-product.

2.3.7. Organic Rankine cycle world capacity

On a worldwide scale, the total installed capacity of the ORC is equal to 4.1 GW, distributed over 2845 power plants, considering all the possible applications [63]. In **Figure 2.8** geothermal is the most diffuse applications for ORC and it contributes to 77.4% of all ORC installed capacity worldwide. An almost equivalent share for waste heat recovery 11.6% and biomass application 10.1% and a minor contribution of the other applications (total 0.93%): waste-to-energy 0.7%, solar 0.2%, remote application 0.03%.

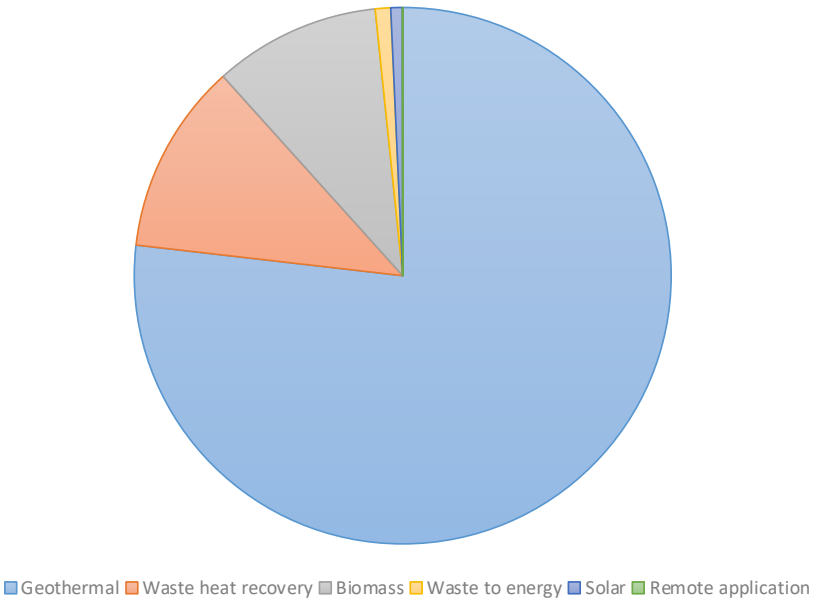

Figure 2.8 *Total installed capacity of the ORC grouped by application [63].*

Figure 2.9 presents the installed capacity (**Figure 2.9 (a)**) and the cumulative installed plants (**Figure 2.9 (b)**) in the period 1975 to 2020 divided by applications and increase between 2016 and 2020. It is worth noting that the trend is firmly increasing and that from the last analysis in 2016 the global ORC market increased by 40 % (+1.18 GW) in terms of installed capacity and 46 % (+851) in terms of installed plants. Actual capacity installed is close to 4.1 GW with more than 2800 installed plants. It is worth to highlight that the installed capacity by year remains relatively low (below 100 MW) until 2008 when it started to rapidly increase by

reaching a maximum value close to 400 MW in 2015 and then stabilizing around 300 MW. Main contribution to the soar of ORC installed capacity is due to geothermal application followed by biomass - especially between 2000 and 2012 - and by waste heat recovery in recent years. Regarding the installed plants, the annual trend is less constant and some peaks appear in the past represented by the installation of a large number of remote units (micro-scale, about 1 kW), while a quick growth is achieved in last two years thanks to small-scale waste heat recovery installations. Current cumulative ORC installed plants is dominated by waste heat recovery 34.5%, and remote 32.3% applications followed by biomass 16.2 %, and geothermal application 15.3 %. Solar and waste-to-energy have a small number of plants equal to 1% and 0.7% of the overall market, respectively.

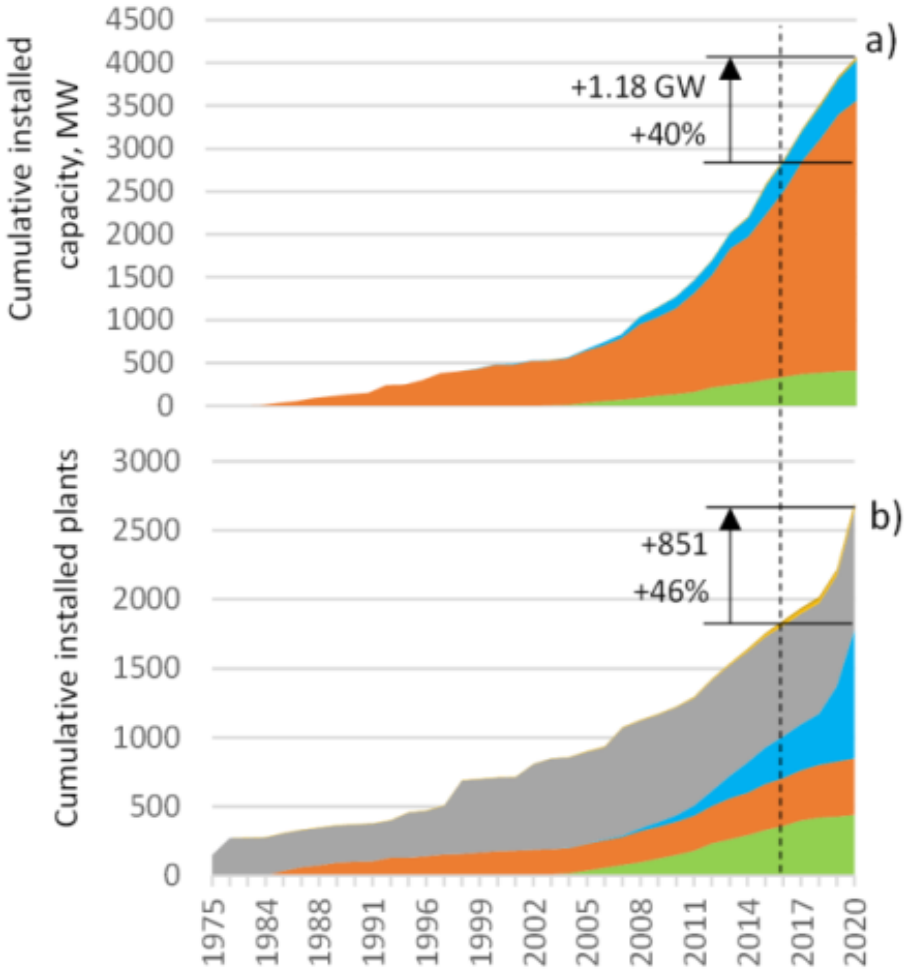

Figure 2.9 *Historical trend of cumulated ORC installed capacity (a) and installed plants (b) divided by applications and increase between 2016 and 2020 [63].*

Figure 2.10 depicts the market increase in 2016-2020 divided by applications in terms of installed capacity **(a)** and plants **(b).** The highest increase in terms of capacity is due to geothermal applications (+970 MW, +45%) while a minor contribution in terms of capacity is due to waste heat recovery, biomass and waste to energy. The latter three fields of applications also show good relative increases between 20% and 36%. Finally, solar capacity has doubled during the last four years but still has a nearly negligible contribution to the overall ORC world market. Regarding installed plants (**Figure 2.10 (b)**) in the last four years, the largest share is

due to waste heat recovery, which increases its installations by 628 plants (+207%), while the other applications increase their units by (9 - 25%).

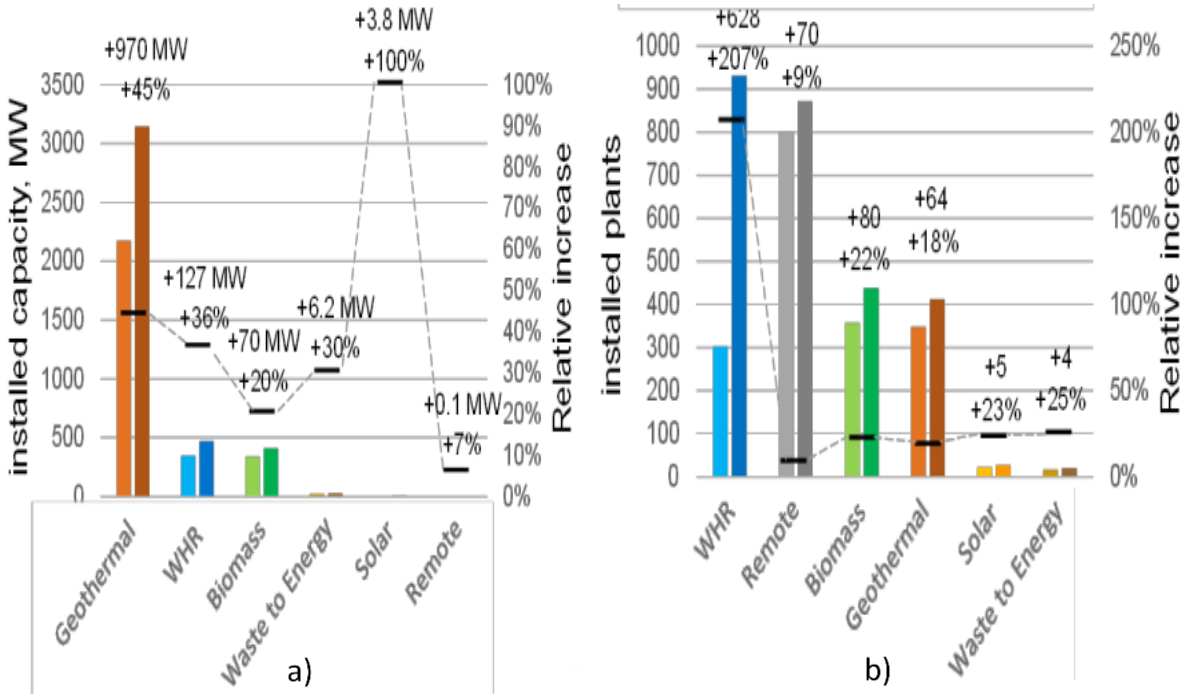

Figure 2.10 *Market increase in 2016-2020 divided by applications in terms of installed capacity (a) and plants (b)* [63].

2.4. Organic Rankine Cycle main components

The ORC systems utilizing low temperature heat resources tend to have a low and limited system efficiency [51,62]. The ORC is made mainly by four classes of components: the heat exchangers, the expander, the pump, and the generator unit. The selection of the expander is an important decision because it is a critical component in a relatively efficient and cost-effective ORC system [80]. Moreover, the total cost of heat exchangers dominates the total power plant investment cost in an ORC system [48]. Hence, the right selection of the turbines and the heat exchangers are very important factors to obtain the optimum ORC design. Beside them, many other components are usually required for a safe and stable operation of the system and for its control. A short list of the components usually present on ORCs is presented in this section.

2.4.1. Heat exchangers

The heat exchanger classification depends on several factors: transfer process, number of fluids, surface compactness, construction, flow arrangements and heat transfer mechanisms [81] to meet the different fluid properties and operating requirements. They are divided into four classes: tubular, plate, extended surface and regenerative. There are three common heat exchanger types used in the ORC system, namely the shell and tube heat exchanger, the plate heat exchanger, and the air-cooled condenser. Large-scale ORC systems typically use shell and tube heat exchangers and the small-scale systems use plate heat exchangers due to their compactness [62,82]. **Table 2-1** provides brief summaries of the main criteria for preliminary selection of heat exchanger types [83]. The main factor of initial selection of the type of heat-

transfer equipment is recommended based on economics considering the same thermal and hydraulic requirement among the available types of the heat exchangers [83]. In addition, maintenance, safety, health, and environmental protection should also be considered during selection to ensure that there are no serious problems due to these aspects.

Table 2-1 *Criteria for the preliminary selection of the appropriate heat exchanger type [83].*

Exchanger type	Maximum pressure range (Mpa)	Temperature range (°C)	Normal area range (m^2)	Fluid Limitations	Key features
Shell-and-tube	30	-200-600+	2-1000	Materials of construction	Very adaptable, many types
Gasketed plate	0.1-2.5	-25-175	1-2500	Limited to Gasket material, avoid gas flow	Modular construction, minimal area cost
Air-cooled	Variable in tube side	Variable in tube side	6-20,000	Materials of construction	Use for heat rejection, standardized design

The principal advantages of plate heat exchangers are minimal risk of internal leakage, compact design, efficient heat transfer, inexpensive materials, ease of control over pressure drops and ease of maintenance [84] as well as availability in a small scale. A small scale of ORC plants [62,82,85,86] use the plate heat exchanger, because the plate type is available with more competitive prices in the markets than shell and tube type. The shell and tube exchanger is the most widely employed type of heat exchanger in the process industry for at least 60% of all heat exchangers used today [83]. Many ORC power plants utilize shell-tube heat exchangers because these types provide relatively large ratios of heat transfer area to volume and weight and are easy to clean. They offer great flexibility to meet almost any service requirement and can be designed for high pressures relative to the environment and high pressure differences between fluid streams [84]. Several studies of ORC plants use these types in their systems [87,88]. In case of lack of cooling water supply at an ORC plant site, an air-cooled condenser is the solution. Air is used to cool and condense liquid streams in finned fan heat exchangers. The tubes are arranged in banks, with the air being pushed through the tubes in a cross flow by fans. Thus, no shell is needed, fouling on the outside of the tubes does not occur. However, the cost of the air-cooled condenser is very high, because the exchanger type requires the largest area of condenser options. This is due to the fact that air has significantly less favourable heat transfer properties than water, such as water has over 4 times higher specific heat ($Cp_{, water}$ =4.19 kJ/kg°C and $Cp_{, air}$ =1.0 kJ/kg°C) and water is 830 times denser than air (the density of water and air at 15 °C is 999 kg/m^3 and 1.2 kg/m^3).

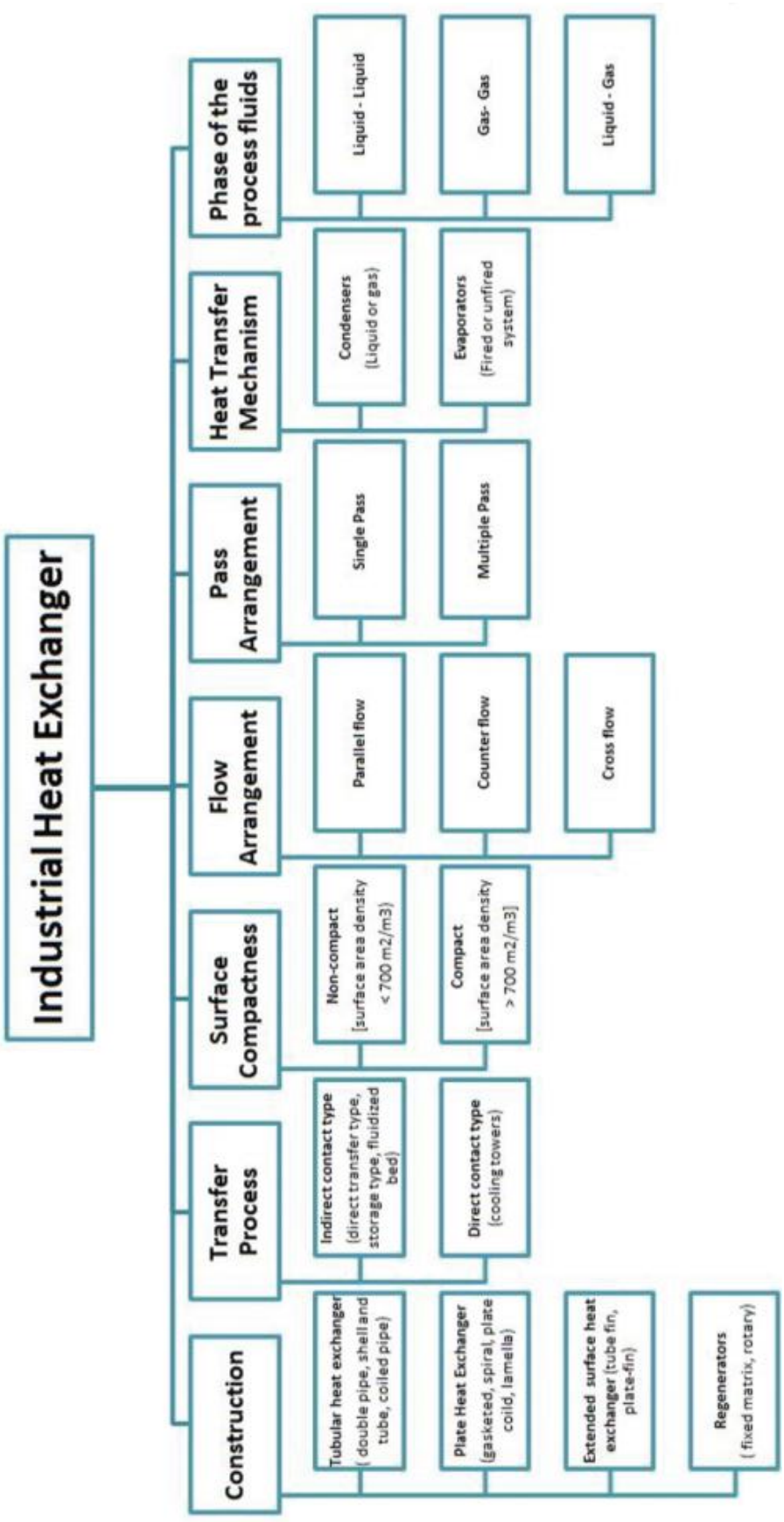

Figure 2.11 *Classification of heat exchanger [89].*

Typically, for high-temperature sources, complex working fluids are used that involve small temperature drops along the expansion path and significant thermal energy available at turbine discharge. A recuperative preheating of the pumped liquid is important to achieve high efficiencies, resulting in limited temperature differences in the evaporator and reducing heat release to the environment. The Recuperator is commonly formed by a finned tube heat exchanger to improve the film transfer coefficient on the tube external side, where vapour flows. Recuperators are realized by several liquid circuits arranged in different staggered rows that form a tube bank. The tubes are finned with continuous plates, the organic liquid flows perpendicular to the vapour and multi-passage paths are usually adopted. The fins are always made of copper unless for aggressive fluids like ammonia, while the material of the tubes depends on the operating temperature. For temperatures below 200°C, the tubes are made of copper while 90/10 cupronickel is used for higher temperatures. The recuperator is placed after the turbine diffuser to reduce the pressure drop in the piping between the two components.

2.4.2. Expansion machines

Performance of the ORC system strongly correlates with that of the expander. The selection of the machine is based on the operating conditions and on the size of the system. Expanders, in general, can be categorized into two types: one is the velocity type, such as axial turbine expanders; the other is the volume type, such as screw expanders, scroll expanders and reciprocal piston expanders [90]. Similarly to refrigeration applications, the volume type machines are more appropriate to the small-scale ORC units, because they are characterized by lower flow rates, higher pressure ratios and much lower rotational speeds than velocity types [91]. According to Chys et al. [92] expanders are classified based on power range: micro system (0.5 - 10 kWe), small system (10 - 100kWe), medium system (100 – 300 kWe) and large systems (300 kWe - 3 MWe).

2.4.2.1. Turbines

Turbomachinery consists of a series of stages, each one consisting of a stator and a rotor. In the stator, the fluid accelerates in converging static channels. Then it enters the rotor where it will possibly further expanded and deflected exchanging momentum with the turbine blades. Rotor disks are connected to the turbine shaft. Based on the relative motion of the fluid with respect to the shaft, turbines can be classified into: axial flow, radial inflow. Turbomachines are appropriate for medium/large power plants and their typical power output range is between 100 kW and 15 MW. Axial turbines for power output higher than 0.5 MW are the most common choice in the ORC field [48].

2.4.2.2. Volumetric expanders

If the power output is less than 100 kW, designing an efficient turbomachine is quite difficult and the use of positive displacement devices may be advantageous. In these machines, pockets of fluid are trapped during rotation, expanded and then discharged. The major types of volumetric expanders are the piston, the scroll, the screw and the vane expanders. These components are cost-effective because they are derived from the refrigerant compressor market and can benefit by large scale economies. Furthermore, they can expand a two-phase fluid with less corrosion issues compared to a turbomachine. The main limitation of these devices is the

difficulty of achieving multiple stage expansion and low efficiency in the presence of a high volume ratio. Both effects restrict the maximum evaporation temperature of the cycle, especially if a highly critical temperature fluid is used.

Quoilin et al. [93] proposed a selection guidance based on allowed power range for each application (low and high temperature waste heat recovery, low temperature solar plant, high temperature combined heat and power) and each type of expansion machine in **Figure 2.12**. The comparison of various types of expanders suitable for ORC system is shown in **Table 2-2**.

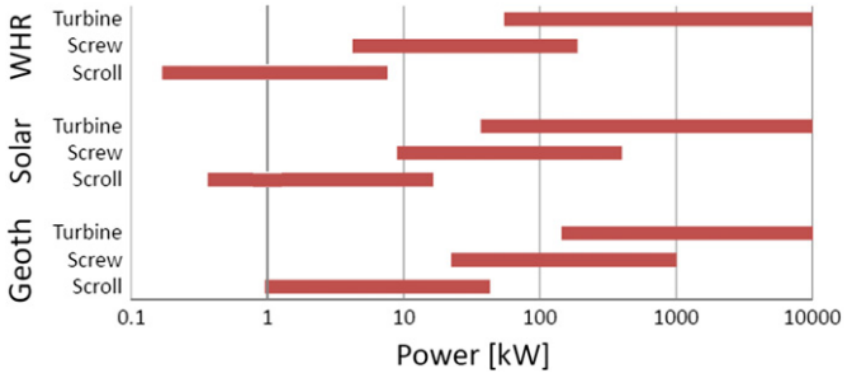

Figure 2.12 *power range for the low temperature applications and each type of expansion machine [62].*

Table 2-2 *Comparison of various types of expanders suitable for ORC system [80].*

Type	**Capacity range (kW)**	**Cost**	**Advantages**	**Disadvantages**
Radial-inflow turbine	50–500	High	Light weight, mature manufacturability and high efficiency	High cost, low efficiency in off-design conditions and cannot bear two-phase
Scroll expander	1–10	Low	High efficiency, simple manufacture, light weight, low rotate speed and tolerable two-phase	Low Capacity, lubrication and modification requirement
Screw expander	15–200	Medium	Tolerable two-phase, low rotate speed and high efficiency in off-design conditions	Lubrication requirement, difficult manufacture and seal
Reciprocating piston expander	20–100	Medium	High pressure radio, mature manufacturability, adaptable in variable working condition and tolerable two-phase	Many movement parts, heavy weight, have valves and torque impulse
Rotary vane expander	1–10	Low	Tolerable two-phase, torque stable, simple structure, low cost and noise	Lubrication requirement and low capacity

2.4.3. Pump

Pumps are generally divided into two large categories: kinetic (including centrifugal and peripheral) and positive displacement (including reciprocating and rotary). For positive displacement pumps, the flow rate is approximately proportional to the rotational speed, while for centrifugal pumps, it also depends on the pressure difference between the evaporating and condensing pressures. ORC pumps are generally multistage variable speed centrifugal pumps

and their design is relatively simple due to the extensive knowledge and use of this component in the power generation, chemical and refining industries. Depending on the cycle configuration, fluid selection and cycle design parameters, the pump may show a consumption that represents a relevant part of the total turbine power output (up to 20-30% for supercritical cycles with high critical pressure fluids) [48]. In this case, the pump efficiency is an important parameter and the component must be carefully designed to achieve a higher cycle efficiency.

2.4.4. Generators, gear boxes

The generator converts mechanical energy into electricity; it normally rotates at the grid frequency and is directly connected to the expander. However, in the ORC field, the variety of working fluids and applications results in expanders having very different optimal rotation speeds. Large plants typically require slow machines while small ORCs require super-fast radial flow turbines. Alternatively, a gearbox can be used between the turbine shaft and the generator shaft. The same component can be used for applications requiring a fast turbine, but above certain gear ratio, the use of a gearbox is not suitable due to the high mechanical losses.

2.5. Cycle configuration

In the ORC field, only a few plant layouts are used on the market while other configurations are proposed in the scientific literature for specific applications. ORC cycles can be divided into two major categories, which are single pressure level cycles and multi-pressure levels cycles; single pressure level cycles can be further divided into subcritical and supercritical (or trans-critical) cycles, while only subcritical configurations are adopted for multi-pressure levels cycles. Besides these two main groups, two other cycles are the triangular cycle and the complete flash cycle.

2.5.1. One pressure level cycles

It is the simplest plant layout and it has the minimum number of components: a pump, a turbine, a condenser and an evaporator. Depending on the size of the plant, the configuration, and the working fluid, the heat exchanger (evaporator) can be formed by a single once through heat exchanger or by different units. In particular, if the cycle is a supercritical one or if a mixture of fluid is used, the once-through heat exchanger is the only option; conversely, for big subcritical power plants a physical division in economizer, evaporator, and possibly super-heater is usually adopted. Because of its simplicity and good efficiencies, make this type of cycles the first option for many different applications. This configuration is divided into two families according to the same plant layout, namely subcritical and supercritical cycles.

2.5.1.1. Subcritical cycles

A subcritical cycle has a maximum pressure that is lower than the critical one. In the literature, this type of ORC cycle is called basic or simple ORC. The improvement scheme of the ORC considered in this study uses the concept of process integration of the basic ORC with an internal heat exchanger (IHE), reheating and regeneration; which have been used in the traditional steam power plants.

When the expander expansion process terminates in superheated region, the integration of an IHE at the exhaust of the expander might be beneficial for preheating the working fluid

before it enters the evaporator. The integration of an IHE, which extracts the remaining latent heat at the expander's exhaust would reduce the heat exchanger and condenser loads, and as well improve performances. **Figure 2.13** depicts the schematic diagram and the *T–s* diagram of the ORC with IHE. It comprises five key components, which are the feed pump, evaporator, expander, IHE and condenser. The latent heat extracted from the superheated vapour–liquid at the expander outlet by the IHE is used to preheat the sub-cooled liquid at the feed pump outlet (state 2 - 3). Afterward, the fluid is heated to its saturated temperature (state 3 - 4) by a heating medium in the heat exchanger at constant pressure and is being injected into the expander (state 4 - 5), where shaft work is produced. Subsequently, the latent heat of the resulting vapour–liquid content is being bled (state 5) and condensed (state 6 - 1) by a cooling medium in the condenser to start the new cycle.

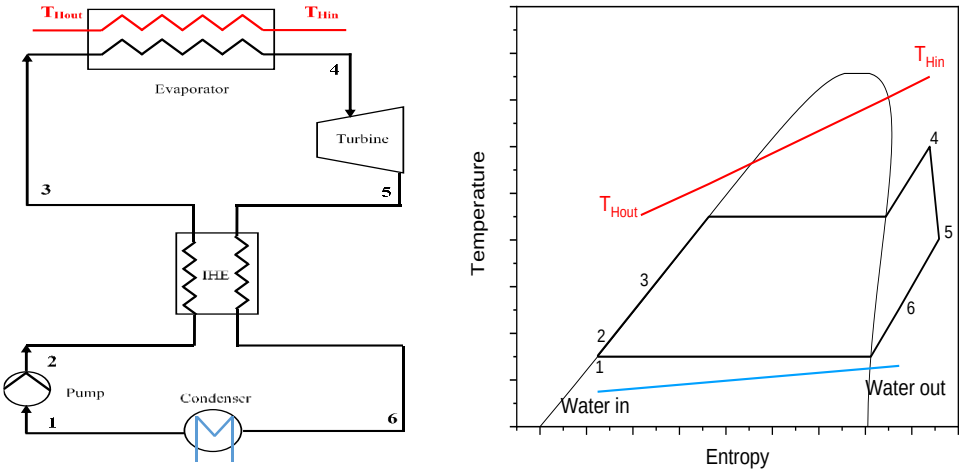

Figure 2.13 *Schematic and T-s diagrams of ORC with IHE (ORC-IHE).*

The reheating is a technique used to increase the expansion work of a thermodynamic cycle or process. The expansion process is completed in stages while the reheating of the working fluid is in between these stages. Generally, it is admitted that increasing the boiler pressure in a simple Rankine cycle using a wetting fluid such as steam increases the efficiency of the power plant. Once the working fluid used in an ORC is a wet fluid for instance water, a reheating would be required to improve fluid dryness because it becomes saturated after an enthalpy drop in the expansion machine while the fluid droplets impingements on the blades of the expansion machine during expansion pose a threat of damage. Thus, to improve fluid dryness, the expansion process is divided into two, and a reheating is introduced between both expansion stages. The reheat ORC is a modification of the simple ORC, in which the working fluid is expanded in the expander in two stages and reheated in between. **Figure 2.14** depicts the schematic cycle configuration of the reheat ORC. It comprises five key components, which are feed pump, heater, high pressure (HP) turbine, low pressure (LP) turbine and condenser. Like the simple ORC, the high pressure saturated fluid is first expanded in the HP expander (state 5 - 6) and the medium pressure fluid is then returned to the heater where it is reheated to its saturated temperature (state 6 - 7) by a heating medium. Afterwards, the medium pressure saturated fluid is expanded in the LP expander (state 7 - 8); where shaft work is produced, with

the resulting vapour–liquid content then condensed (state 8 - 1) by a cooling medium in the condenser to start the new cycle.

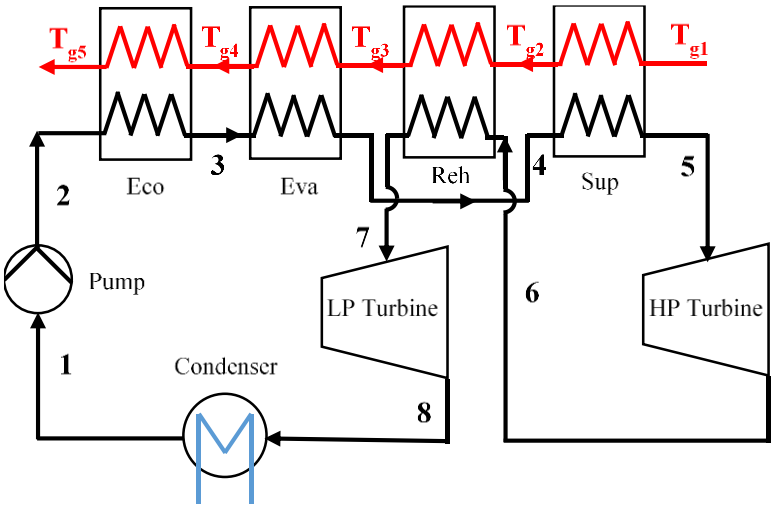

Figure 2.14 *Schematic diagram of reheat ORC.*

The regeneration is the process of transferring energy within a cycle from a working fluid at high temperature in part of the cycle to a lower temperature in another part of the cycle to reduce the amount of external heat transfer that is required to power the cycle. This technique is used to raise the temperature of the liquid leaving the pump (by the latent heat of the feed fluid) before it is heated by the heating medium in the heat exchanger. For instance, in steam power plants, 'extracting' or 'bleeding' steam at different points from the turbine is performed to attain a practical regeneration process. This steam, which could have produced more work by expanding further in the expansion machine, is used to preheat the feed water instead [94]. The regenerative ORC is a modification of the simple ORC, which is accomplished by 'extracting' or 'bleeding' vapour from the expander. **Figure 2.15** presents the schematic cycle configuration of the regenerative ORC and the *T*–*s* diagram of its thermodynamic process. It illustrates the system working principle with a bleed point for preheating the working fluid in an open feed fluid-heater. A fraction of the vapour flow rate is bled (point 6) at the intermediate pressure between the heating and the condensing pressure, which is directed to the heat exchanger to preheat the pressurized feed fluid. The working fluid is pressurized with the condensate pump (state 1 – 2), then preheated in the feed fluid-heater (state 2 – 3) and is being pressurized to a high pressure with the feed pump (state 3 – 4). The high pressure fluid is heated (state 4 - 5) by a heating medium in the heat exchanger and injected into the expander (state 5 – 7); where it is expanded, with the resulting vapour–liquid content being bled (point 6) for the preheating of the working fluid (at point 2) and condensed (state 7 - 1) by a cooling medium in the condenser to start the new cycle.

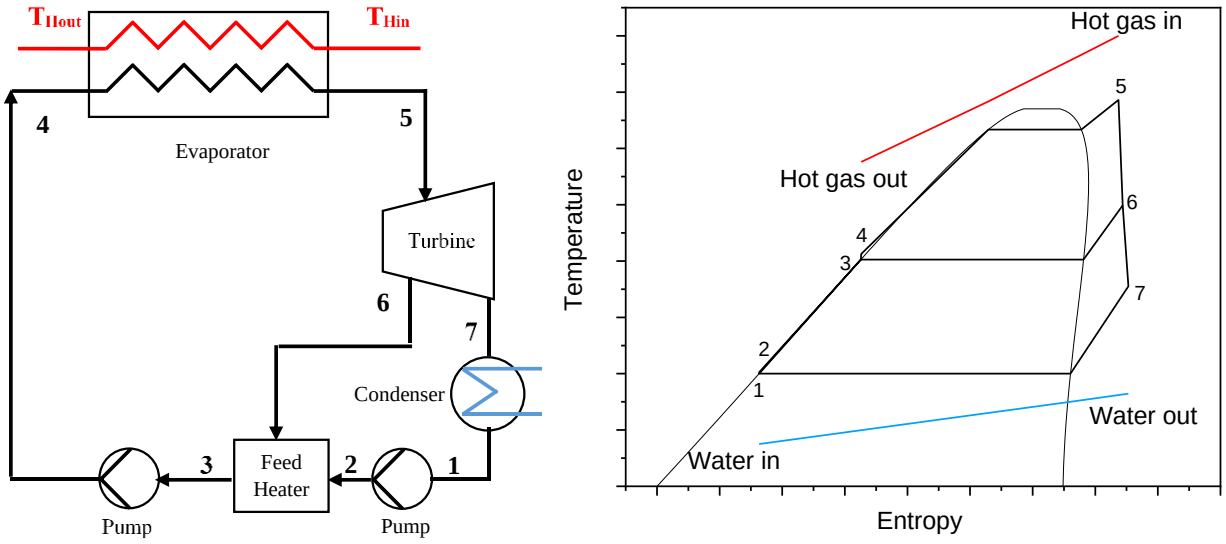

Figure 2.15 Schematic and T-s diagrams of regenerative ORC.

2.5.1.2. Supercritical cycles

A supercritical cycle is a cycle with a maximum pressure higher than the critical one. In the literature, this configuration is called supercritical cycle [95–98] or transcritical [99–101]. Working fluid is heated up from a subcooled liquid region to superheated vapour with a smooth transition above the critical point. There is no phase change and all the physical and thermodynamic properties vary without discontinuity in the heat introduction process. The supercritical ORC can lead to higher efficiency mainly for low critical temperature fluids for medium and high temperatures of the heat input [95,102]. The proper selection of the working fluid and operating parameters lead to a heating curve that matches the temperature variable heat source well, thus reducing the overall logarithmic temperature difference and the efficiency losses caused by the heat input with limited temperature differences. However, this configuration of the ORC also presents some challenges to overcome. However, some disadvantages of the supercritical process have to be considered such as operation at high pressure compared to the subcritical cycles, safety concern and expensive investment cost due to special materials of the system. Moreover, an experimental study conducted in investigating the performance of ORC using low-temperature heat resources under (<100 C°). The authors concluded that supercritical operation was difficult to be achieved [103].

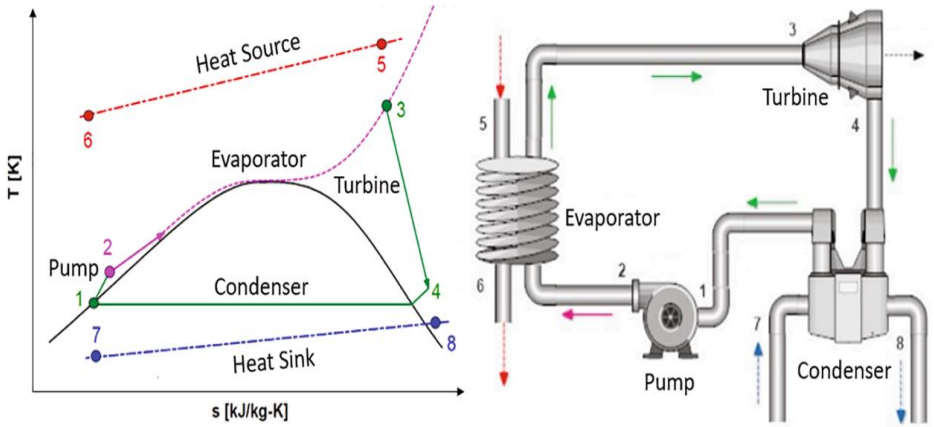

Figure 2.16 Schematic and T-s diagrams of supercritical ORC [104].

Figure 2.16 shows a schematic of the cycle and the *T-s* diagram of the system. The organic fluid exiting the condenser is pumped above its critical pressure and then heated in the evaporator to the turbine inlet temperature by the heat source. The supercritical organic fluid is then expanded in the turbine to the condenser pressure, generating power before entering the condenser to be condensed back to the saturated liquid state.

2.5.2. Two pressure levels cycles

Having a multi-pressure heater in an ORC can improve the performance of the cycle by achieving a smaller average temperature difference between the two fluids, thus reducing the thermodynamic losses in the heat exchangers [105]. This kind of cycle can achieve higher efficiency compared to subcritical one level cycle and performances similar to the supercritical ones. The adoption of two pressures of evaporation allows following better the variable temperature heat source but it requires more expensive equipment: including a second set of heat exchangers, pump, and turbine and a more complicated plant layout. **Figure 2.17** presents the schematic cycle configuration of the dual pressure ORC and the *T–s* diagram of its thermodynamic process. The working fluid is condensed into a saturated liquid in the condenser, and then it is divided into two parts after pressurization by a low-pressure pump. One part goes into the Low Temperature Evaporator (LTE), and the other part goes into the High Temperature Evaporator (HTE) after pressurization by a high-pressure pump. The working fluid evaporated in the HTE enters the high pressure turbine to expand. The working fluid evaporated in the LTE is mixed with the high pressure turbine exhaust, and the mixed working fluid enters the low pressure turbine to expand. Finally, the working fluid at the outlet of the low pressure turbine enters the condenser to be condensed back to the saturated liquid state.

An example of applications where two or more pressure level cycles might be profitable is deep geothermal reservoirs with high exploration and drilling costs, and industrial waste heat recovery from plants like cement and steel production industries. An example of the comparison between one level and two pressure level cycle for geothermal application is reported in reference [106]. A two-pressure levels cycle in the most general configuration can be superheated on both evaporation levels and it can present an IHE on both levels. Finally, turbines can be arranged in series or in parallel depending on the two temperatures of evaporation and the mass flow ratio between high and low pressure streams.

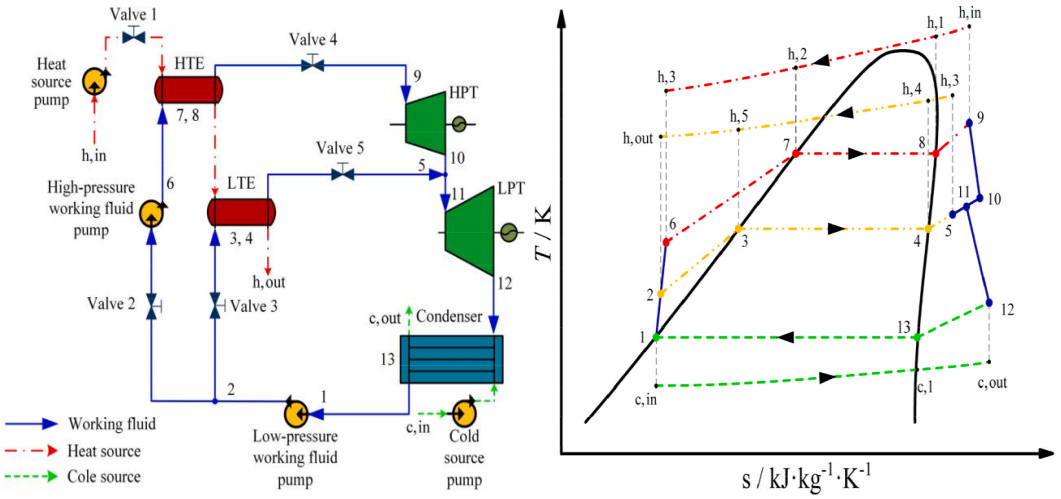

Figure 2.17 Schematic and T-s diagrams of dual pressure ORC [107].

2.5.3. Trilateral cycles

The trilateral cycle system is basically a power plant in which expansion starts from the saturated liquid rather than the saturated, superheated or supercritical vapour phase. In such a configuration, the transfer of heat from a heat source stream to the working fluid is achieved with a high degree of temperature matching [108]. Theoretically, the trilateral cycle has a lot of advantages in term of the efficiency and simplicity in configuration, which has made it become a subject of novel research. Moreover, the heat transfer without pinch-point limitation, there are thermal matching between the exergy of the temperature profiles of the heat source and the working fluids. However, the main challenge for the successful implementation of this configuration concerns the design of two-phase expanders with good isentropic efficiency, which must be higher than 75% [109].

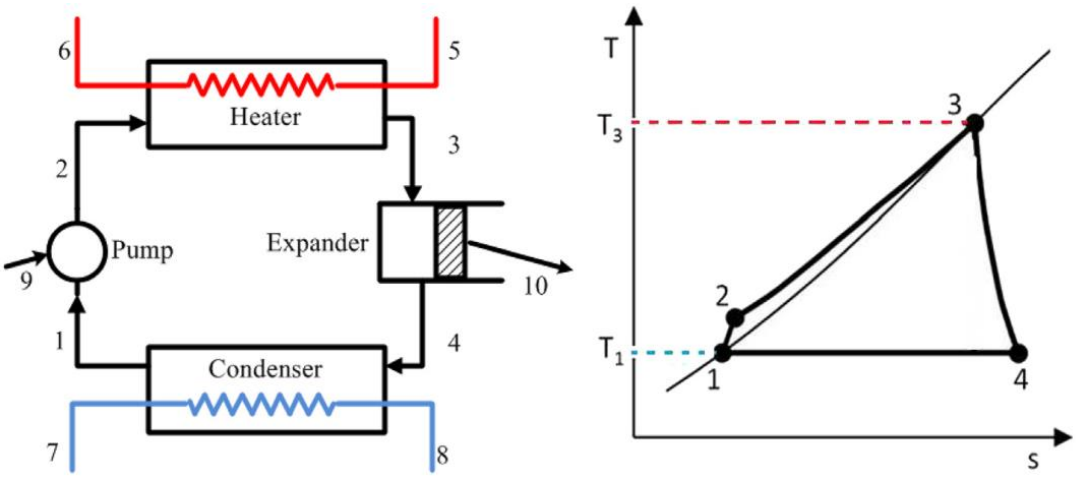

Figure 2.18 Schematic and T-s diagram for trilateral cycle [108].

The schematic and *T-S* diagram of trilateral cycle system are depicted in **figure 2.18.** The trilateral cycle system consists of a heat exchanger, a condenser, a pump and a two-phase expander. The working fluid is first pumped from the low pressure to the high pressure by the pump. The working fluid is then heated to the boiling point by absorbing heat from the hot source in the heat exchanger. At saturated liquid, the working fluid directly enters the two-

phase expander to deliver work. The resulted vapour-liquid mixture is then fully condensed in the condenser.

2.5.4. Organic Flash Cycle

For trilateral cycles, there are some transformations and organic flash cycle is one of the most important system, which can potentially replace the two-phase expander required in trilateral cycle and therefore reduce the capital cost of the system. Flash cycles have been traditionally implemented in geothermal direct steam plants. Heat is transferred to the ORC until the working fluid reaches a saturated liquid state. In the heat exchanger, boiling of the working fluid is avoided, resulting in a better match between the temperature profiles of the heat carrier and the working fluid. The fluid would then be flash evaporated to produce a two-phase mixture, and the saturated vapour would be separated and then expanded to produce power. The liquid phase is directly returned to the condenser. In order to increase the mass flow rate of vapour, several flash tanks can be connected in series. A schematic of the organic flash cycle configuration and its *T-S* diagram are shown in **figure 2.19.**

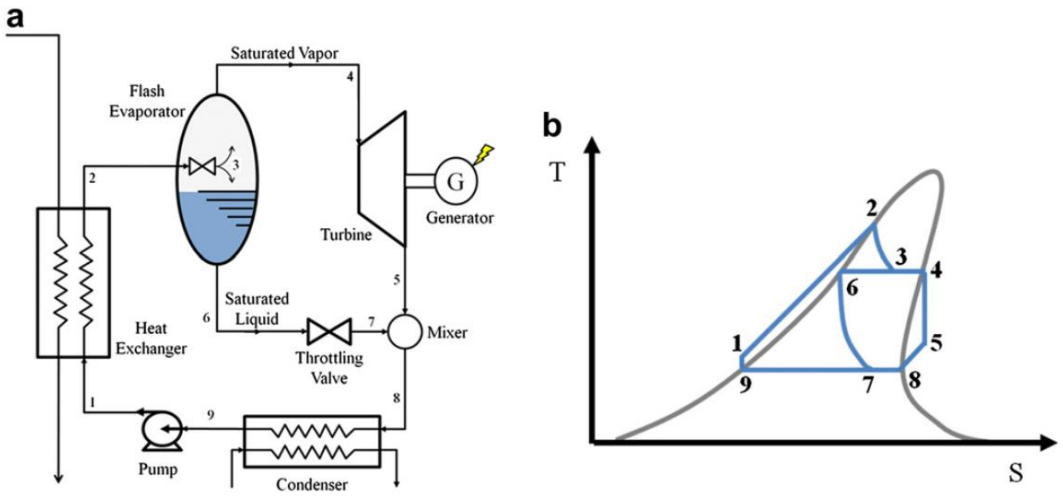

Figure 2.19 *Schematic and T-s diagram for Organic Flash Cycle [110].*

2.6. Working fluid

For the design of the ORC cycle, one of the most important steps is the identification of the appropriate working fluid as the thermo-physical properties of the working fluids strongly influence the efficiency of the system, the sizes of the system components, the design of expansion machine, the system stability and safety and environmental concerns [111–113]. For the Rankine cycle in general and the steam cycle in particular, water is a perfect working fluid with good properties, i.e. it is abundant, cheap, chemically stable, thermally stable, non-toxic, non-flammable; it has low viscosity, zero ODP, zero GWP. However, this fluid cannot be economically used for electricity generation from a low temperature heat source due to the relatively high phase change temperature (100°C) at atmospheric pressure. In addition, the use of water as a working fluid also has some disadvantages: Need for high superheat to avoid condensation of the fluid during the expansion stage of the Rankine cycle and complex and expensive turbines.

Various kinds of substances can be used as working fluids in Rankine cycles [19,40]. The working fluids in the ORC system can be classified into several categories depending on the classification method. Below are summarized main families of potential fluids for ORCs.

- Alcohols: methanol, ethanol.
- Inorganic fluids: Water (R718), Carbon dioxide (R744) and Ammonia (R717).
- Hydrocarbons (HCs): natural flammable substances able to react with halogens: Propane (R290), Propyne, Isobutane (R600a), Isopentane (R601a), Benzene, etc.
- Perfluorocarbons (PFCs): fully fluorinated HCs. e.g. R116, R218.
- Chlorofluorocarbons (CFCs): all hydrogen atoms in a hydrocarbon molecule are replaced with chlorine, fluorine or bromine. e.g. R12, R113, R115.
- Hydrofluorocarbons (HFCs): partially halogenated and chlorine free HCs. e.g. R134a, R152a, R236ea.
- Hydrochlorofluorocarbons (HCFCs): partially halogenated hydrocarbons. e.g. R22, R141b.
- Ethers and Hydrofluoroethers (HFEs): e.g. HFE7000, RE170, HFE7100.
- Siloxanes, e.g. Octamethyltrisiloxane (MDM), Hexamethyldisiloxane (MM), Octamethylcyclotetrasiloxane (D4).
- Mixtures:

Azeotropic mixtures: mixtures of two or more compounds possess the same equilibrium vapour and liquid phase compositions at a given pressure. e.g. R500, R502.

Zeotropic mixtures: mixtures of two or more compounds that change volumetric composition and saturation temperature as they boil. e.g. R404, R407.

The working fluids could be categorized according to the saturation vapour curve in the temperature-entropy *T-s* diagram, which is one of the most crucial characteristics of the working fluids in an ORC. This characteristic affects the fluid applicability, cycle efficiency, and arrangement of associated equipment in a power generation system. Based on the slope of the vapour saturation curve on the *T-s* diagram, there are three kinds of working fluids: dry, isentropic and wet fluids, see **Figure 2.20**. A dry fluid with positive slopes, a wet fluid with negative slopes, and an isentropic fluid with nearly infinitely large slopes. Wet fluids need to be superheated before flowing into the turbine. If the fluid comes to the turbine as a saturated vapour, it drops under the dome region after expansion, which can cause degradation of the turbine blades. Typically, the minimum dryness fraction at the outlet of a turbine is kept above 95% [114]. Despite the fact that the superheat can help to improve the system efficiency, it is considered a drawback due to the low heat exchange coefficients that lead to large and expensive exchangers [111]. On the other hand, the isentropic and dry fluids do not need superheat, and as a result, turbine degradation can be avoided. If the fluid is “too dry”, the expanded vapour will leave the turbine with substantial “superheat”, this is considered a waste and increases the cooling load in the condenser [19]. A recuperator is very often used to recover

energy from the superheated steam leaving the turbine to preheat the working fluid before entering the evaporator. This recovery improves the efficiency of the system but also increases the complexity and therefore the capital cost of the system, which exists trade-off. In the work of Hung et al. [41], isentropic fluids are generally considered the best candidates for recovering low-temperature waste heat. In their latter study [115] on the effect of types of the saturation vapour curve for a fluid on system efficiency and irreversibility, the results indicated that wet liquids with steep saturated vapour curves in a *T*-*S* diagram have better overall energy conversion performance efficiency than dry fluids and isentropic fluids.

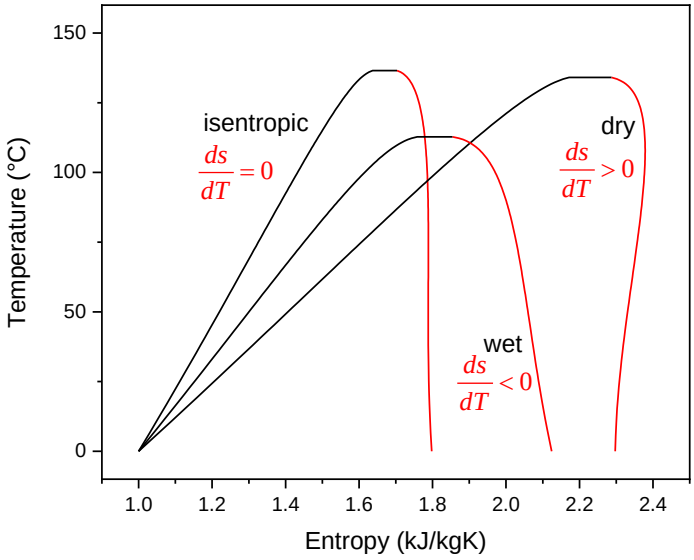

Figure 2.20 *Three types of working fluids: isentropic, wet and dry.*

2.6.1. Criteria and methodology for fluid selection

2.6.1.1. Ideal working fluid

Badr et al. [116] presented an early study on the working fluids selection for an ORC, and discussed the properties that a working fluid should ideally have. It is quickly established that no single working fluid meets all the required criteria, and it is often up to the designer to choose a fluid according to their selection criteria. The desired properties discussed are summarized in the following list. These same selection criteria have been reiterated within a number of more recent research papers [55,62,80].

- The working fluid must result in an optimal thermal cycle efficiency resulting in an optimal conversion of the input heat into power.
- The evaporation pressure should not be excessive, moderate pressure is recommended in order to avoid mechanical stress problems.
- The condensation pressure should be kept above atmospheric pressure to avoid the requirement of operating the condenser under a vacuum. Therefore, for safety and economic reasons, the pressure in the heat exchange units should be kept above one bar for condensers and below 25 bars for evaporators.

- The triple point must be well below the minimum ambient temperature that is desired. This ensures that the fluid does not solidify at all operating points of the system.
- Low viscosity, high latent heat of vaporisation and high thermal conductivity of the working fluid are preferred. These properties ensure that pressure drops across exchangers and auxiliary pipes are low and that the heat exchange rate in exchangers is high.
- A good fluid should have low vapour and low liquid specific volumes. These properties affect heat transfer rates in heat exchangers. The vapour specific volumes relate directly to the size and cost of the expander.
- The slope of the fluids saturated vapour line should be close to vertical.
- The fluid should be non-corrosive.
- The working fluid must be chemically stable at all temperature levels used in the system. The thermal decomposition resistance of the working fluid in the presence of lubricants and container materials is an important criterion.
- Non-toxicity, non-flammability, non-explosiveness and non-radioactivity are also desirable characteristics.
- The fluid should have good lubrication properties.
- Low cost and high availability are desired.

Along with serious environmental problems (e.g. climate change, ozone depletion, etc.), environmental criteria (ODP, GWP) are increasingly cited in the work [40,42,117,118] of the ORC fluid selection. Due to the Montreal and Kyoto protocols, a number of potential working fluids have already been banned, with others set to be phased out. A possible working fluid should therefore have a low environmental impact with a low GWP, a low atmospheric lifetime, and a low ODP. With a large number of design criteria to meet and a large array of possible working fluids available, it is inevitable that a number of researchers have attempted to classify working fluids in a bid to recommend which working fluids would be optimal for particular applications. Tchanche et al. [40] coupled a thermodynamic ORC model with working fluid considerations in order to recommend fluids for a low temperature solar ORC working with a heat source temperature of 90°C. It was concluded that no fluid successfully met all criteria, but R134a was suggested as the most suitable candidate for this application, although R152a, butane and isobutane were also suggested as suitable candidates. Required main characteristics of organic working fluids are illustrated on **Figure 2.21**.

Figure 2.21 *Required main characteristics of organic working fluids [119].*

2.6.1.2. Methodology

In reality, there is no one fluid that satisfies all the criteria of the ideal fluid discussed above. Therefore, a compromise must be adopted for each particular application. As already mentioned in the literature [40,120], the selection of working fluids for the ORC is carried out through several steps. The general procedure for the identification of potential working fluids for the ORC involves the following steps:

1. Data collection (conduct a state of the art survey of working fluids).
2. First selection taking into account the following criteria:
   - Environmental properties of the fluids.
   - Safety/health: flammability, toxicity.
   - Chemical, thermal stability: the stabilities of the fluids at the maximum cycle temperature are important criteria for the selection of working fluids.
   - Cycle operating conditions.
   - Thermo-physical properties from heat source and cold sink temperature level data, type of ORC used (subcritical or supercritical).
   - Availability, compatibility with materials and lubricating oil, and cost.
3. Modelling the system with the pre-selected fluids.
4. Thermo-economic optimization taking into account environmental and economic criteria.
5. Decision and classification.

A comprehensive list of working fluids for waste heat recovery applications, with their classification and properties, is included in appendix 1.

A summary of the most relevant publications about ORC working fluid selection is reported in **Table 2-3**.

Table 2-3 Recommended fluids for different applications, working conditions and performance indicators.

Reference	Application	T_{Hot}	Performance indicators	Recommended fluid
[40]	Solar	90°C	Efficiencies, volume flow rate, mass flow rate, pressure ratio, toxicity, flammability, ODP and GWP	R134a
[118]	Combined heat and power	-	Thermodynamic performance of the cycle	Ethanol, R123 and R141b
[54]	Geothermal	90°C	Power output per unit mass flow rate of hot source Total heat transfer area to net power output Electricity production cost	R236ea, E170, R600, R141b
[56]	Geothermal	90°C	Thermal efficiency and exergy efficiency High recovery efficiency Heat exchanger area per unit power output levelized energy cost	R123, R218, R152a
[121]	Waste heat recovery	150°C	Maximum net power output, suitable working pressure, total heat transfer capacity and expander size parameter	-R114, R245fa, R123, R601a, n-pentane, R141b and R113
[122]	Waste heat recovery	147°C	Exergy efficiency	R11, R141b
[123]	Waste heat recovery	120°C	Exergy efficiency	R600a
[124]	Geothermal	110°C 130°C 150°C	work output per unit mass of geothermal hot brine	R32, R134a and propylene
[125]	Geothermal	120-180°C	Exergy efficiency	R143a, RC318 and R236ea
[126]	Waste heat recovery	170°C	Net power output	R1234yf
[127]	Geothermal	160°C	Exergy efficiency, Specific Investment Cost, Net Power Output	R245fa
[128]	Geothermal	150°C	Exergy efficiency, Cost per net output power	R141b
[129]	-	90°C 120°C 150°C	Net power output	R1234yf, R1234ze(e), Isobutene
[130]	Waste heat recovery	150°C	Exergy efficiency and system total cost per unit net power output	R245ca, R365mfc

2.7. Organic Rankine Cycles optimization

The main challenge in designing an ORC is the large number of possible combinations of variables: the number of possible working fluids, even if only pure liquids and not mixtures are considered, is more than 50 and the number of cycle configurations is not negligible too. At this stage, the characteristics of the heat source and heat sink, the size of the plant, and the expected performance must be considered, along with any other technical limitations, in order to exclude certain working fluids, cycle configurations, or to set certain design parameters to reduce the computational time needed to make the optimization procedure. For example, maximum cycle pressure or the need to avoid condenser vacuum may influence the choice of cycle configuration by limiting the investigation to certain plant configurations or working fluids. In other applications, such as automotive engine exhaust heat recovery, a lightweight installation and small occupied volume requiring simple installation layouts with a limited number of components are required. Remote applications, such as small solar power plants in a rural setting require simplicity, reliability and low maintenance costs. At the end of this step, a number of favourable working fluids and plant layouts to exploit a given heat source are pre-selected. The search for their optimal combination is carried out in the next step.

For each combination of working fluids and cycle configuration, a plant optimization must be performed to determine the best ORC system according to a certain objective function. For the general system, many cycle parameters must be specified and most of them must be optimized to maximize or minimize the selected parameter. The objective function varies depending on the application and the plant requirements. Typically, two specific types of optimization are performed:

Thermodynamic optimization: It is performed with the aim of maximizing power production. The efficiency of the cycle is maximized and reliable limits must be assumed in the pinch points temperature differences in the heat exchangers.

Techno-economic optimization: The objective is to minimize the electricity production cost or the specific cost of a plant calculated as a ratio of total cost to the nominal power production. In this optimization, a greater number of design variables are generally considered with a simplified design of the main components.

The optimization design variables of the system are, for example, the evaporation and the condensation temperatures, the superheat degree and pinch point temperature differences (PPTD) in the heat exchangers. Each parameter of them has a different effect and weight on the final solution, but in certain cases some of them can be assumed to be constant because their effect on the objective function is univocal. An example is a pure thermodynamic analysis of an ORC system where there is no need to optimize the PPTDs in the heat exchangers: in fact, the decrease of the PPTDs always allows a reduction of the entropy production in the heat transfer with a positive effect on net power production. Optimizing these variables in thermodynamic optimization implies pushing them to lower bound leading to extreme heat exchanger surfaces and a less reliable solution. In a techno-economic optimization instead variation of the PPTDs results in two contrasting effects on the electricity production cost and the optimal value for these variables is the result of a trade-off between an increasing of power production and increased equipment cost resulting from the larger heat transfer surfaces.

2.8.Conclusion

This chapter aims to introduce the operating principle of the ORC. The ORC is almost similar to that of a steam cycle, and similarly, the concept has been applied in real actual power systems with incredible growth in technological development. The main reason for the success of ORC power systems is their great flexibility. It is a technology that can be employed to convert external sources of thermal energy at very different temperature levels and over a wide range of capacities. This characteristic ranks ORC systems at the forefront of technologies suitable for renewable of renewable-equivalent thermal energy conversion (geothermal energy, biomass combustion, solar, industrial waste heat recovery, waste heat recovery from reciprocating engines and gas turbines, OTEC). A brief history of ORC systems was presented, citing important events in the development of this type of thermodynamic cycle. The scientific knowledge of several potential ORC configurations was discussed. The cumulative global capacity of ORC power systems for the conversion of renewable and waste thermal energy is undergoing a rapid growth, which started a decade ago, in accordance with recent developments in the energy conversion scenario. Currently, the subcritical ORC is the most widely used configuration due to its simplicity, safety and stability of operation. Despite the

large number of working fluid studies for ORC applications, their conclusions do not lead to one single optimal fluid for a given temperature level and a given application. This is mainly due to the diversity of the selected objective functions when screening working fluids. **Table 2-4** provided the proposed terminology for properties that can be used to classify ORC power plants.

Table 2-4 *Proposed terminology for properties that can be used to classify ORC power plants*

Maximal cycle temperature (°C)	**Power capacity**
High >250	Micro <3kW
Medium 150–250	Mini 3–50 kW
Low <150	Small 50–500 kW
	Medium 0.5–5 MW
	Large >5MW
Working fluid class	**Thermal energy source**
Hydrocarbons: Alkanes, aromatics, alcohols	Geothermal (Pressurized) water, steam
Fluorocarbons: Perfluorocarbons, hydrofluorocarbons	Biomass (solid or biogas) Combustion
Siloxanes: Cyclic, linear	Solar radiation Parabolic trough, fresnel
Carbon dioxide	Industrial heat Process cooling, flares, landfill gas
Mixture: Components also from different classes	Prime mover flue gas/cooling Stationary, mobile
Configuration	**Working fluid cooling**
Saturated: Simple, regenerated, multi-P levels	Air
Superheated: Simple, regenerated, multi-P levels	Water
Supercritical: Simple, regenerated, multi-P levels	Air with intermediate loop
Cascaded: Combinations of cycle variants	Water (for CHP purposes)
Expander type	**Working fluid heating**
Turbine: Axial, radial inflow/outflow, mixed flow	Direct
Volumetric expander: Scroll, screw, piston, vane	Indirect: Thermal oil loop, water loop
Turbine/generator connection	**Turbogenerator assembly**
Direct With inverter	Hermetic
Indirect With/without gearbox	Open: Shaft seals

3. Performance analysis and optimisation of a reheat organic Rankine cycle

3.1. Introduction

In recent years, a large number of studies have examined the thermodynamic performance of ORCs by means of first and second law analysis. In most of these studies, some criteria, the most common the thermal and exergetic efficiency as well as the power output have been assessed for varying conditions and working fluids considering a multitude of different design options and energy integration scenarios (geothermal, solar, biomass, industrial waste heat) [117,128–130]. Other authors have focused on the multi-objective optimization of ORC systems with the aim to optimize certain design parameters. The equipment components (heat exchangers, expanders, pumps) are sized depending on the selected design points and boundary conditions (working fluids, pressures, temperatures, heat fluxes, power output values). Most of the multi-objective optimization approaches utilize various optimization methods in order to pinpoint the values of the design variables that maximize the objective functions. Typically, these studies focus on a single criterion, whereas a number of them include multiple objectives within the optimization process. An overview of these studies, along with a presentation of their methodology and main conclusions, is presented in the following.

3.1.1. Working fluid selection

Wang et al. [131] investigated the effect of the boiling temperature of working fluids on the ORC performance operating with 13 different working fluids. The heat source temperature had a range of 100-220 °C and the PPTD had a range of 5-30 °C. The authors revealed that the boiling temperature of working fluids greatly affected the optimal evaporating pressure to affect the cycle performance. R123 was the best fluid for the temperature range of 100-180 °C and R141b was the optimal fluid with the temperature higher than 180 °C.

He et al. [118] proposed a thermodynamic screening of 22 working fluids for subcritical ORCs. The waste heat source temperature and the PPTD were fixed to be 150 °C and 5 °C, respectively. The authors concluded that the larger net power output was produced when the critical temperature of working fluid approached the waste heat source temperature. They pointed that R114, R245fa, R123, R601a, n-pentane, R141b and R113 are suitable as working fluids for subcritical ORC under the studied conditions.

Wang et al. [132] proposed a theoretical model to analyse the influence of working fluid properties on the thermal efficiency, the optimal operation condition and exergy destruction for low-grade waste heat recovery. Meanwhile, the effect of different heat sources on the optimal performance of ORCs with 25 working fluids has been evaluated using pinch point and exergy analysis method. The authors emphasized that it is recommended to get the most from the heat source rather than always seek of high thermal efficiency in the low temperature

range. Additionally, fluids with low critical temperature, low specific liquid heat and high vaporization latent absorb more energy from the hot source.

Xu and Yu [133] investigated the effect of critical temperatures on the performance of subcritical ORC. More specifically, they screened 57 fluids for heat source temperature range of (100-300 °C), consisting of flue gas flow rate of about 11 kg/s. They concluded that the critical temperature should be in a range from 100 K higher than to 20–30 K lower than the waste gas inlet temperature. Based on their conclusion, R245fa and R141b were selected as the optimal working fluids.

A theoretical model was proposed by Long et al. [120] to analyse the impact of working fluids on the performance of the ORC. They chose exergy efficiency as the objective function and considered 10 different working fluids for varying heat source temperature from 90 to 150°C. The results suggested that the working fluids selection depends significantly on optimal evaporation temperature. In addition, fluids with lower critical temperature lead to a higher optimal evaporation temperature, which results in higher overall exergy efficiency. R600A is selected as the optimum working fluid under the studied waste heat conditions.

Darvish et al. [134] investigated the performance of ORCs for low-grade waste heat recovery (120°C) with nine different working fluids. Thermodynamic models are used to explore thermodynamic parameters such as output power and efficiency. R134a and isobutane are found to exhibit the highest energy and exergy efficiencies, the exergy efficiencies for the systems using R134a and isobutane are observed to be 19.6% and 20.3%, respectively.

Peng et al. [135] investigated eleven pure working fluids based on the first and second law of thermodynamics. They set the heat source temperature of 130 °C and the superheat degree of 5 °C. The authors showed that the evaporating temperature was the most important parameter of the ORC performance. The cyclohexane suggests the highest thermal and exergetic efficiencies, and it shows outstanding overall performances and thus can be selected as the most suitable fluid under the given condition.

Zhu et al. [136] performed a thermo-economic optimization of ORCs for marine diesel engine waste heat recovery. They examined seven different working fluids for varying diesel-engine temperatures from 293 to 387 °C and the rate of exhaust energy from diesel engines is in the range of 223.7 kW-488.10 kW. The authors shown that there is an optimal evaporation temperature, at which the ORC system has the maximum thermal efficiency, and minimum exergy destruction rate and water pump power consumption. Furthermore, under the optimized parameters, R141b performs the most satisfactorily with the thermal efficiency of 19.87%, exergy efficiency of 45.84% and the maximum net power of 97 kW followed by R113, cyclohexane; R600a performs the least favourably.

Uusitalo et al. [137] studied the use of 35 working fluids for low-temperature ORCs including hydrocarbons, fluorocarbons and siloxanes. They studied the dependence of the critical temperature and molar mass of the fluid on the cycle design and on important process operating parameters. They concluded that the higher cycle efficiency can be obtained if the evaporation pressure slightly lower than the critical pressure of the fluid for all the studied fluids. Furthermore, the increase in the fluid superheating does not have significant influence on the cycle efficiency, and the cycle efficiency slightly increases as the degree of superheating increases.

3.1.2. Cycle configuration

One aspect that is more significant when designing an ORC is its configuration, since the cycle performance can be improved by including additional equipment such as IHE and feed-heaters.

Meinel et al. [138] compared three ORC configurations considering basic, recuperated and regenerative ORCs in order to convert the waste heat from internal combustion engine to power. Two studies were investigated, the first considering that the exhaust gas outlet is limited to 130°C to stay above the acid dew point; In the second study, the pinch point of the exhaust gas heat exchanger was set at 10°C. Results show that regenerative ORC has large thermal efficiency for isentropic and wet fluids, less exergy destruction and could be operated for possible conjoined heat and power generations. Whereas, dry fluids can be applied in a recuperator ORC configuration in a more efficient way.

Four ORC configurations including basic ORC, basic ORC with IHE, regenerative ORC and regenerative ORC with IHE were compared by Safarian and Aramoun [139]. The authors investigated the influence of factors such as degree of thermodynamic perfection and influence coefficient of each element on the cycle performance. The considered inlet hot gas to the evaporator is a steady stream of nitrogen at the temperature of 300 °C and the pressure of 0.1 MPa. They reported that the regenerative ORC with IHE has the highest thermal and exergy efficiencies (22.8% and 35.5%) and the lowest exergy loss (42.2 kW) and the evaporator is the element, which has the greatest impact on the system performance.

Li et al. [140] performed an extensive study on the energetic and exergetic evaluation of ORC with IHE, basic, reheat and regenerative ORCs for a fixed power output of 30 kW. Unlike most studies, the scope of the investigation was not limited to a specific application but considered waste heat, biomass as well as geothermal and solar energy sources. He studied 14 working (only dry or isentropic) fluids and performed parametric investigations to examine the impact of the evaporation pressure level and the condensation temperature of the cycle on the ORC performance. The results can be summarized as follows: as the working fluid critical temperature increases the thermal efficiency increases, the condensation temperature influences the thermal efficiency more than the evaporator temperature. Among the studied configurations, the ORC with IHE and the regenerative ORC have a lower exergy destruction value compared to the basic ORC, while the reheat ORC has a marginally larger exergy destruction.

The influence of superheat and IHE on the thermo-economic performance of basic ORC, superheated ORC and ORC-IHE are analysed by Zhang et al. [141]. They examined nine different working fluids for flue gas temperature range (150- 270°C). They concluded that, parameters such as temperature of the heat source, heat source load, working fluid type, critical temperature and specific heat of working fluid affected the use of IHE in the ORC system; they also found that at low heat source temperature and load superheated ORC is more suitable than basic and ORC with IHE for wet fluids. Additionally, for high heat source temperature and load ORC with IHE can achieve higher thermal and exergy efficiency compared to basic ORC.

Kezrane et al. [142] compared basic ORC, ORC with IHE and ORC with superheat for waste heat recovery application (160 °C, 50 kg/s). The following organic working fluids were considered: isopentane, n-pentane, cyclohexane, n-hexane and toluene. The authors found that the use of IHE improves the thermal efficiency by 7.7% and maintaining maximum power

output. In addition, result revealed that the superheating is not required for working fluids as they already quit the expander at a superheated state. Depending on the operating conditions, isopentane coupled with ORC with IHE could be suggested the most appropriate (cycle configuration-working fluid) couple.

Valencia et al. [143] investigated the energetic and exergetic analyses of three ORC configurations for waste heat recovery from the exhaust gases of a 2-MW natural gas engine. A basic ORC, an ORC with IHE and an ORC with double-pressure configurations are considered; cyclohexane, toluene, and acetone are selected as working fluids. They also investigated the effect of evaporating pressure on the net power output, thermal efficiency, specific fuel consumption, overall energy conversion efficiency, and exergy destruction. The authors revealed that ORC with IHE operated with toluene improves the operational performance by achieving a net power output of 146.25 kW, an overall conversion efficiency of 11.58%, an ORC thermal efficiency of 28.4%, and a global exergy efficiency 59.76%.

3.1.3. Optimization

Additionally, various studies have focused on the multi-objective ORC optimization. Wang et al. [144] implemented genetic algorithm (GA) to optimize a low temperature ORC (150°C, 15Kg/s). They examined the influence of turbine inlet pressure and temperature, approach and PPTD on objective function, i.e. ratio of net power output to total heat transfer area. Showing that the ORC with isobutene as a working medium which has the best performance. Moreover, results show that turbine inlet pressure, turbine inlet temperature, PPTD and approach temperature difference have significant effects on the net power output and surface areas of both the evaporator and the condenser.

By means of the GA using exergy efficiency as the objective function, three different ORCs including the basic ORC, the single-stage regenerative ORC and the single-stage regenerative ORC using six different working fluids (R245fa, R245ca, R141b, R123, R113, R11) and under the same given waste heat condition are investigated [145]. The optimization variables include the evaporation pressure (all configurations), the fractions of the flow rate (regenerative ORCs). They showed that the double-stage regenerative ORC demonstrated the highest exergetic efficiency, equal to 56.87% compared to single-stage regenerative ORC at 55.01% and 50.61% for basic ORC, respectively. The R11 and R141b working fluids are selected as the most appropriate working fluids.

Imran et al. [146] carried out a thermo-economic optimization of three cycle configurations: a basic as well as a single and a double stage regenerative ORCs for waste heat recovery over a power range of 30-120 kW. The constraint set consist of evaporation pressure, superheat, PPTD in evaporator and condenser and the optimization was performed for five different working fluids. The results of optimization revealed that R245fa is the best working fluid under their operating conditions. The author also identified the evaporation pressure of the cycle as the dominant parameter on both the thermo-economic performance. The single-stage regenerative ORC improved the thermal efficiency by 1.01% with an extra cost of 187 $/kW while the double stage regenerative ORC enhanced the thermal efficiency by 1.45% with an extra cost of 297 $/kW compared to the basic ORC.

Yang et al. [147] carried out a multi-objective optimization of an ORC for a diesel engine waste heat recovery, considering both thermodynamic and economic aspects. The GA is employed to solve the Pareto solution of the thermodynamic performances and economic

indicators for maximizing net power output and minimizing total investment cost under diesel engine various operating conditions using R600, R600a, R601a, R245fa, R1234yf and R1234ze as working fluids. According to the authors, the increase of evaporation pressure improves both the thermodynamic and economic performance, while the impact of the superheating degree is minimal. R245fa is considered as the most appropriate working fluid for the ORC with comprehensive consideration of thermo-economic performances, environmental impacts and safety levels.

Feng et al. [148] considered micro-scale ORCs for waste heat recovery. More specifically, they optimized basic and regenerative low-temperature (150 °C) systems, operating with R123 as working fluid. Five system parameters are used as decision variables, these variables included the evaporator outlet temperature and pressure, the superheating degree, the PPTD in the evaporator and the condensation temperature. The exergy efficiency and the heat exchanger area per unit net power output are selected as the objective functions. Based on the optimization results, the author suggested that there is a trade-off between the thermodynamic and economic performance of the system. The regenerative ORC exhibited a maximum exergy efficiency of 59.93 %, corresponding to a heat exchange area to 3.07 m^2/kW, which are higher by 8.10 % and 15.89 % respectively compared to those of the basic ORC.

Gotelip Correa Veloso et al. [149] optimized an ORC with IHE for low-grade waste heat recovery, operating with 25 working fluids. The objectives considered were net power output, the heat exchanger area. The influence of the evaporation pressure, superheating degree, heat exchanger effectiveness and PPTD in the evaporator and condenser was investigated. According to the authors, the higher net power output was obtained with R245cb2 as working fluid, generating up to 2063 kW with a heat transfer area of 2997 m^2, providing a 23.6% increase in exergy efficiency of the system.

3.1.4. Scope and motivation of the present work

Regardless of the large number of studies on the analysis of ORCs, most of these have focussed on the basic ORC, ORC with IHE and regenerative ORC systems, but relatively little has examined the potential of reheat ORC. In addition, even considering the limitations of studies on reheat ORC, most of them concentrate on dry or isentropic fluids, while wet fluids have not been explored. The purpose of this research is to investigate the performance of reheat ORC system with different working fluid types in the application of low-grade waste heat recovery. The relationship of the main operating parameters, such as evaporation pressure, reheat pressure and superheat degree to the performance of the reheat ORC system is discussed. Moreover, a multi-objective optimization was implemented to maximize the exergy efficiency and minimize total thermal conductance taking into consideration evaporation pressure, reheat pressure, superheat degree and PPTD as decision variables. Besides, the present work also considers the possible presence of an IHE within the ORC and its influence on overall system performance.

3.2. System analysis and optimization

3.2.1. System description

The schematic diagram of a reheat ORC cycle is shown in **Figure 3.1**. The diagram of temperature-transferred heat corresponding to reheat ORC is given by **Figure 3.2**. Working fluid enters the pump at state 1 as saturated liquid sate and is compressed to the pressure of the

evaporator. The evaporator is divided into three sections (economizer, evaporator and superheater). The working fluid absorbs thermal energy from the waste heat source and to be saturated liquid at state 3, from state 3 to state 4 a phase change occurs in the working fluid from a saturated liquid to a saturated vapour. The working fluid enters the superheater as a saturated vapour at state 4 and leaves as a superheated vapour at state 5. The generated vapour expands, initially, in the high-pressure turbine to the reheat pressure and the reheat process takes place between the two turbines. In this process, the working fluid is reheated at constant pressure, generally at the inlet temperature of the high-pressure turbine. Working fluid then expands in the low-pressure turbine, the pressure of the working fluid at the exit of the low-pressure turbine decreases to the condenser pressure at state 8.

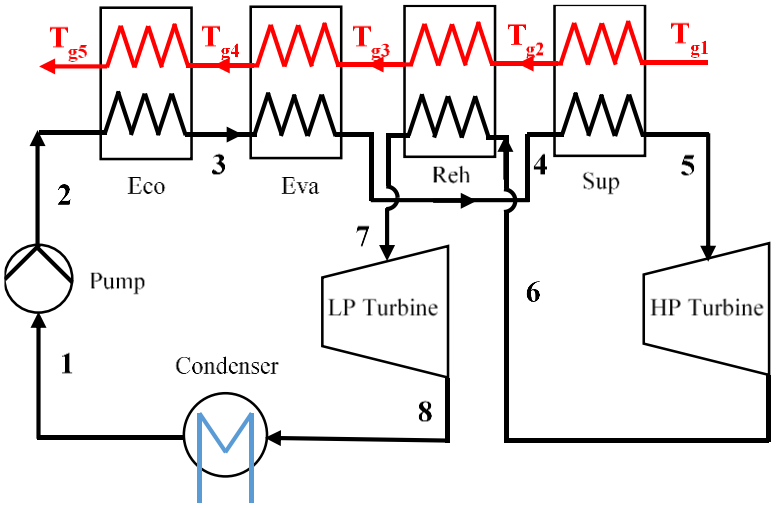

Figure 3.1 *A schematic diagram of reheat ORC.*

For thermodynamic analysis, the reheat ORC was modelled based on the following assumptions:

- The system operates under steady state condition.
- The pressure drop in the evaporator, condenser, reheater and pipes are neglected.
- To ensure maximum energy recovery and to avoid corrosion at low temperatures, the exhaust gas outlet temperature is limited to the minimum allowed temperature 82 °C [141,150].

The optimal reheat pressure in steam Rankine cycle is one-fourth of the evaporating pressure [92], in the present work the reheat pressure is taken as the mean pressure of maximum and minimum [140].

Table 3-1 shows parameters used during the simulation of reheat ORC. PPTD value are the initialization values used taken from literature and which are further investigated as a range of temperature difference options in the optimization section, later in the chapter.

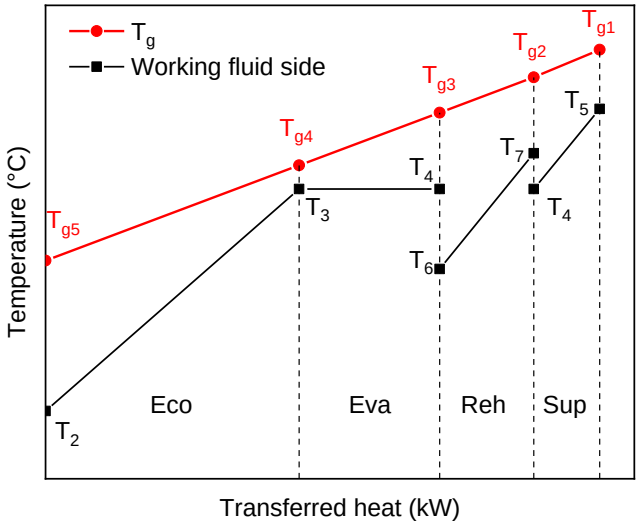

Figure 3.2 *The temperature-transferred heat diagram of reheat ORC.*

Table 3-1 *Operating conditions of the reheat ORC.*

Parameters	**Value**
Environment temperature (°C)	20
Temperatures of heat source (°C) **[151]**	150
Mass flow rate of hot gas (kg/s) **[152]**	14
Specific heat at constant pressure for hot gases (kJ/kg·K) **[152]**	1.1
Condensing temperature (°C) **[142]**	30
LP and HP turbine efficiency (%) **[152]**	80
Feed pump isentropic efficiency (%) **[153]**	80
PPTD in evaporator (°C) **[152]**	8
PPTD in condenser (°C) **[154]**	5
Circulating pump head (m) **[153]**	20
Circulating pump efficiency (%) **[153]**	80

3.2.2. Model description

To evaluate the performance of the system, both the thermal and exergy efficiency have been used. It is necessary to use the exergy analysis since the energy analysis cannot provide any information about the irreversibility of the system. Supposing the reheat ORC system works under steady state, the mass balance of each control volume can be expressed as

$$\sum_{in} m = \sum_{out} m \tag{3.1}$$

The energy balance equation can be expressed as:

$$\sum_{i} E_i + Q = \sum E_0 + W \tag{3.2}$$

The heat balance equations in the evaporator between the hot gas and the working fluid are represented as follows:

Economizer

$$\dot{Q}_{eco} = \dot{m}_{wf}(h_3 - h_2) = \dot{m}_g Cp_m(T_{g4} - T_{g5}) \tag{3.3}$$

Evaporator

$$\dot{Q}_{eva} = \dot{m}_{wf}(h_4 - h_3) = \dot{m}_g Cp_m(T_{g3} - T_{g4}) \tag{3.4}$$

Super heater

$$\dot{Q}_{Sup} = \dot{m}_{wf}(h_5 - h_4) = \dot{m}_g Cp_m(T_{g1} - T_{g2}) \tag{3.5}$$

The heat balance equations in the reheater can be expressed as

$$\dot{Q}_{\mathrm{Re}h} = \dot{m}_{wf}(h_7 - h_6) = \dot{m}_g Cp_m(T_{g2} - T_{g3}) \tag{3.6}$$

Where T_g and h are the temperature and the enthalpy of the hot source and the working fluid at each state respectively, $\dot{m}_g$ and $\dot{m}_{wf}$ are the mass flow rate of the hot source and the working fluid respectively, Cp_m is the average specific heat capacity at constant pressure of the hot source.

Therefore, the heat absorbed by the working fluid is the sum of Q_{eco}, Q_{eva}, Q_{Sup} and $Q_{\mathrm{Re}h}$ which can be expressed as:

$$Q_{in} = m_{wf}(h_5 - h_2) + m_{wf}(h_7 - h_6) \tag{3.7}$$

Since there is, tow turbine (high-pressure turbine and low-pressure turbine) the turbine power for both HP and LP turbine can be calculated as:

$$W_T = m_{wf}(h_5 - h_6) + m_{wf}(h_7 - h_8) \tag{3.8}$$

The heat rejected by the working fluid in the condenser is given by :

$$Q_{con} = m_{wf}(h_8 - h_1) \tag{3.9}$$

The power consumed by the pump can be expressed by:

$$W_P = \dot{m}_{wf}(h_2 - h_1) \tag{3.10}$$

The power consumed by the circulating pump in the cooling system can be expressed by [153,155]:

$$W_{CP} = \frac{\dot{m}_{cw} g H}{\eta_{CP}} \tag{3.11}$$

$\dot{m}_{cw}$ is the cooling water flow rate, H is the circulating pump head, g is the gravitational acceleration and η_{CP} is the efficiency of circulating pump.

The cooling water flow rate is:

$$\dot{m}_{cw} = \frac{Q_{con}}{\Delta T_{cw} Cp_{cw}} \tag{3.12}$$

Q_{con} is the condenser heat transfer rate, Cp_{cw} is heat capacity at constant pressure of the cooling water and ΔT_{cw} is the cooling water temperature rise when heated by the working fluid.

The net power output produced by the reheat organic Rankine cycle is:

$$W_{net} = W_T - W_P - W_{CP} \tag{3.13}$$

Cycle efficiency is expressed as the ratio of net power output to the heat supplied to the system.

$$\eta = \frac{W_{net}}{Q_{in}} \tag{3.14}$$

The exergetic efficiency can be determined by the use of the following equation:

$$\eta_{ex} = \frac{W_{net}}{\dot{Q}_{in}(1 - \frac{T_L}{T_H})} \tag{3.15}$$

Because that the hot source temperature was changed, thus T_H will calculate as [156]:

$$T_H = \frac{T_{g1} - T_{g5}}{ln(\frac{T_{g1}}{T_{g5}})} \tag{3.16}$$

Where T_{g1} and T_{g5} are the inlet and outlet temperature of the hot source.

T_L is the average temperature of low-temperature reservoir and it can be calculated as [156]:

$$T_L = \frac{T_{cw\_out} - T_{cw\_in}}{ln(\frac{T_{cw\_out}}{T_{cw\_in}})} \tag{3.17}$$

Where T_{cw_in} and T_{cw_out} are the inlet and outlet temperature of the heat sink.

The total heat thermal conductance (UA) of the cycle is considered as a parameter to estimate the heat transfer area of the heat exchangers. The following energy balances is used to calculate the hot source temperature at each state.

$$T_{g4} = T_3 + \Delta T_{PP} \tag{3.18}$$

$$T_{g2} = T_{g1} - (\frac{m_{wf}}{C_h})(h_5 - h_4) \tag{3.19}$$

$$C_h = m_g Cp_g \tag{3.20}$$

Where C_h heat capacity rate of the hot source.

$$T_{g3} = T_{g4} + (\frac{m_{wf}}{C_h})(h_4 - h_3) \tag{3.21}$$

$$T_{g5} = T_{g4} - (\frac{m_{wf}}{C_h})(h_3 - h_2) \tag{3.22}$$

The logarithmic mean temperature difference (LMTD) method is considered to evaluate the heat transfer amount in the heat exchangers and it can be established as following:

$$Q = UA\Delta T_{LMTD} \tag{3.23}$$

$$\Delta T_{LMTD} = \frac{\Delta T_{in} - \Delta T_{out}}{\ln(\frac{\Delta T_{in}}{\Delta T_{out}})} \tag{3.24}$$

$$UA_{Evap} = UA_{eco} + UA_{eva} + UA_{\sup} + UA_{\mathrm{Re}h} \tag{3.25}$$

$$UA = UA_{con} + UA_{Evap} \tag{3.26}$$

3.2.3. Selected working fluid

The working fluid choice plays a critical factor in the design of an ORC system. The selection of the working fluid, which must be safe, environmentally friendly and low-cost, must be specifically taken into account. [157–159]. There is no working fluid that satisfies all selection criteria [19,160], thus the fluid selection method balancing the environmental, safety, physical, and chemical properties of a working fluid.

Based on environmental and safety concerns, four wet fluids are selected, namely R152a, cyclopropane, dimethyl ether and propyne. In addition, R236ea [161,162] and R600a [126,163] are broadly recommended in ORC systems. The thermodynamic properties of these six working fluids are presented in **Table 3-2**, and the related *T-s* diagram is presented in **Figure 3.3**.

Table 3-2 *Properties of the selected organic fluids used in the study.*

Name	M [kg/mol]	T_c (°C)	P_c (bar)	GWP	ODP	Fluid type
R152a	66.051	113.26	45.2	133	0	Wet
Cyclopropane	42.081	125.15	55.8	11	0	Wet
Dimethyl ether	46.07	127.23	53.37	1	-	Wet
Propyne	40	129.23	56.26	~20	0	Wet
R236ea	134	139.29	34.20	858	0	Isentropic
R600a	58	135	36.29	~20	0	Dry

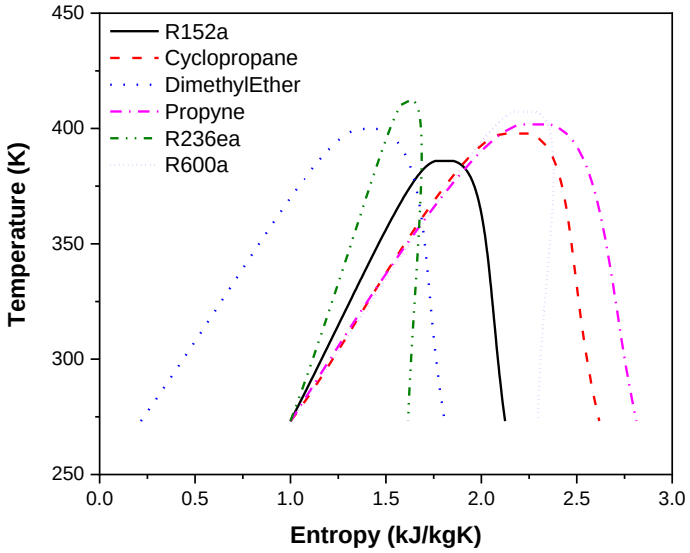

Figure 3.3 *T-s diagram of selected working fluid.*

3.2.4. Data validation

To validate the present model, the energy balance equations of reheat ORC are solved with the same parameters as in Ref. (G. Li 2016) [140]. The hot source was geothermal water and the evaporator inlet pressure was 10 bars. The pump and turbine isentropic efficiencies were 0.8 for each one. The validation was conducted with R245fa, R236ea and R600 as the working fluid, the comparison between the obtainable results and the results of the cited reference shows a very good agreement, as shown in **Table 3-3** and **Figure 3.4**. Thus, the proposed model was considered to be verified.

Table 3-3 *Comparison of the present results with Reference [140].*

Working fluid	η_{th} [%]		I_{tot} [kW]	
	this work	Reference [140]	this work	Reference [140]
R236ea	10.66	10.60	34.4	34.2
R600	11.02	11	32.19	32.1

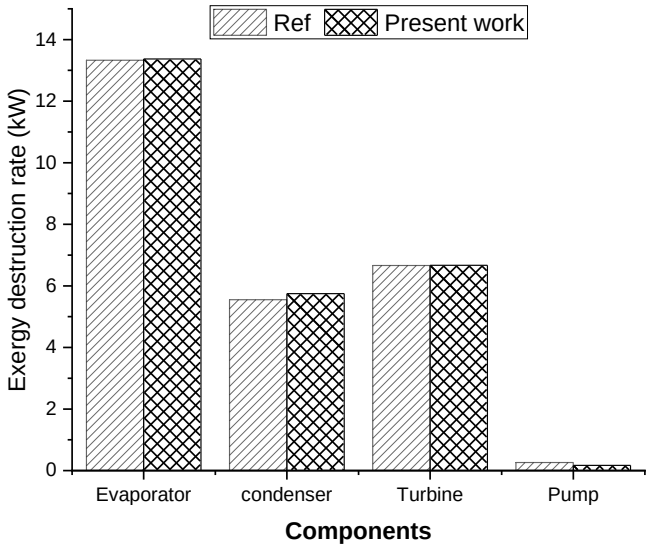

Figure 3.4 *Exergy destruction rate for each component comparisons with reference (G. Li, 2016) [140] .*

3.2.5. Optimization

Non-linear constrained optimization methods can be divided into two main categories: deterministic methods and stochastic methods. Deterministic methods, e.g. gradient descent, the conjugate gradient method and Newton's method, are generally applied in the case of a search for the local optimum, and are based on the determination of the derivatives of the objective function and the constraints. These two characteristics (the determination of the derivative and the search for the local optimum) mean that these methods are not robustly applicable to the resolution of a problem such as the one presented here. Indeed, the present case is one of global non-linear optimization and the objective function, which depends on several variables, is calculated following a numerical process involving systems of non-linear equations, making the explicit determination of the derivative of the objective function very complex. In this case, it is generally recommended to use so-called stochastic methods and more particularly evolutionary methods such as Genetic Algorithms (GAs) which have shown success in several engineering problems [119,164].

3.2.5.1. Genetic algorithm

In particular, the GA has attracted much attention for solving complex engineering problems [165,166]. Basically, it only needs function values (not the derivative) and can handle many decision variables. GAs are based on the principles of natural selection and are a type of stochastic method. Many practical optimum design problems are characterized by mixed continuous-discrete variables that cannot be efficiently solved using standard non-linear programming techniques. GAs are well adapted to solve such problems and, in most cases, they are able to locate the global optimal solution with high probability. The basis of the method is Darwin's theory of survival of the fittest. GAs use the principles of natural genetics and natural selection. The GA differs from the traditional optimization techniques because it involves a search from a population of solutions and not from a single point, and it prevents convergence to sub-optimal solutions in the process of searching for the optimum.

Multi-objective optimization problems have received interest form researches since early 1960s. In a multi-objective optimization problem, multiple objective functions need to be optimized simultaneously. In the case of multiple objectives, there does not necessarily exist a solution that is best with respect to all objectives because of differentiation between objectives. A solution may be best in one objective but worst in another. Therefore, there usually exist a set of solutions for the multiple-objective case, which cannot simply be compared with each other. For such solutions, called Pareto optimal solutions or non-dominated solutions, no improvement is possible in any objective function without sacrificing at least one of the other objective functions. Different GAs exist, classified according to the way in which a new generation is created from the previous one, i.e. the mutation or crossover operators corresponding to **figure 3.5.**

The algorithm chosen in the present work is the one presented by Deb et al. [167]. Moreover, among the GAs, Non-dominated Sorted Genetic Algorithm-II (NSGA-II) converges rapidly and allows for multiple objectives to be considered simultaneously. It allows a simple and efficient parametric optimization as described by Deb et al [168].

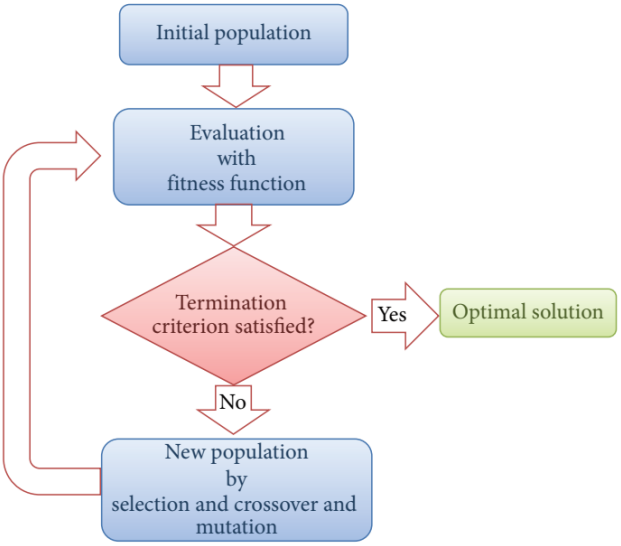

Figure 3.5 *The schematic flowchart of genetic algorithm [169].*

Many optimization problems in engineering are non-linear, having multiple conflicting objectives. A multi-objective optimization problem can be described as follows:

$$\min/\max \quad f(\bar{x}) = [f_1(\bar{x}), f_2(\bar{x}), \ldots, f_n(\bar{x})]$$

$$\text{Subject to} \quad \begin{aligned} g_i(\bar{x}) &\le 0, & i &= 1,2,\ldots,m \\ h_j(\bar{x}) &= 0, & j &= 1,2,\ldots,k \\ x_{m,\min} &\le x_m \le x_{m,\max} & m &= 1,2,\ldots,p \end{aligned}$$

$(\bar{x})$ represents the vector of decision parameters, $f(\bar{x})$ is the vector of objectives, $g_i(\bar{x})$ and $h_j(\bar{x})$ are the inequality and equality constraints, respectively, $x_{m,\min}$ and $x_{m,\max}$ represent the range to which the decision parameters belong.

In the study, each individual has five genes corresponding to the parameters that allow to optimize the cycle:

- Evaporation pressure
- Reheat pressure
- Superheat degree
- PPTD in evaporator
- PPTD in condenser

The first generation is created randomly in a previously defined domain. The objectives achieved by each individual are calculated completely independently of each other. The objectives of each individual are then compared and thus allow an evaluation of the "viability" of the individuals, to use the metaphor of evolutionary theory. The new generation is created from the previous one using three operators:

- Selection
- Crossover
- Mutation

Selection rules select the individuals, called parents that contribute to the population at the next generation. The selection is generally stochastic, and can depend on the individual's scores.

In natural world, the genes of children are from both of their parents. In order to imitate this situation, we do crossover of chromosomes of selected parents to generate offspring. Crossover just happens between two chromosomes (one couple), so the first stage of crossover is arranging the chromosomes of selected parents' population in pairs which is made random.

Different from crossover, mutation occurs quite rarely in GA. The aims of the mutation operator are:

- To generate a string in the neighbourhood of the current string, thereby accomplishing a local search around the current solution.
- To safeguard against a premature loss of important genetic material at a particular position.
- To maintain diversity in the population.

The use of these three operators successively yields new generation with improved values of average fitness of the population. If any bad strings are created at any stage in the process, they will be eliminated by the reproduction operator in the next generation.

In this section, two objective functions of the reheat ORC system, the exergy efficiency and the total thermal conductance, are used to perform the multi-objective optimization. The evaporation pressure, reheat pressure, superheat degree and PPTD are set as five decision variables.

The objective functions for the reheat ORC are set by

$$f_1(x) = \text{maximize}\ (\eta_{ex}) = \frac{W_{net}}{Q_{in}(1-\frac{T_L}{T_H})}$$

$$f_2(x) = \text{minimize}\ (UA) = UA_{con} + UA_{Evap}$$

- Evaporation pressure

The evaporation pressure greatly affects the efficiency of ORCs [136,137,146,147], as it directly impacts the work produced in the expander and the work consumed by the pump. In addition, it strongly affects the heat transfer regime in the evaporator, by affecting the matching between the heat source and the working fluid temperature profiles and by determining the heat input to the ORC, when a constant pinch point is assumed. Lastly, the expander inlet pressure also influences the expander type and configuration selection and thus the expansion efficiency. The evaporation pressure is varied from a minimum value corresponding to a saturation temperature of 50°C. This minimum pressure is considered in principle necessary for the production of sufficient work by the expander, enough to overcome the power consumption of the pump. Furthermore, it is assumed that the maximum evaporation pressure must not exceed 0.9 of critical pressure to ensure that the system operates under subcritical condition. Additional constraints on the evaporation pressure result from its association with the expander inlet temperature and the PPTD in the evaporator, and are necessary in order to avoid temperature crossovers with the heat source stream.

- **Reheat pressure**

The second optimization variable is the reheat pressure. The purpose of a reheating cycle is to remove the moisture carried by the vapor at the final stages of the expansion process. In a reheat ORC, the expansion takes place in two expanders. The working fluid expands in the high-pressure turbine to some intermediate pressure, then passes back to the reheater, where it is reheated at constant pressure to a temperature that is usually equal to the original superheat temperature. This reheated working fluid is directed to the low-pressure turbine, where is expanded until the condenser pressure is reached.

- **Superheating degree**

From a technical perspective, the superheating degree influences the heat transfer in the evaporator as well as the volume flow rate of the working fluid at the expander outlet. The superheating degree is varied from a minimum of 0 °C to a maximum of 20 °C.

- **Pinch point temperature difference**

Lower PPTD values lead to higher power outputs but also to increase heat exchanger sizes. Meanwhile, the pinch point affects the mass flow rate of the working fluid. The range of the PPTD is selected to be from 5°C to 10°C, which is a typical practical range [170]. Of course, the upper bound of this variable is additionally constrained by the expander inlet temperature of the working fluid and the heat source temperature and the condenser temperature (in order to avoid temperature crossovers).

- **Boundary conditions**

The optimization variables and the main assumptions regarding their search bounds are summarized in **Table 3.4**.

Table 3-4 *Constraints and bounds for optimization.*

Parameters (constraints)	**Lower bound**	**Upper bound**
Evaporation pressure (bar)	$P_{sat}(50°C)$	$0.9*P_{cr}$
Reheat pressure (bar)	$1.1*P_{cd}$	$0.9*P_{ev}$
Superheat (°C)	0	20
PPTD evaporator (°C)	5	10
PPTD condenser(°C)	5	10

3.2.5.2. Decision-making in multi-objective optimization

In the case of multi-objective optimization, the resulting solutions are a set of optimum points (Pareto front). In order to select the final solution from the optimum points, The Technique for Order Preference by Similarity to an Ideal Solution (TOPSIS) is commonly applied in decision-making process and used to determine the final optimal result [126,163,171]. The TOPSIS was developed by Yoon and Hwang [172]. The basic concept of this method is that the selected alternative should have the shortest distance to the positive ideal solution and the farthest distance from the negative ideal solution. To be precise, for thesis case study, alternatives are represented by the exergy efficiency and the total thermal conductance, respectively. The positive-ideal solution is the one that maximizes the benefit criteria and minimizes the cost criteria, while the negative-ideal solution does the opposite. It minimizes

the benefit criteria and maximizes the cost criteria [173]. The method assumes to have m alternatives, n attributes/criteria and the final goal is represented by the score of each alternative concerning each criterion [173].

The TOPSIS method is illustrated in the following steps

Step 1: Consider a matrix D , with $A_1, A_2, ..., A_m$ alternatives and $C_1, C_2, ..., C_n$ criteria. The rating of the alternative $A_i (i = 1, \dots, \mathrm{m})$ according to $C_j (j = 1, \dots, \mathrm{n})$ is represented by x_{ij}. The weight vector $W = (w_1, w_2, \dots, w_n)$ is composed considering the individual weights w_j with $j = 1, ...,$ n for each criterion C_j, satisfying $\sum_{j=1}^{n} w_j = 1$. In general, the criteria are classified into two types: benefit and cost. The benefit criterion means that a higher value is better while for the cost criterion is valid the opposite.

Step 2. Normalized decision matrix construction.

The data of the decision matrix D come from different sources, so it is necessary to normalize it in order to transform it into a dimensionless matrix, which allow the comparison of the various criteria. In this work, we use the normalized decision matrix $R = [r_{ij}]_{mxn}$ with $i = 1, \dots, m$, and $j = 1, \dots, n$. The normalized value r_{ij} is calculated as:

$$r_{ij} = \frac{x_{ij}}{\sqrt{\sum_{i=1}^{m} x_{ij}^2}}, \text{ with } i = 1, \dots, m; j = 1, \dots, n \tag{3.27}$$

This passage permits to get a dimensionless matrix and compares different types of criteria: various attributes dimensions are transformed into non-dimensional attributes. This allows comparisons across criteria.

Step 3. Weighted normalized decision matrix construction.

Given the set of weights for each crit erion w_j, with $j = 1, ...,$ n, multiply each row of the normalized decision matrix by its associated weight to get the weighted normalized evaluation v_{ij}.

Step 4. Positive and negative ideal solutions identification.

Identify the positive ideal solutions A^+(benefits) and negative ideal solutions A^-(costs) as follows:

$$A^+ = (v_1^+, v_2^+, ..., v_m^+) \tag{3.28}$$

$$A^- = (v_1^-, v_2^-, ..., v_m^-) \tag{3.29}$$

Where

$$v_j^+ = \left(\max_i v_{ij}, j \in J_1; \min_i v_{ij}, j \in J_2\right)$$
$$v_j^- = \left(\min_i v_{ij}, j \in J_1; \max_i v_{ij}, j \in J_2\right)$$

Where J_1 and J_2 represent the criteria benefit and cost, respectively.

Calculate the Euclidean distances [172]from the positive ideal solution A^+(benefits) and the negative ideal solution $A^-$of each alternative A_i, respectively as follows:

$$S_i^+ = \sqrt{\sum_{j=1}^{n} (v_{ij} - v_i^+)^2} \ , i = 1, \dots, m \tag{3.30}$$

$$S_i^- = \sqrt{\sum_{j=1}^{n} (v_{ij} - v_i^-)^2} \ , i = 1, \dots, m \tag{3.31}$$

Step 6. Calculation of the relative closeness to the ideal solution.

C_i denotes the relative closeness for each alternative A_i with respect to positive ideal solution.

$$C_i = \frac{S_i^-}{(S_i^+ + S_i^-)} \ i = 1, .., m \text{ , where } C_i \in \{0,1\} \tag{3.32}$$

Step 7. Rank of alternatives according to the relative closeness.

Sort C_i in decreasing order and select the best alternative with the highest value. It will be the one with the shortest distance from positive-ideal solution and the farthest distance from negative-ideal solution.

3.3. Results and discussions

3.3.1. Parametric study

To investigate the effect of several parameters on the performance of the reheat ORC a parametric study has been carried out. The considered decision parameters for the present work are evaporation pressure, reheat pressure, superheat degree and PPTD in the evaporator.

Figure 3.6 illustrates the variation of exergy efficiency with the evaporation pressure when the degree of superheat and the PPTD are 5°C and 8°C respectively. Exergy efficiencies of wet fluids continually increase with the increase of evaporation pressure to attain their maximum, while for dry and isentropic fluids, exergy efficiencies initially increase and then diminish at higher evaporation pressures. The increase in evaporation pressure results in an increase in the enthalpy decline through both high and low pressure turbines and a reduction in mass flow rate of working fluids. Nevertheless, the enthalpy decline increases more rapidly than the reduction of the mass flow rate, which leads to an increase in the exergy efficiency for wet fluids. Exergy efficiency for dry and isentropic fluids decreased as a result of the decrease in mass flow rate which becomes dominant. The highest exergy efficiency was reached by propyne followed by cyclopropane and dimethyl ether.

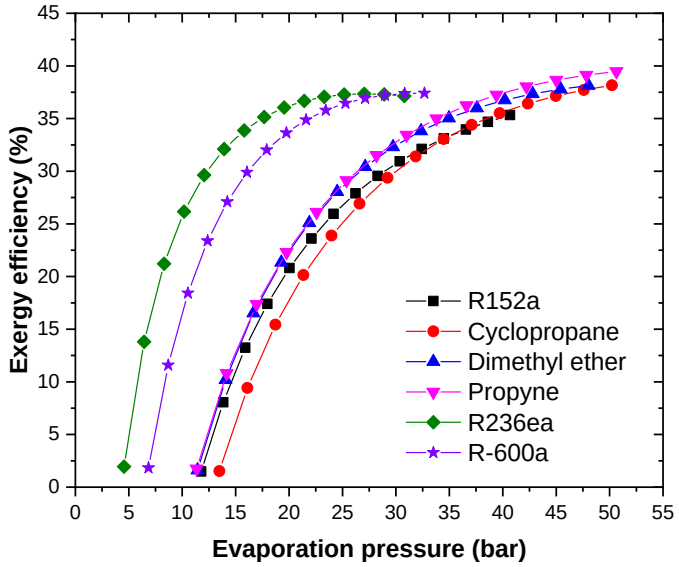

Figure 3.6 Effect of evaporation pressure on exergy efficiency.

The effect of the evaporation pressure on the output power appears in **figure 3.7**. Alluding to **figure 3.7**, wet fluids have large evaporation pressure compared to dry and isentropic fluids. It can be remarked that for all organic fluids the power output varied with a maximum curve. The variation of the output power can be explained by equations 3.13. The increase of evaporation pressure results in a higher enthalpy difference through the high and low pressure turbines, as well a reduction in mass flow rate of organic fluid, with power output resulting due to the influence evaporation pressure and corresponding enthalpy rise. However, the progressive drop in mass flow rate dominates the increasing enthalpy drop, thus the output power decreases immediately afterwards. R236ea has the highest power output followed by R152a and R600a.

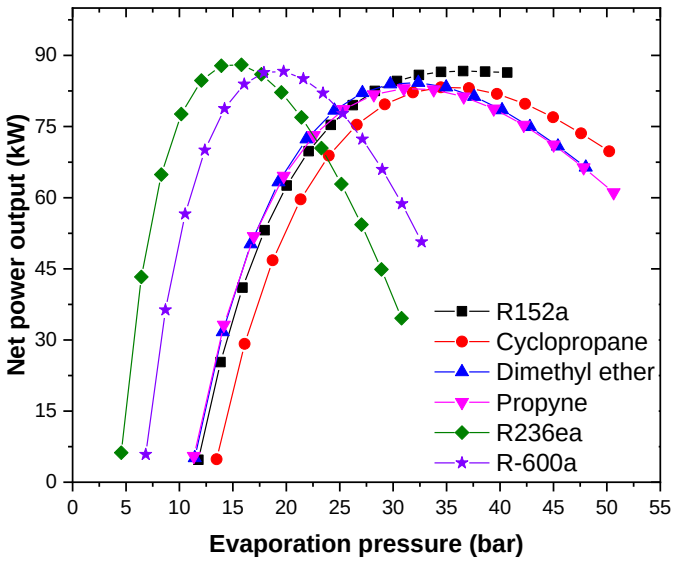

Figure 3.7 Effect of evaporation pressure on net power output.

Figure 3.8 displays the variation of the total thermal conductance as a function of evaporation pressure. The total thermal conductance diminishes inversely with the increase in evaporation pressure for all fluids. This latter is due to the fact that as the evaporation temperature increases at the same time, the gas outlet temperature of the evaporator increases

respectively, succeeding in a reduction in the heat transfer rate of the evaporator and condenser, which contributes to the drop in thermal conductance. R236ea and R600a have the lowest values of thermal conductance.

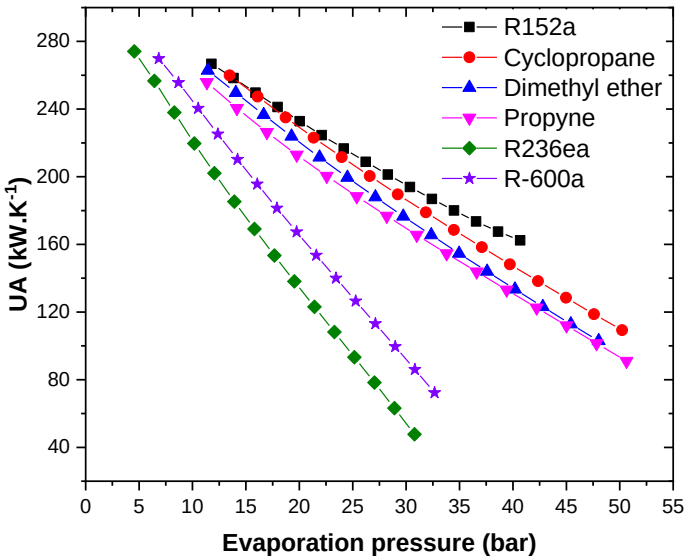

Figure 3.8 Effect of evaporation pressure on total thermal conductance.

Figure 3.9 shows the variation of the exergy efficiency as a function of reheat pressure. The exergy efficiency varied with a maximum curve for all working fluid types. While the net power output increases with the increase in reheat pressure for all working fluid types (**Figure 3. 10**). The increase in reheat pressure leads to an increase in both enthalpy drop through the low-pressure turbine and mass flow rate. Therefore, the power output increases, since the power output and exergy efficiency are related (through Equation 3.15), and therefore, the exergy efficiency will also increase. R152a has the highest power output followed by cyclopropane and dimethyl ether, while propyne has the highest exergy efficiency followed by R600a and R236ea.

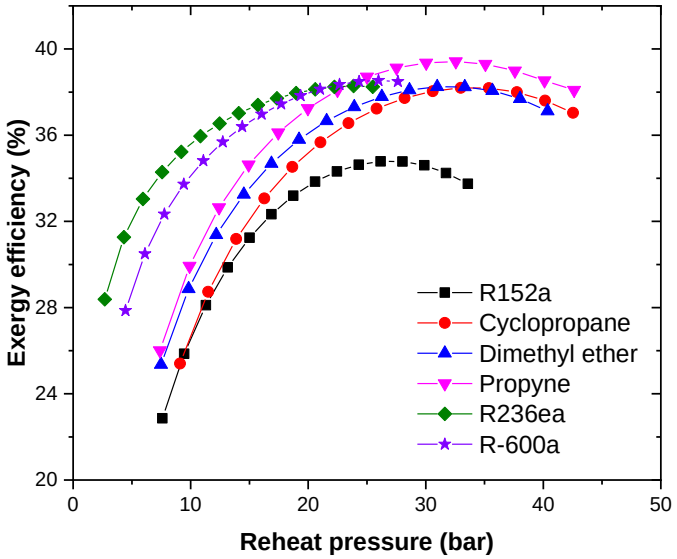

Figure 3.9 Effect of reheat pressure on exergy efficiency.

Figure 3.11 illustrates the variations of total thermal conductance value with reheat pressure for selected organic fluids. As the reheat pressure increases, the values of total thermal conductance increase for all types of organic fluids. The quantity of heat transferred and the

logarithmic mean temperature are the parameters that affect the total thermal conductance. The increase of reheat pressure yields an increase in the heat absorbed and rejected by the organic fluid and consequently, the total thermal conductance increases. R236ea and R600 have the lowest value of total thermal conductance.

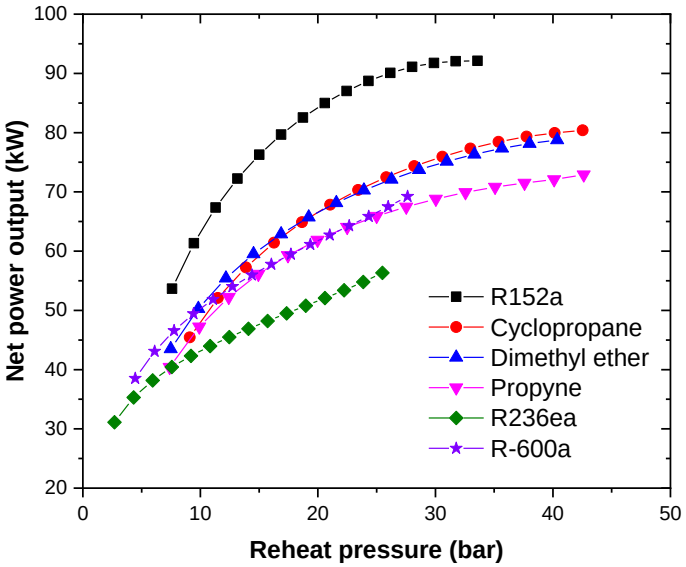

Figure 3.10 *Effect of reheat pressure on net power output.*

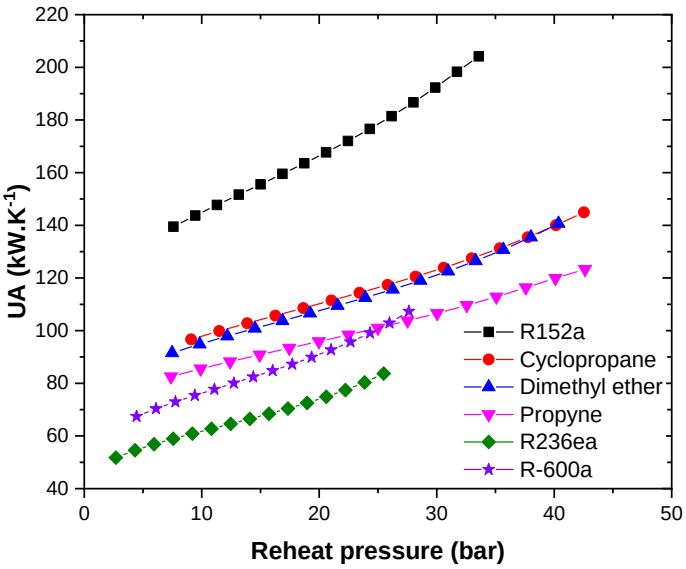

Figure 3.11 *Effect of reheat pressure on total thermal conductance.*

Exergy efficiency for various superheat degrees, for constant evaporation pressure and reheat pressure is plotted in **Figure 3.12**. The exergy efficiency increases with the increase of superheat degree for all working fluids; wet fluids have a slightly higher increase followed by dry and isentropic fluids. **Figure 3.13** demonstrates that effect of the superheat degree on power output. The increase of superheat degree permits a higher enthalpy drop in both high and low pressure turbines and dwindling mass flow rate of organic fluid. The enthalpy drop increases faster than the mass flow rate of wet fluids and inversely for dry and isentropic fluids, resulting in the slight increase in the power output for wet fluids. Nevertheless, as the superheat degree increases, the exergy destruction in the evaporator decreases and thus the exergy efficiency increases.

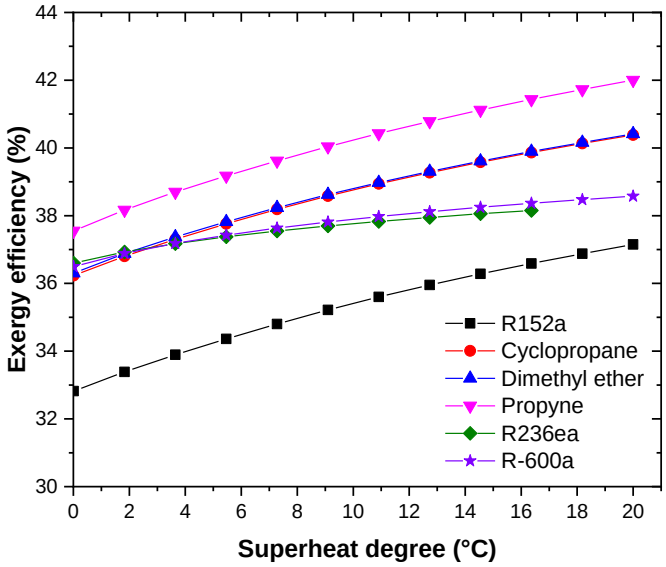

Figure 3.12 *Effect of degree of superheat on exergy efficiency.*

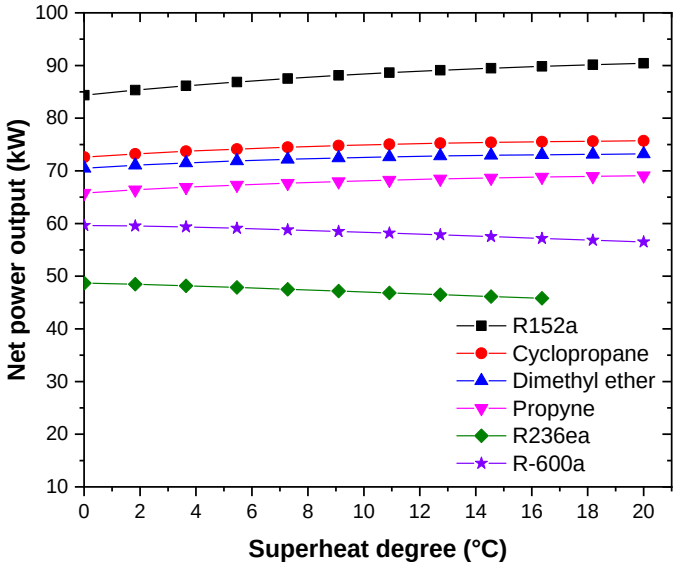

Figure 3.13 *Effect of degree of superheat on net power output.*

Figure 3.13 indicates the effect of superheat degree upon the total thermal conductance. By noting the trend, the thermal conductance decreases slightly at first, then increases with the superheat degree for propyne, R236ea and R600a. Due to the mass flow rate decrease of working fluids with the increase of superheat degree, the heat transfer quantity in the economizer and evaporator decreases respectively, causing a decrease of total thermal conductance at first. Furthermore, the increase of superheat degree leads to a decrease in LMTD in the superheat section, leading to an increase in thermal conductance of the superheated section, and thus the total thermal conductance increases as a result. Isentropic and dry have better performance than wet fluids in this regard.

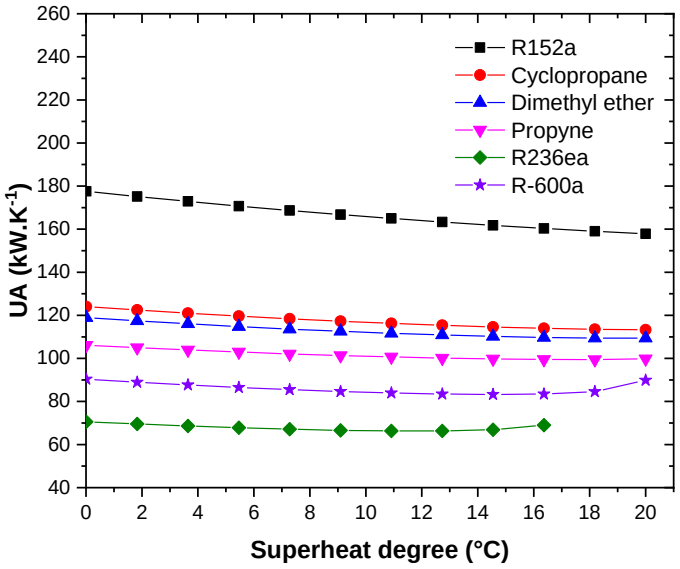

Figure 3.14 *Effect of degree of superheat on total thermal conductance.*

Figures 3.15 and 3.16 exhibit the variations of exergy efficiency and power output as a function of PPTD in evaporator. Both exergy efficiency and power output decrease with the increase of PPTD for all working fluid types. With the elevation of PPTD, the mass flow rate and the enthalpy difference in both turbines decrease, resulting in a net power output reduction. The drop of exergetic efficiency is caused by the lower mass flow rate and lower power output.

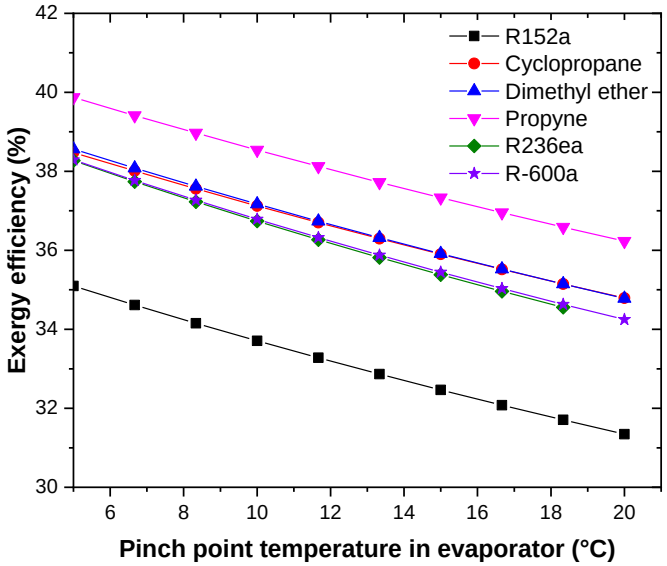

Figure 3.15 *Effect of evaporator PPTD on exergy efficiency.*

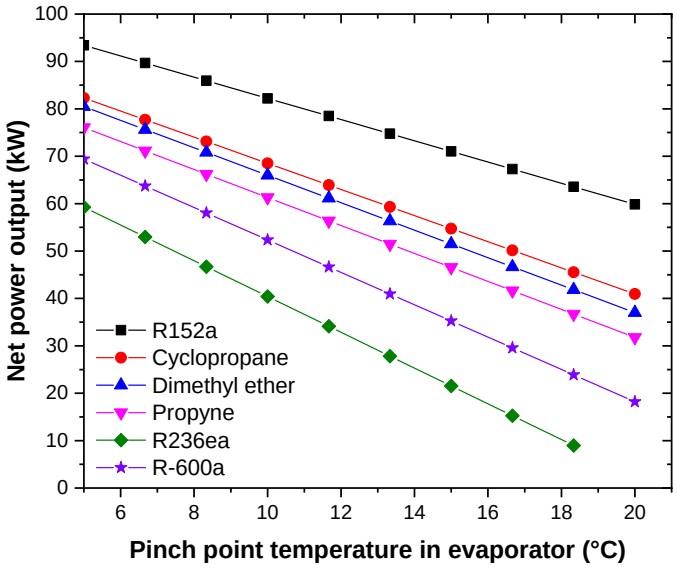

Figure 3.16 Effect of evaporator PPTD on net power output.

Figure 3.17 expresses the effect of PPTD in evaporator upon the total thermal conductance. The total thermal conductance decreases with the increase of pinch point temperature for all organic fluids. At higher PPTD, the temperature gradient between the fluids is high, which bounds the low temperature fluid to exit the evaporator at an early stage from a lower heat transfer area. This means that less heat transfer area is required for the high pinch point condition and eventually leads to lower thermal conductance.

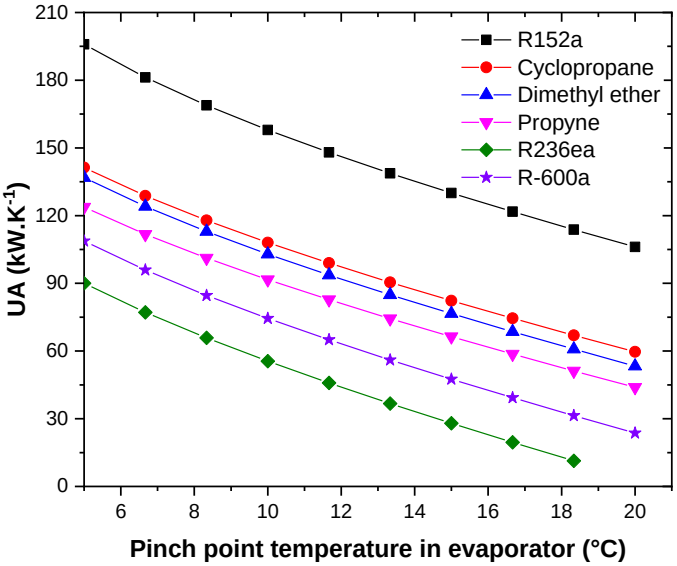

Figure 3.17 Effect of evaporator PPTD on total thermal conductance.

3.3.2. Optimization results

Results using NSGA-II algorithm to conduct a multi-objective optimization of reheat ORC are discussed in this section.

Figure 3.17 shows the Pareto fronts for reheat ORC (without IHE) with selected organic fluids. It can be remarked that, the exergy efficiency and total thermal conductance are two compromising objective functions. As the exergy efficiency increases the total thermal

conductance increases also. The overall range of exergy efficiencies and total thermal conductance of reheat ORC with all organic fluids are 11.52-42.40% and 29.34-170.44 kW.K^{-1}, respectively. The maximum exergy efficiency is 42.40 % for propyne, and the minimum thermal conductance is 29.34 kW.K^{-1} for R236ea. It can be concluded that, R236ea has the smallest total thermal conductance when the exergy range is between 20-39%, among the selected organic fluids and R152a has the highest total thermal conductance at the same exergy range. At the higher end of the exergy range efficiency (39-42.40%), propyne shows optimal performance, followed by cyclopropane and dimethyl ether while, R152a has the largest thermal conductance compared to R236ea and R600a. As can be observed in **Figure 3.18**, the optimal point is picked with the TOPSIS method.

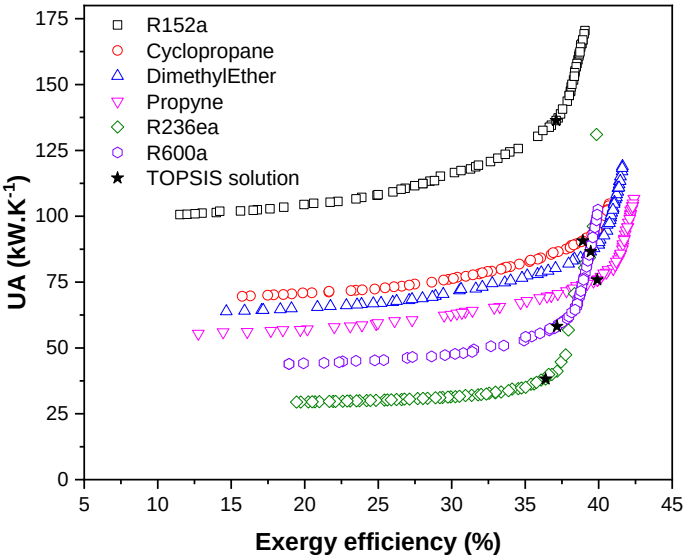

Figure 3.18 *Pareto-frontier (optimal solutions) for candidate working fluids (ORC without IHE).*

In cases where the working fluid leaving the turbine is in the vapour phase, an IHE is added to the cycle to recover waste heat from the superheated turbine exhaust. It reduces the heat needed to preheat the fluid before it enters the evaporator and the amount of heat discharged by the working fluid at the condenser. The IHE effectiveness was considered as a decision variable and assumed to vary between 0.6 and 0.9 [125].

Optimal Pareto-fronts for reheat ORC (with IHE) were obtained in **Figure 3.19**. It is obvious that dry and isentropic fluids exhibit the best performance compared to wet fluids. The results reveal that a maximum of 49.1 % exergetic efficiency can be achieved by the reheat ORC-IHE system, which corresponds to a 13.6% improvement compared to the system without IHE. The off-spring diversity of dry and isentropic fluids is much larger than wet fluids. Narrow ranges of exergy efficiency of wet fluids lead to a limited distribution of thermal conductance. Thus, there is limited optimization space for wet fluids. This confirms that the integration of IHE is more effective for dry and isentropic fluids. As can be seen in **Figure 3.19**, the exergy efficiency and the total thermal conductance of dry and isentropic fluids fall in the range from 23% to 49.1% and 27.55 kW.K^{-1} to 82.6 kW.K^{-1}, respectively. The exergy efficiency and the total thermal conductance of wet fluids range from 29.8 % to 47.04 % and 66.24 kW.K^{-1} to 185.8 kW.K^{-1}, respectively.

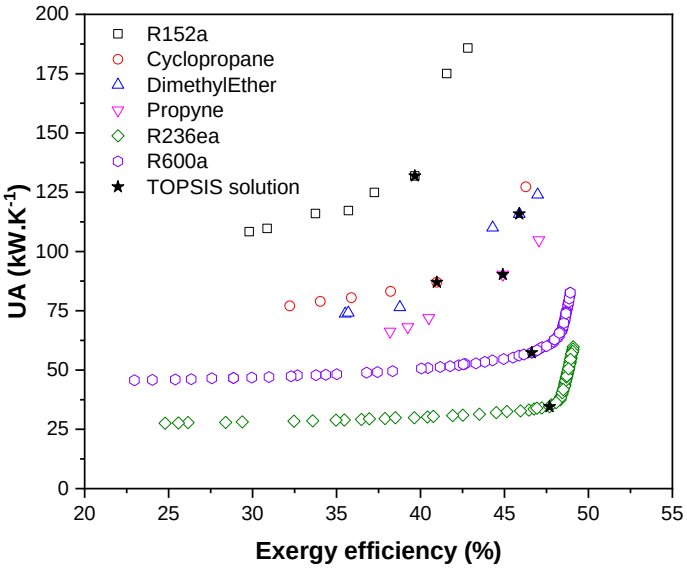

Figure 3.19 *Pareto-frontier (optimal solutions) for candidate working fluids (ORC with IHE).*

The results of reheat ORC without IHE parameters for all fluids are tabulated in **Table 3-5**. While the optimized parameters of ORC with IHE as well as the values obtained for the objective functions are listed in **Table 3-6**. For reheat ORC without IHE, results indicate that wet fluids need a higher superheat degree than dry and isentropic fluids. Further it can be observed that, the PPTD in evaporator reaches its upper bound, while the optimum PPTD in condenser approaches its lower bound for all fluids. R236ea has the lowest exergy efficiency, total thermal conductance and power output. R152a produces more power output with a higher thermal conductance, while propyne has the optimal exergy efficiency among all fluids. The reheat pressures of the selected working fluids were optimized to maximize the exergy efficiency and minimize the total thermal conductance. The reheat pressure ranges 45-54% of the evaporation pressure for the optimal condition.

It is interesting to note that the reheat ORC with IHE has higher superheat degree compared to the system without IHE. Furthermore, it can be noted in **table 3-6** that the optimal IHE effectiveness locates in the range of 0.83-0.89 for selected working fluids. The gain in exergy efficiency of the ORC-IHE using R236ea and R245fa is 23.7% and 20.2% compared to the ORC without IHE. As seen from tables **3-5 and 3-6**, comparing the values of net power output of both systems, wet fluids produce higher net power output compared to dry and isentropic fluids. Further, the ORC with IHE has a substantial amount of waste heat still available in its exhaust gas outlet. This is mainly caused by the higher inlet temperature of the working fluid in the economizer due to the heat absorbed by the working fluid in the IHE. Therefore, in order to improve the overall system performance, the exhaust gas can be further utilized e.g. combined heat and power applications. The thermal conductance for R236ea is quite less compared to other working fluids and the desired increase in the exergetic efficiency highlights it as the optimal choice for ORC with IHE. The optimum reheat pressure to evaporation pressure ratio is between 0.27–0.48 for studied working fluid.

Table 3-5 *Optimum values of objectives and design parameters obtained from TOPSIS solutions (ORC without ORC).*

Optimum parameters	**Working fluids**					
	R152a	Cyclopropane	Dimethyl ether	Propyne	R236ea	R600a
Evaporation pressure (bar)	39.83	47.27	47.15	49.67	30.18	32.38
Reheat pressure (bar)	21.61	23.74	23.26	22.42	14.75	15.85
Superheat degree (°C)	19.95	18.23	18.87	15.22	10.60	14.96
PPTD evaporator (°C)	9.88	9.97	9.96	9.93	9.98	9.97
PPTD pp condenser (°C)	5.05	5.06	5.03	5.07	5.22	5.22
Exergy efficiency (%)	37.10	38.92	39.46	39.91	36.39	37.16
UA (kW/°C)	136.31	75.98	86.58	75.83	38.23	58.16
Power output (kW)	83.23	63.22	60.57	54.81	28.09	41.55
Reheat pressure to turbine inlet pressure ratio	0.54	0.50	0.49	0.45	0.48	0.48
Hot gas outlet temperature (°C)	90.77	110.14	112.66	117.14	132.34	123.7

Table 3-6 *Optimum values of objectives and design parameters obtained from TOPSIS solutions (ORC with IHE).*

Optimum parameters	Working fluids					
	R152a	Cyclopropane	Dimethyl ether	Propyne	R236ea	R600a
Evaporation pressure (bar)	39.98	48.95	46.79	49.16	30.60	32.03
Reheat pressure (bar)	16.61	14.47	22.73	19.02	9.56	8.84
Superheat degree (°C)	19.64	19.63	19.12	19.57	12.78	17.59
PPTD evaporator (°C)	9.47	9.19	5.83	7.41	9.96	9.97
PPTD pp condenser (°C)	5.29	5.38	5.06	5.38	5.01	5.01
IHE effectiveness	0.86	0.83	0.85	0.85	0.89	0.89
Exergy efficiency (%)	39.66	40.97	45.88	44.90	47.69	46.62
UA (kW/°C)	131.85	87.03	115.83	90.28	34.53	57.29
Power output (kW)	76.73	55.35	73.24	60.18	23.31	37.14
Reheat pressure to turbine inlet pressure ratio	0.41	0.29	0.48	0.38	0.32	0.27
Hot gas outlet temperature (°C)	101.26	117.91	111.17	118.22	139.12	131.87

The percentage of exergy destruction in the ORC components with different fluids and with and without IHE is shown in **figure 3.20** and **3.21**. **Figure 3.20** and **3.21** prove that the evaporator and condenser are the components with the highest exergy destruction contribution, respectively. Besides, exergy destruction in the pump is low, accounting for only 2-4% of the total exergy destruction, which can be ignored. In addition it can be seen that the ORCs with IHE represent the lower exergy destruction of evaporator and expander. This exergy reduction is mainly due to the presence of the IHE. These results show that, evaporator and condenser must be better designed to decrease the exergy destructions in these components.

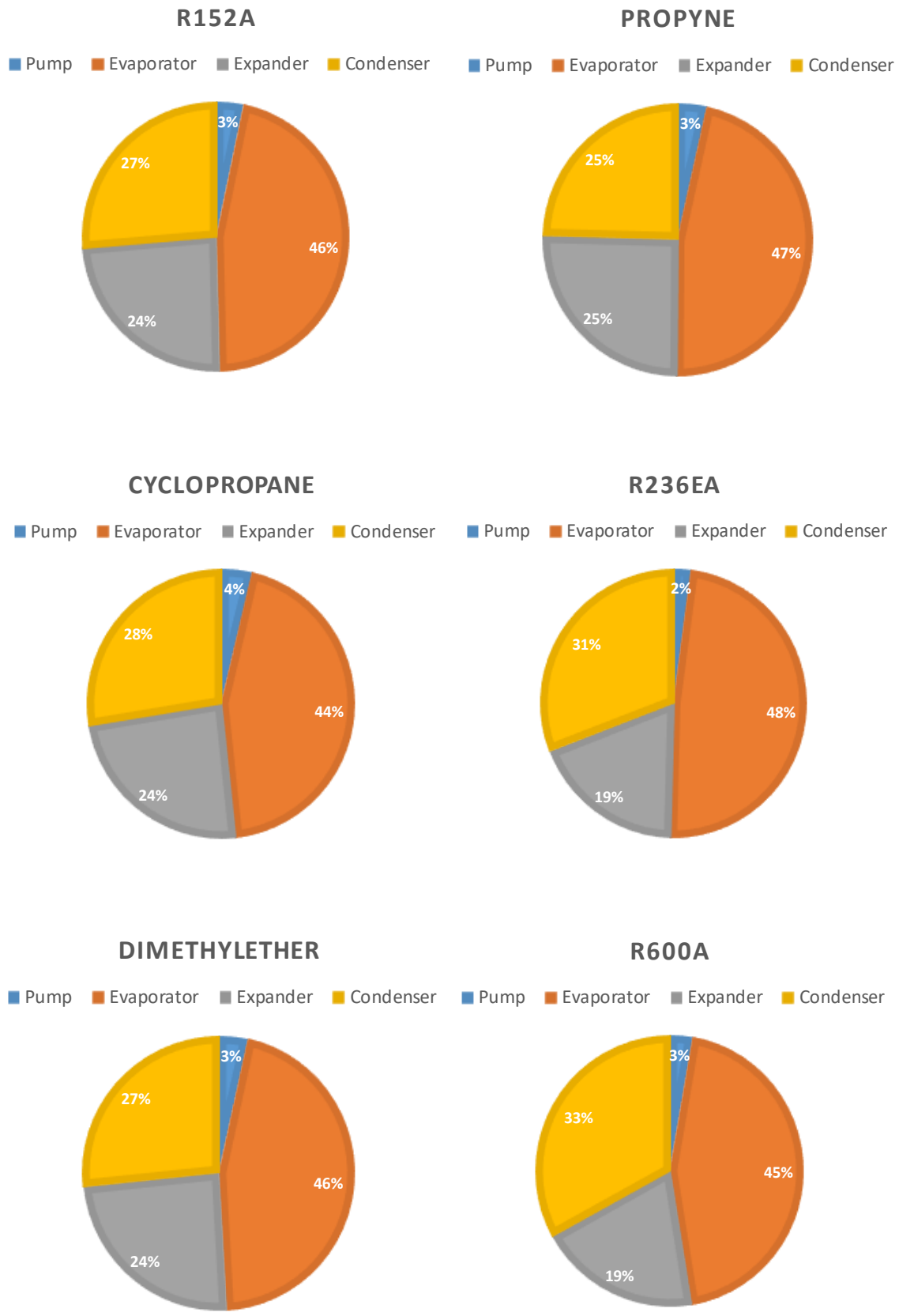

Figure 3.20 *Percentage of the exergy destruction in the reheat ORC components with different working fluids.*

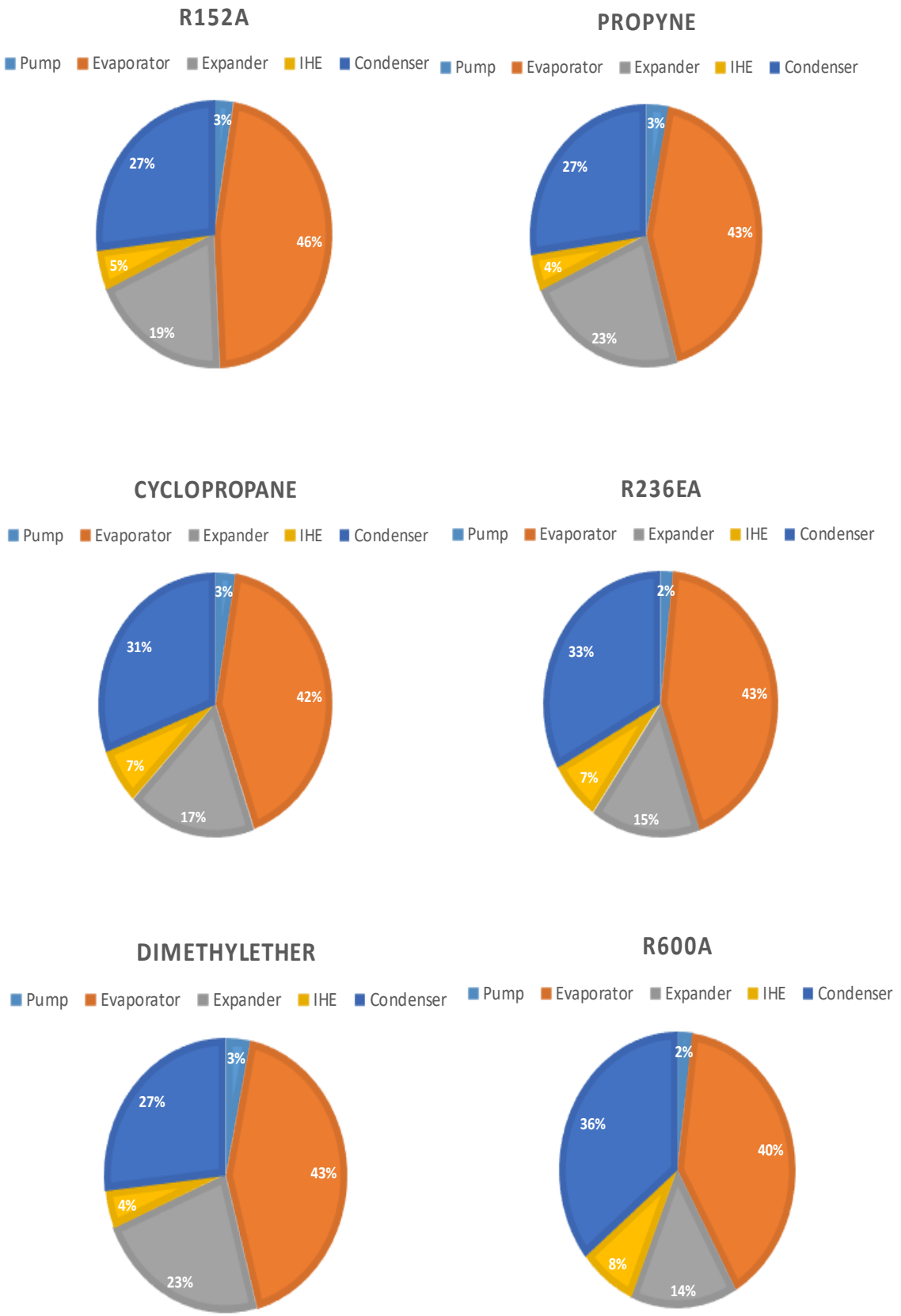

Figure 3.21 *Percentage of the exergy destruction in the reheat ORC-IHE components with different working fluids*

3.4. Conclusion

In this work, the performance analysis and optimization of a reheat ORC is investigated to recuperate low-grade heat source using six different organic fluids (R152a, cyclopropane, dimethyl ether, propyne, R236ea and R600a). The system optimization is performed using NSGA-II by considering exergy efficiency and total thermal conductance as objective functions and evaporation pressure, reheat pressure, superheating degree, PPTD and IHE effectiveness as decision variables. The essential conclusions obtained from the study are:

The parametric study indicates that for each working fluid there is an optimal evaporation pressure, which simultaneously maximizes and minimizes the exergy efficiency and total thermal conductance, respectively. The increase of reheat pressure increases the exergy efficiency, total thermal conductance value and power output. Wet fluids produce more power output compared to dry and isentropic fluids. In the case of wet fluids, superheat has a positive impact on exergy efficiency, however, for dry and isentropic fluids the increase of superheat degree decreases the power output.

Considering the optimization outcomes, there is an optimal reheat pressure which maximizes the exergy efficiency and minimizes the total thermal conductance, the reheat pressure to evaporation pressure ratio ranges are 0.27-0.48 and 0.45- 0.54 for ORC with and without IHE, respectively. The optimum superheat degree approaches its upper bound for wet fluids. The gain in exergy efficiency of the ORC-IHE using R236ea and R245fa is 23.7% and 20.2% compared to the ORC without IHE. This confirms that the integration of IHE is more effective for dry and isentropic fluids compared to wet fluids. The results revealed that R236ea and propyne are the best working fluids for the ORC with and without IHE, respectively. The outlet temperatures of the hot gas in ORC with IHE was higher than those of basic that it can be further utilized e.g. combined heat and power applications.

The evaporator and condenser are the components with the highest exergy destruction contribution, respectively. The ORCs with IHE represent the lower exergy destruction of evaporator and expander. This exergy reduction is mainly due to the presence of the IHE. These results show that, evaporator and condenser must be better designed to decrease the exergy destructions in these components.

4. Thermo-economic optimization of different organic Rankine cycle configurations

4.1. Introduction

The performance of ORCs is affected by heat source conditions [172,173], working fluid selection, heat sink conditions, cycle configuration and components [174] and process variables. The application of the ORC with IHE has also been proposed as a strategy to improve the efficiency of basic ORCs. Similarly to the case of ORC with IHE, in regenerative ORCs the working fluid is preheated before entering the evaporator. However, in contrast to ORC with IHE, the heat is provided via vapour that is extracted at an intermediate expansion stage. In the most commonly investigated variation of the regenerative ORC, the preheating occurs in an open-type heat exchanger, in which the sub-cooled liquid and vapour streams are mixed. In the same time, a large number of studies have focused on the thermo-economic assessment of ORC systems in order to improve some design parameters. The ORC components are sized according to the selected design points and boundary conditions. Some specific costs correlations are applied to each component to estimate the capital investment cost of the system and thereby evaluate its economic feasibility. The most common evaluation criteria include the specific investment cost, the Electricity Production Cost (EPC), and the payback period of the system. In the following, an overview of working fluid selection, along with a cycle configuration and optimization, is presented.

4.1.1. Working fluid selection

Astolfi et al. [122] compared the performance of subcritical/transcritical ORCs considering 54 working fluids and geothermal heat source (120–180 C). At 120 °C, 150 °C and 180 °C the highest exergy efficiency was achieved by R143a, RC318 and R236ea, respectively. The authors indicated that for most cases, the optimum cycle performance was reached when the ratio between the critical temperature of the working fluid and the temperature of the heat source was 0.88-0.92. Furthermore, among fluids with a similar critical temperature, fluids with high molecular complexity are preferable because of the possibility to reduce the average temperature difference in the evaporator, therefore limiting the exergy losses.

Xinxin et al. [175] studied the effect of turning point on the performance of an ORC. They used the model of near-critical region-triangle to evaluate the performance of 57 dry and isentropic fluids. The performance includes the relation between turning point temperature and cycle thermal efficiency, the relation between near-critical region triangle area and exergy at turning point temperature. Furthermore, working fluid selection was also conducted in terms of heat source type. The authors pointed out that R123 and dodecane are good candidates for the closed and open type heat sources, respectively.

Chen et al. [176] used the reduced temperature to predict the ORC performance and select the optimal working fluid under multiple heat source temperatures. Eighteen organic working fluids with critical temperature from 100 to 200 °C are evaluated. The authors found that as the heat source temperature gets closer to the critical temperature of the working fluid, the maximum exergy efficiency is obtained. R236ea, R245fa, R245ca and R365mfc were selected as the optimal working fluids for 130 °C, 150 °C, 170 °C and 190 °C, respectively.

Rad et al. [177] performed a study on the energetic and exergetic performance of basic ORC for waste heat from industrial complexes with temperature in the range of 120–300 °C. According to the results, a heat source temperature of 120 °C had the highest energy and exergy efficiencies for working fluid of R245fa. Also, the optimum working fluids for the heat source temperatures of 150 and 200 °C were R152a and R141b, respectively. Furthermore, for the heat source temperatures of 250 and 300 °C, benzene and water had the highest efficiencies, respectively. They also noted that a fluid with the nearest critical temperature to the heat source temperature must be selected as the appropriate working fluid.

Kose et al. [178] carried out a thermodynamic performance analysis of a triple combined system (gas turbine-steam Rankine cycle-ORC). Although the authors evaluated the performance of both the steam and organic Rankine cycle for different operating conditions, they did not optimize either the steam or organic Rankine cycle parameters. By using R141b as the working fluid, they calculated that the system thermal and exergetic efficiencies equal to 47.65 % and 67.35 %, respectively. By this way, the waste heat recovery corresponding to 734.57 kg/h natural gas which is equivalent to 2203.73 kg-CO2/h emissions was carried out.

Based on the economic and the environmental assessment, the comparison from aspects of both thermodynamic performance and economic factors using R245fa, R12333zd(E), R1234ze(Z) and R1366mzz(E) have been analysed by Ye et al. [179]. The authors revealed that R12333zd(E) has the best performance followed by R1234ze(Z), R1366mzz(E) and R245fa based on the economic and environmental assessment. The evaporation and condensing temperature and superheat has a crucial effect on the performance and cost. In addition, the evaporation and condensing temperature and superheat have a crucial effect on the performance and cost. Furthermore, The physical properties of R1233zd(E) and R245fa are extremely approximate, which makes R1233zd(E) be an alternative refrigerant without redesigning components of ORC system.

Wang et al. [180] examined the environmental and economic performance of a basic ORC driven by waste heat, considering waste heat source temperature (90–230 °C) and 14 working fluids. The authors performed parametric study to analyse the matching relationship between the heat source temperatures and corresponding fluids. The results showed that ORCs with lower global warming potential fluids generated lower greenhouse gas emissions. Regarding the environmental benefits, R600a exhibited the maximum greenhouse gas emission reduction at a heat-source temperature of 150 °C, followed by R152a, R600, and R601a, respectively. Whereas the suitable working fluid corresponding to the best economic performance was R245fa.

Yang et al. [181] investigated the performance of five low-GWP fluids in ORC with an energetic-economic-environmental model. R1233zd(E), R1234ze(Z), R1336mzz(Z) and R1224yd(Z) are proposed as potential drop-in replacements to R245fa because of extremely

low GWPs. The heat source was exhaust gas at 150 °C, with a mass flow rate of 0.33 kg/s. As a result, they observed that both the cycle thermal efficiency and the economic indicators are sensitive to evaporator outlet temperature, compared to the rest variables. R1224yd(Z) shows the highest cycle thermal efficiency around 15.9%, which is 11.2% higher than R245fa; Concerning the economic cost, R1234ze(Z) saves 9.85% more than R245fa.

Alshammari et al. [182] carried out a comparative assessment of the effects of working fluid types on the performance of basic ORC coupled with 7.25ℓ heavy-duty diesel engine. The considered working fluids are R123 (dry), R21 (wet) and R141b (isentropic). The system is analysed under superheated conditions and near saturated vapour curve, at various operating conditions. The authors revealed that wet fluids offer attractive cycle performance in the superheated region, while near the saturated vapour curve, isentropic fluids are found to present best cycle performance.

4.1.2. Cycle configuration

Bina et al. [183] applied thermo-economic analysis to four different ORCs, using dry organic fluid as working fluid. These cycles were designed to use the geothermal energy as a heat source. Evaluations were made to determine the effects of important operating parameters such as turbine inlet pressure, condenser temperature, pinch point temperature and mass flow rate of geo-fluid on energy and exergy efficiencies, as well as total production cost. Among cycles, the maximum energy and exergy efficiency of 20.57% and 63.72% were calculated in the ORC-IHE. Whereas the lowest energy production cost and the lowest total energy cost were calculated to be related to the regenerative and basic ORCs, respectively.

Liu et al. [184] studied different ORC layouts including basic ORC, ORC with IHE and regenerative ORC with four different working fluids. The authors reported that the optimal layout of ORC systems vary with the performance indices of ORC system. The optimal layout for thermal efficiency is regenerative cycle with R123, and the optimal configuration for capital cost is superheated ORC with R123. The optimal scheme for the index of power output and exergy efficiency is superheated with R152a when the geothermal temperature varies from 80–85 °C. However, the superheated configuration with R134a is better for power output and exergy efficiency when the geothermal temperature increased to 95 °C.

Braimakis and Karellas [185] conducted an energetic analysis of different ORC configurations applied for waste heat energy utilization. They compared the performance of three regenerative ORCs operating with different working fluids to that of a basic ORC. The authors concluded that both recuperative and regenerative ORCs perform significantly better for drier fluids. Moreover, the recuperative basic ORC cycle performs better than the non-recuperative regenerative ORCs from both energetic and economic aspects, but the recuperative regenerative ORCs are better than the recuperative basic ORC from thermodynamic point of view.

Gholizadeh et al. [186] integrated a gas turbine cycle and an ORC to extract more power by the waste heat of the gas turbine cycle. Two configuration of ORCs including basic and regenerative was selected and the influence of several parameters on the thermodynamic and thermo-economic system performance were discussed. The results revealed that the combined gas turbine-basic ORC and gas turbine-regenerative ORC systems could produce net output

electricity of 1308 kW and 1368 kW, respectively. Furthermore, the thermal and exergy efficiency increase of regenerative ORC was equal to 4.39% and 4.4%, respectively, with a decrease in overall product cost of 0.25 $/GJ.

Jimenez- Arreola et al. [187] performed a comparative study of the dynamic behaviour of a direct and an indirect evaporator, with the purpose of recovering waste heat from the heavy-duty diesel engine, with the use of R245fa as working fluid. The authors reported that indirect evaporation has a much higher capability of damping the heat fluctuations, hence protecting the system from extreme changes in boundary conditions even when control measures are not present. However, direct evaporation has important advantages over indirect evaporation, mainly because of its considerably lower volume and potential for higher thermal efficiency.

Bademlioglu et al. [188] studied the thermodynamic performance of ORC-IHE; they examined the effect of nine parameters on the thermal and exergy efficiencies. The variance of analysis method is selected to obtain the contribution ratio of each parameter on the target function. They pointed out that evaporation temperature, expander efficiency, heat exchanger effectiveness and condensation temperature are the main process parameters which affect the thermodynamic performance of ORC system. The thermal and exergy efficiencies of the system are found as 18.1% and 65.52%, respectively.

4.1.3. Optimization

Multi-objective optimization has received much attention in recent studies. Imran et al. [124] compared and optimized various ORC systems including basic-ORC, ORC-IHE, and regenerative ORC for geothermal brine (160 °C, 5 kg/s). Six different working fluids have been selected to maximize the exergy efficiency and minimize the specific investment cost within logical limits of evaporation temperature, superheat degree and pinch-point temperature difference (PPTD). For exergy efficiency < 45%, the basic ORC is the most appropriate configuration; however, the regenerative ORC shows the best performance for exergy efficiencies over 45%.

Wang et al. [125] performed an exergo-economic analysis, bi-objective optimization and grey-relational analysis on basic, recuperative and extractive ORCs for medium temperature geothermal applications. Their results revealed that from both thermo-economic points of view the basic ORC performed better than the other two cycles when using R245fa as working fluid. Meanwhile, R141b found to give the best performance among all fluids.

Turgut and Turgut [189] have optimized two ORC configurations including basic and regenerative ORCs by considering exergy efficiency and specific investment cost as objective functions. Twelve different organic fluids were used for each system configuration, and results revealed that the R600 and R245fa gave the best performance of basic and regenerative CROs, respectively.

Hu et al. [190] performed a multi-objective optimization to select the optimum working fluid and working conditions of basic ORC. The ratio of heat source mass flow rate to net power output and total investment cost were considered. It concluded that the evaporation temperature is the most parameter that affects the thermo-economic performance, however lower super heat degree is more attractive for the system performance.

Wang et al. [191] presented a multi-objective optimization of basic ORC and selected the investment cost per unit power and exergy efficiency as objectives. They pointed that the increase of superheat degree has a positive effect on net power output and investment cost per unit power, while thermal and exergy efficiencies decrease with the rise of superheat degree.

Herrera-Orozco et al. [192] carried out a multi-objective optimization of a basic and recuperative ORC system considering 15 working fluids. They revealed that the heat exchangers exhibit the highest exergy destruction, while (Toluene-ORC-IHE) is selected as the best couple (working fluid-cycle configuration).

From the previous studies, the performance of ORC is strongly affected by the working fluid type, cycle configuration and superheat degree. However, there is a lack of studies on the comprehensive effect of the type of working fluid on ORC configuration. It can be noted that most studies do not consider wet fluids in order to avoid turbine blades damage which under particular pressure and temperature conditions can occur at or near the trailing edge of the turbine rotor (i.e., at rotor outlet). However the performance advantage of wet fluids is demonstrated when in superheated condition [182,184]. Moreover, there is a still need on studies, which combines exergy efficiency and net power output with EPC to compare the performance of different ORC configurations. Furthermore, the thermo-economic performance of recuperative and regenerative systems has not been sufficiently investigated in many indexes (exergy efficiency, electricity production cost and net power output), while the relationship between the optimal evaporation temperatures to the inlet temperature of the heat source ratio for these configurations needs to be determined.

The main objectives of the present chapter are given below:

- To perform a thermo-economic optimization of a basic-ORC, ORC-IHE and regenerative ORC with the use of a low-grade heat source. Two case studies are investigated, the first is to use exergy efficiency and EPC together as objectives, and the second combines the net power output and EPC.
- For each case study and (working fluid-cycle configuration), a technique for order preference by similarity to ideal situation (TOPSIS) is applied to define an optimum solution between the Pareto solutions.
- To compare the cycle configurations and indicate the best couple (working fluid type - cycle configuration).
- To investigate the relationship between the optimal evaporation temperatures to the inlet temperature of the heat source ratio.

4.2. Methodology

With ongoing efforts in the industrial sector to improve energy efficiency, recovering and converting industrial waste heat into electricity offers an interesting opportunity for a lower cost, emission-free energy source. As mentioned in [193], more than 50% of the waste heat in industrial processes is classified as low-grade waste heat, which is generally below 300–350°C. An example of an application of waste heat utilization is the exhaust gases for melting glass fibers, whose temperature ranges (140–160°C) [193]. The ORC is most appropriate for heat sources at relatively low temperatures. It generally employs fluids that are more volatile than

water, which allows operating pressures at lower temperatures than the traditional Rankine cycle.

4.2.1. System description

Figure 4.1 presents the main components and *T-s* chart of the basic ORC. As **Figure 4.1** illustrates, the working fluid absorbs energy from the hot gas in the evaporator (2–3) which is then expanded in the turbine (3–4) to produce work. It is then cooled and condensed in the condenser (4-1) before it is pumped (1–2) back to the evaporator. The red line indicates the source of waste heat while the blue line indicates the coolant medium.

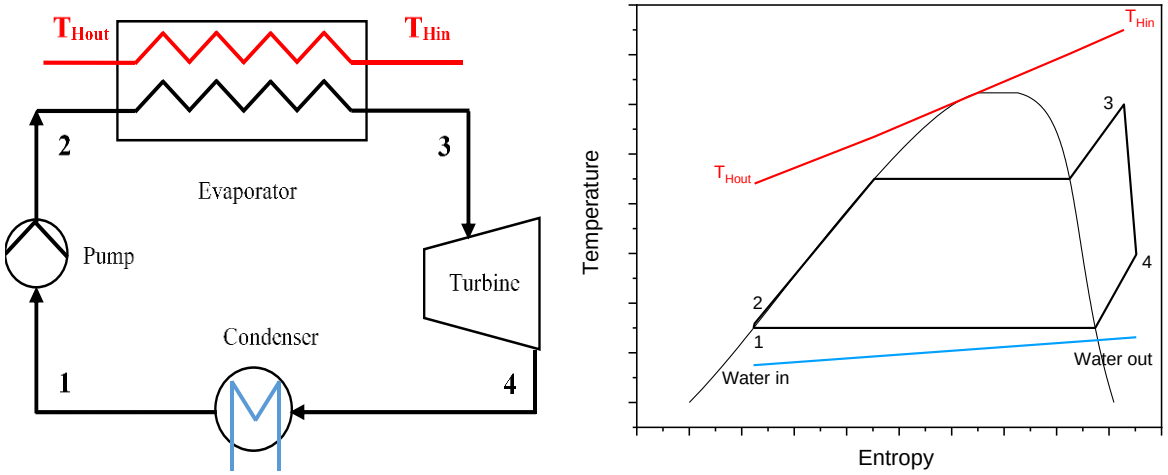

Figure 4.1 Schematic and T-s diagrams of basic ORC.

In cases where the working fluid at the turbine outlet is in the vapour phase, an IHE (2–3, 5–6) is added to the cycle to recover the energy of the liquid leaving the pump. The IHE reduces the heat required to preheat the fluid before it enters the evaporator and the amount of heat discharged by the working fluid at the condenser. This scheme is presented in **Figure 4.2**. Alternatively, to improve the performance of the basic-ORC, a part of the vapour is extracted from the turbine to the feed heater, to preheat the working fluid (2–3) before it enters the evaporator. The layout of the regenerative ORC and its *T–s* chart is demonstrated in **Figure 4. 3.**

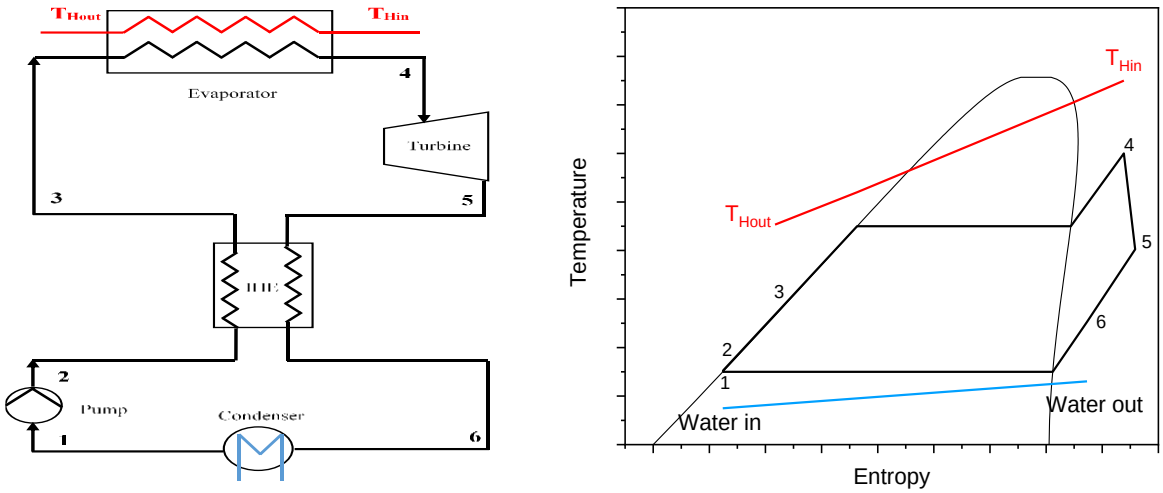

Figure 4.2 Schematic and T-s diagrams of ORC with IHE (ORC-IHE).

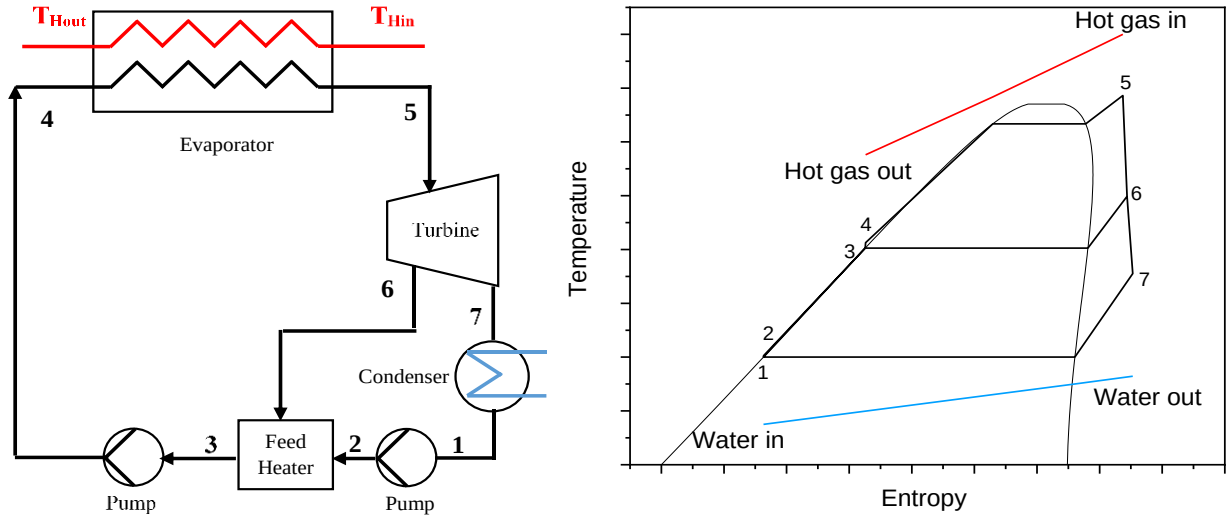

Figure 4.3 Schematic and T-s diagrams of regenerative ORC.

4.2.2. Thermodynamic model

For thermodynamic analysis, the ORCs were modelled based on the first and second-laws of thermodynamics. The following hypotheses are taken into consideration:

- The studied system operates in a steady state condition.
- Heat and friction losses in the heat exchangers and pipes are neglected.
- The heat source consists of exhaust gas at the exit of industrial boilers. The mass flow rate and inlet temperature of waste heat source are 10 kg.s^{-1} and 150°C, respectively [194]. In order to recover as much energy as possible and to avoid corrosion at low-temperatures, the outlet temperature of exhaust gas is fixed at its minimum allowed temperature 82°C [141].
- The turbine and pump isentropic efficiencies are 0.75 and 0.8, respectively. It is widely understood that pump efficiency can significantly suffer off-design and real-world operations can indicate very low efficiencies, but for the current model's rated point scenario it was considered satisfactory to assume 0.8 as a fixed value, in order to assess the stated working fluid and configuration architecture.
- The generator efficiency was assumed at 95%.
- Water at 20°C is used as a cooling medium; the condensation temperature is assumed as 30 °C.
- The thermo-physical properties of different organic-fluids are evaluated with CoolProp [195].

Table 4-1 summarizes the relations used in the first law analysis of the cycles.

The net output power of the system is defined as:

$$W_{net} = W_T - W_P \tag{4.1}$$

The thermal efficiency of the ORC system is calculated as follows:

$$\eta_{th} = \frac{W_{net}}{Q_{eva}} \tag{4.2}$$

The exergy flow is given by:

$$\dot{E}x = Q_{eva}(1-\frac{T_0}{T_H}) \tag{4.3}$$

T_0 Represents the ambient temperature and T_H is the logarithmic mean temperature of the hot source, which can be evaluated as follows:

$$T_H = \frac{T_{hot,in} - T_{hot,out}}{\ln(\frac{T_{hot,in}}{T_{hot,out}})} \tag{4.4}$$

Thus, the exergy efficiency of the system can be determined:

$$\eta_{ex} = \frac{W_{net}}{Q_{in}(1-\frac{T_0}{T_H})} \tag{4.5}$$

Table 4-1 *Thermo-economic models for different ORC configurations.*

Component	Model	Configuration
	Thermodynamic models	
Pump	$W_P = m_{wf}(h_2 - h_1)$	Basic ORC, ORC-IHE
	$W_P = m_{wf}[(1-X)(h_2 - h_1) + (h_4 - h_3)]$	Regenerative ORC
Evaporator	$Q_{eva} = m_{wf}(h_3 - h_2)$	Basic ORC
	$Q_{eva} = m_{wf}(h_4 - h_3)$	ORC-IHE
	$Q_{eva} = m_{wf}(h_5 - h_4)$	Regenerative ORC
Turbine	$W_T = m_{wf}(h_3 - h_4)$	Basic ORC
	$W_T = m_{wf}(h_4 - h_5)$	ORC-IHE
	$W_T = m_{wf}\left[(h_5 - h_6) + (1-X)(h_6 - h_7)\right]$	Regenerative ORC
Condenser	$Q_{con} = m_{wf}(h_4 - h_1)$	Basic ORC
	$Q_{con} = m_{wf}(h_6 - h_1)$	ORC-IHE
	$Q_{con} = m_{wf}(h_7 - h_1)$	Regenerative ORC
Open feed heater	$x = \dot{m}_6 / \dot{m}_5$	Regenerative ORC
	Economic models	
Evaporator/ Condenser	$\log_{10} C_p = K_1 + K_2 \log_{10}(A) + K_3(\log_{10}(A))^2$	
Turbine/ Pump	$\log_{10} C_p = K_1 + K_2 \log_{10}(W) + K_3(\log_{10}(W))^2$	
Generator	$C_{P,gen} = 60(W_{gen})^{0.95}$	
	$C_{BM} = C_p F_{BM}$	
	$F_{BM} = B_1 + B_2 F_M F_P$	
	$\log_{10} F_p = C_1 + C_2 \log_{10}(P) + F_3(\log_{10}(P))^2$	
The total cost	$C_{tot} = C_{BM,eva} + C_{BM,T} + C_{BM,con} + C_{BM,p} + C_{BM,gen}$	Basic ORC
	$C_{tot} = C_{BM,eva} + C_{BM,T} + C_{BM,con} + C_{BM,p} + C_{BM,IHE} + C_{BM,gen}$	ORC-IHE
	$C_{tot} = C_{BM,eva} + C_{BM,T} + C_{BM,con} + C_{BM,p} + C_{BM,FH} + C_{BM,gen}$	Regenerative ORC

To calculate the heat transfer area of evaporator, condenser and IHE, the logarithmic mean temperature difference (LMTD) method is used.

$$\Delta T_{LMTD} = \frac{\Delta T_{\max} - \Delta T_{\min}}{\ln(\frac{\Delta T_{\max}}{\Delta T_{\min}})} \tag{4.6}$$

ΔT_{LMTD} Represents the logarithmic mean temperature difference, while $\Delta T_{\max}$ and $\Delta T_{\min}$ represent the maximal and minimal temperature differences at the ends of the heat exchangers, respectively.

$$Q = UA\Delta T_{LMTD} \tag{4.7}$$

U and A is the overall coefficient of heat transfer and the heat transfer surface of the heat exchanger, respectively. The following values are taken as heat transfer coefficients for the evaporator, the condenser and the IHE 0.9, 1 and 0.2 kW/(m^{2}K) [196], respectively.

4.2.3. Economic model

A comprehensive detailed economic analysis is a very complex process, which depends on several specific criteria and varies from site to site and from time to time. As a result, the total cost of the ORC system will be estimated by the cost of the basic components, including heat exchangers, turbines and pumps [197]. It is important to note that the effect of the working-fluid cost on the total capital cost is small and the variation in working fluid mass flow rate with PPTD and evaporation temperature is slight. Consequently, the cost of the working-fluid is not taken into account in the work, as mentioned in reference [127,194].

Among the different correlations that are presented in this study, for many of the ORC components, the methodology presented by Turton [198] is applied for providing cost estimates. This methodology has been recently gaining popularity among ORC researchers [181,127,169]. According to the methodology, first the purchase cost of the equipment at ambient operating pressure and assuming carbon steel construction C_p is calculated from the equation:

$$\log_{10} C_p = K_1 + K_2 \log_{10}(X) + K_3(\log_{10}(X))^2 \tag{4.8}$$

Where, X is the capacity or size parameter of the equipment component (such as the area of a heat exchanger or the power capacity of pumps and compressors/turbines); K_1 , K_2 , K_3 , B_1 , B_2 are constants which are illustrated in **Table 4-2**.

The bare module cost is defined as:

$$C_{BM} = C_p F_{BM} \tag{4.9}$$

C_p is the purchase cost and F_{BM} is the bare module factor.

$$F_{BM} = B_1 + B_2 F_M F_P \tag{4.10}$$

Where F_M is the material factor; F_P is the pressure factor.

$$\log_{10} F_p = C_1 + C_2 \log_{10}(P) + F_3(\log_{10}(P))^2 \tag{4.11}$$

P is the operating pressure in bar; C_1, C_2 , C_3 are constant, listed in **Table 4-2**.

The total cost of the system is the summation of all components. The economic model for each component of the considered ORC configurations are given in **Table 4-1**.

$$C_{tot} = C_{BM,eva} + C_{BM,Tur} + C_{BM,cond} + C_{BM,p} \tag{4.12}$$

The chemical engineering plant cost index (CEPCI) is commonly used in estimating the construction cost at different periods; the total capital cost of the ORC system in 2018 is derived from:

$$C_{tot,2018} = C_{tot,2012} \cdot \frac{CEPCI_{2018}}{CEPCI_{2012}} \tag{4.13}$$

The Capital recovery factor (CRF) is the ratio of the annual payments to the present value. The CRF is estimated using the equation:

$$CRF = \frac{i(1+i)^{time}}{(1+i)^{time} - 1} \tag{4.14}$$

i means the interest rate which is set as 5 %, $time$ means the period of capital recovery which is set as 20 years.

The EPC can be expressed as follows:

$$EPC = \frac{CRF.C_{tot,2018} + C_{OM}}{W_{net}.h_{full-load}} \tag{4.15}$$

C_{OM} means maintenance and operation costs and assumed to be 2% of $C_{tot,2018}$. $h_{full-load}$ means the full load operation hours, which is set as 7500 h.

Table 4-2 Equipment cost parameters [198].

Equipment	K_1	K_2	K_3	C_1	C_2	C_3	B_1	B_2	F_m	F_{BM}
Pump	3.3892	0.0536	0.1538	0	0	0	1.89	1.35	1.5	
expander	2.2476	1.4965	-0.1618	0	0	0	/	/	/	3.3
evaporator	4.6656	-0.1557	0.1547	0	0	0	0.96	1.21	1	
condenser	4.6656	-0.1557	0.1547	0	0	0	0.96	1.21	1	

4.2.4. Selected working fluid

As declared before, the working-fluid choice is an important and critical factor in the design of the ORC system due to its effect on the performance of the cycle in addition to its environmental impact. The following criteria have to be taken into account when choosing a working fluid: safety, environmentally-friendliness and low-cost [156,157,199].

The selection criteria used in this work are:

- Little impact on environment (zero ODP and the GWP of the working fluid has to be lower than 1000).
- Fluids with critical temperature much higher than the heat source temperature were excluded. Fluids with a highly critical temperature above the evaporation temperature lead to a higher expansion pressure ratio and result in larger components [151].

Taking into account the precedent criteria, four wet fluids, three dry fluids and five isentropic fluids are selected. Their properties are shown in **Table 4-3**.

Table 4-3 Properties of working fluids.

Name	M (kg/kmol)	T_c (°C)	P_c (kPa)	GWP (100 years)	ODP	Fluid type
R152a	66	113.26	4450	124	0	Wet
Cyclopropane	42.08	125.15	5579.7	11	0	Wet
Dimethyl ether	46.07	127.23	5337	1	-	Wet
Propyne	40	129.23	5626	~20	0	Wet
R600a	58.12	134.67	3640	0	0	Dry
Butene	56.10	146.14	4005.1	-	-	Dry
R600	58	151.98	3796	~20	0	Dry
R124	136.48	122.28	3624	609	0.02	Isentropic
R236ea	152.04	139.29	3502	710	0	Isentropic
Isobutene	56.10	144.94	4009.8	-	-	Isentropic
R1234zez	114.04	150.12	3533	1	0	Isentropic
R245fa	134.05	153.86	3640	950	0	Isentropic

4.2.5. Validation

The present models are validated with the work of Zhang et al. [141] and Zare [200] using basic ORC-cyclopropane, ORC-IHE-cyclopropane and regenerative ORC-R600a as cycle configuration-working fluid combinations. The comparison between the obtained results and the results of the cited reference shows a very good agreement, as shown in Table 4. Thus, the proposed model was considered to be verified.

Table 4-4 Validation of the present ORC models.

ORC configuration		η_{th} (%)	η_{ex} (%)	W_{net} (kW)	m_{wf} (kg/s)	EPC ($/kWh)
Basic ORC	Present work	11	46	77.11	1.35	0.075
	[141]	11	46	76.32	1.39	0.074
ORC-IHE	Present work	11	44	73.44	1.57	0.094
	[141]	12	43	73.91	1.59	0.091
Regenerative ORC	Present work	14.97	53.92	2690	-	-
	[200]	14.96	52.94	2605	-	-

4.2.6. Optimization

The NSGA-II is selected for optimizing ORCs performance. **Table 4–5** outlines the application of multi-objective optimization for ORC cycle.

Defining appropriate objective functions is a crucial step in the optimization of ORCs. Taking only a thermodynamic function could lead to an uneconomical design. Thus, the economic considerations must be taken into account. According to Imran et al. [124] it exists a trade-off between the exergy efficiency, net power output and cost. Therefore, two case studies are investigated; in the first, the exergy efficiency and the EPC are selected as the objective functions, while the second deals with the net power output and EPC as objectives.

The first case

$$max(\eta_{ex}) = f_1 \quad (4.16)$$

$$\min(EPC) = f_2 \quad (4.17)$$

The second case

$$max(W_{net}) = f_1 \quad (4.18)$$

$$\min(EPC) = f_2 \quad (4.19)$$

The following system parameters are selected for the optimization of the ORC configurations: evaporation pressure, PPTD in evaporator and condenser, superheating degree, IHE effectiveness and intermediate pressure. The previous parameters have been chosen because of their strong influence on the system performance from both thermodynamic and economic point of view [201]. Experimentally, Abbas et al. [202] showed that both the evaporation pressure and PPTD are significant parameters affecting the thermodynamic performance of the ORC. In addition, the superheat degree can affect the ORC performance. According to [203] the increase of superheat degree can lead to improved thermal efficiency of the system, as well as protecting the turbine from damage. Lin et al. [204] practically tested a basic ORC, and noted that the pressure ratio and superheat degree show a significant sensitivity to the performance of the system. The decision variables and their bounds are listed in **Table 4–6**.

Table 4-5 Summary of optimization on ORC.

Refs.	Cycle configuration	Considered fluids	Objective function	Optimization Algorithm
[125]	Basic ORC ORC-IHE Regenerative ORC	Dry Isentropic Wet	-Exergy efficiency -Cost per net output power	NSGA-II
[205]	Basic ORC	Dry Wet	-Total investment cost -Mass flow rate of heat source per net power output	NSGA-II
[206]	Basic ORC ORC-IHE Transcritical ORC	Dry Isentropic Wet	-Exergy efficiency -Payback period	NSGA-II
[207]	Basic ORC	Dry	-Net power output - Total cost rate	NSGA-II
[208]	Basic ORC	Dry Isentropic	-thermal efficiency - Net revenue	Multi-objective genetic algorithm
[209]	Basic ORC	Dry	-Exergy efficiency -total heat transfer requirement	NSGA-II
[210]	Basic ORC	Dry Wet	-Exergy efficiency -Levelized energy cost	NSGA-II
[189]	Basic ORC Regenerative ORC	Dry Isentropic	-Exergy efficiency -Specific investment cost	Artificial Cooperative Search
[211]	Basic ORC	Dry	-Exergy efficiency -Levelized energy cost	NSGA-II

In the case of multi-objective optimization, the resulting solutions are a set of optimum points (Pareto front). In order to select the final solution from the optimum points, the TOPSIS method has to be used to select the final optimum one. [126]. The TOPSIS method selects the point closest to the positive optimal point on the Pareto-Optimal frontier as the optimal solution.

Table 4-6 Lower and upper bounds for the variables included in the optimization.

Variable	Lower bound	Upper bound
P_{eva}	$1.3*P_{con}$	$P_{sat}(T_c-10)$
P_{int}	$1.1*P_{con}$	$0.9*P_{sat}(T_c-10)$
ε_{IHE}	0.6	0.9
$T_{pp,eva}$	5	20
$T_{pp,con}$	5	10
T_{sup}	0	20

4.3. Results and discussion

In the present section, the results of the optimization process for the selected cases are reported and discussed. **Table 4–7** reports the TOPSIS solutions of the basic-ORC operated with different fluid types. As shown in **Table 4–7**, for the same working fluid the distribution of EPC with exergy efficiency and net power output is different. A performance comparison between studied cases with different fluids shows that case 2 gives the most satisfactory results. For the second case, the exhaust gas outlet temperature and the PPTD in the condenser hit minimum and maximum allowable limits, respectively. The degree of superheating varies with case study type and working fluid type.

The optimal PPTD on the evaporator is always below 10 °C, except for R152a, because of the critical temperature limitation. With respect to wet fluids, the optimal superheat degree approaches its upper bound. However, a variable superheat degree was remarked to be within a range of (0 – 8 °C) for dry and isentropic fluids except R124. It is important to point out that, in the second case, the working fluid must be superheated regardless of the type of working fluid, a similar remark was mentioned in [212]. In addition, the superheat temperatures are lower for the exergy efficiency case than the net power output case. The net power outputs of case 2 at optimal condition are increased by 4%, 4% and 7% for R245fa, R1234zez and Propyne, respectively. R236ea is seen to produce the highest net power output for case 1 with the minimum EPC, while Dimethyl ether delivers the maximum net power output for case 2, but also has the highest EPC of 0.119 $/kWh when power is maximized.

Figure 4.4 illustrates the influence of evaporating temperature on the net power output, exergy efficiency and the EPC with R1234zez as working fluid. A PPTD of 5°C is selected for both the evaporator and the condenser. A minimum value for the EPC is remarked around 105°C (dashed line) for the second case. However, this minimum does not coincide with maximum exergy efficiency of 50.76 % obtained at 111°C (solid line). As the evaporating temperature increases, the EPC decreases due to the increase in net power output. For each working fluid, there is a specific value for the evaporation temperature where the net power output is maximum and therefore, the EPC is at its minimum value. Moreover, as the evaporation temperature increases, the cost of the heat exchanger increases, but the increase in net power output is greater than the increase in the cost of the heat exchanger. The net output power dropped further after a specific value of the evaporation temperature (95°C in this case) and the heat exchanger cost increased - resulting in an increase in EPC. This observation can be extended to other working fluids and cycle configurations used in this investigation.

Table 4-7 Results of optimization for the ideal solutions for basic ORC (Works in kW, efficiencies in %, EPC $/kWh, temperature in °C).

Fluid	Objective function	T_{eva}	$PPTD_{eva}$	$PPTD_{con}$	T_{sup}	T_{out}	W_{net}	η_{ex}	EPC
R152a	Case 1	100.23	12.13	5.47	20	82	84.28	47.18	0.127
	Case 2	102.82	11.41	10.00	18.28	82	85.59	46.68	0.120
Cyclopropane	Case 1	111.39	5	7.08	19.52	87.07	87	51.11	0.124
	Case 2	105.81	5	10.00	19.12	82	90.49	49.35	0.119
Dimethyl ether	Case 1	111.72	5	6.36	20	86.63	87.08	51.10	0.124
	Case 2	107.16	5	10.00	18.53	82	90.51	49.36	0.119
Propyne	Case 1	112.49	5	6.70	19.54	91.27	83.31	51.63	0.125
	Case 2	108.09	5	10.00	4.27	82	90.25	49.22	0.120
R600a	Case 1	116.99	5	5.11	3.45	82.34	89.68	50.65	0.125
	Case 2	112.49	5.71	10.00	7.85	82	88.45	48.23	0.119
Butene	Case 1	111.68	5	5.55	1.95	85.57	86.8	50.56	0.125
	Case 2	108.11	5.12	10.00	2.13	82	89.62	48.87	0.118
R600	Case 1	111.08	5	5.40	0	84.10	87.72	50.37	0.124
	Case 2	107.55	5.57	10.00	2.41	82	88.59	48.31	0.117
R124	Case 1	111.55	8.24	6.17	14.29	82	87.38	48.82	0.123
	Case 2	111.57	6.94	10.00	19.49	82	87.92	47.95	0.119
R236ea	Case 1	117.66	5.17	6.11	0	82	89.74	50.14	0.122
	Case 2	113.35	5.67	9.92	6.00	82	87.89	47.95	0.118
Isobutene	Case 1	111.64	5	5.88	1.24	83.62	88.54	50.39	0.123
	Case 2	109.82	5	10.00	1.70	82	89.88	49.01	0.118
R1234zez	Case 1	111.27	5	6.12	4.58	87.77	85.22	50.76	0.123
	Case 2	105.13	5	10.00	7.63	82	89.47	48.79	0.116
R245fa	Case 1	114.05	5	5.02	0	87.65	84.87	50.84	0.125
	Case 2	107.42	5	9.81	6.64	82	88.82	48.49	0.117

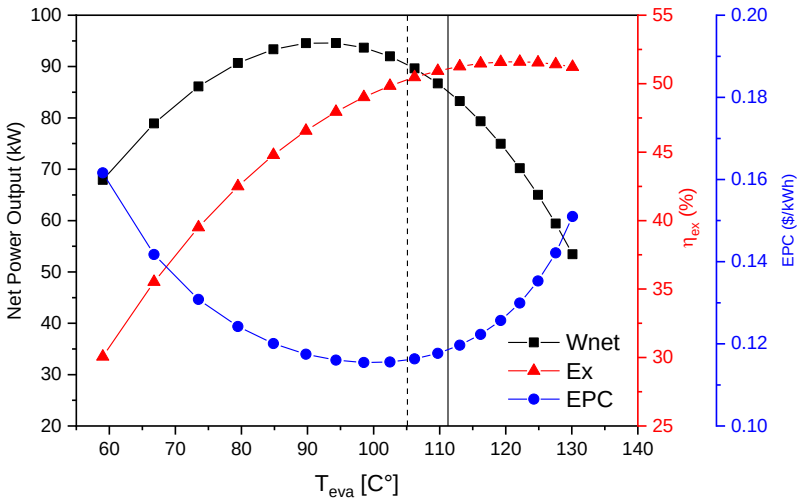

Figure 4.4 case 1 and case 2 optimum for R1234zez.

Table 4–8 reports the optimal values of the decision variables for the ORC with IHE. In this configuration, the EPC are considerably higher than for basic ORC, a consequence of the IHE addition. When optimized for case 1, the highest exergy efficiency is observed for dry and isentropic fluids. R124 delivers the highest net power output, however wet fluids can produce higher net power output compared to other working fluids. In comparison, the results obtained using the two cases are different. Firstly, the optimal superheat degree reaches upper bound for all fluids for the case 1, this means that the superheat is necessary even for dry and isentropic fluids when considering ORC-IHE a similar result is found in [157,213]. Secondly,

for the second case, the heat source temperature is cooled to the minimum cooling limit of 82°C indicating full utilization. Thus, more waste heat of the exhaust gas can be recuperated by the second case. It can be noted that the net power output of case 2 at optimal condition is higher than that of case 1 by 2–32% with low EPC of 0.6-20%, respectively. It is important to highlight that the increase in net power output is mainly due to the improved evaporating temperature matching with the heat source.

Table 4-8 *Results of optimization for the ideal solutions for ORC-IHE (Works in kW, efficiencies in %, EPC $/kWh, temperature in °C).*

Fluid	Objective function	T_{eva}	$PPTD_{eva}$	$PPTD_{con}$	T_{sup}	ε_{Rec}	T_{out}	W_{net}	η_{ex}	EPC
R152a	Case 1	102.12	10.14	5.20	20	0.64	82	88.37	49.48	0.155
	Case 2	99.83	11.38	9.38	18.40	0.72	82	86.33	47.27	0.154
Cyclopropane	Case 1	112.57	5.01	5.03	20	0.89	91.40	86.02	53.84	0.168
	Case 2	103.56	5.00	9.97	18.10	0.63	82	91.68	50.01	0.147
Dimethyl-ether	Case 1	112.96	5.01	5.01	20	0.81	91.04	86.04	53.61	0.162
	Case 2	105.14	5.00	9.86	16.58	0.67	82	91.98	50.20	0.148
Propyne	Case 1	116.61	5.01	5.01	20	0.83	97.09	79.26	53.71	0.169
	Case 2	100.53	5.00	9.92	19.09	0.72	82	90.93	49.62	0.149
R600a	Case 1	117.66	5.10	5.07	18.26	0.88	101.37	78.23	56.75	0.176
	Case 2	110.41	5.00	9.88	3.32	0.81	82	95.24	51.97	0.154
Butene	Case 1	122.15	5.14	5.06	20	0.90	111.06	65.59	57.36	0.188
	Case 2	102.06	5.01	9.98	7.58	0.73	82	91.95	50.15	0.149
R600	Case 1	122.97	5.11	5.10	19.88	0.90	113.88	62.54	58.38	0.194
	Case 2	103.72	5.01	9.80	0.95	0.80	82	93.15	50.86	0.152
R124	Case 1	110.94	5.03	5.45	19.85	0.78	86.14	93.36	54.73	0.156
	Case 2	110.13	6.19	9.84	12.42	0.78	82	95.24	51.99	0.151
R236ea	Case 1	116.19	5.03	5.43	18.87	0.87	100.93	78.79	56.66	0.172
	Case 2	109.71	5.02	9.95	1.29	0.88	82	96.35	52.61	0.157
Isobutene	Case 1	120.94	5.05	5.31	20	0.89	108.98	68.59	57.30	0.184
	Case 2	102.99	5.00	9.95	6.79	0.76	82	92.60	50.51	0.150
R1234zez	Case 1	113.57	5.04	5.20	19.89	0.80	100.29	78.27	55.75	0.163
	Case 2	102.11	5.00	9.56	5.60	0.74	82	92.03	50.31	0.147
R245fa	Case 1	116.15	5.10	5.28	19.05	0.87	104.19	74.64	56.81	0.172
	Case 2	103.72	5.01	9.96	2.38	0.74	82	93.15	50.81	0.147

Table 4–9 lists the results of the decision variables for the regenerative ORC. Referring to **Table 4–9**, for most of the working fluids, case 2 has lower value of the evaporation temperature than case 1. For wet fluids, operated optimally at a significant degree of superheating reaches its upper bound – an expected and well-known outcome. However, the pinch point in the condenser attains its upper bound for all working fluids. Compared to case 1, the EPC benefits that can be achieved by case 2 vary, from a minimum of 3% (R124) to a maximum of 15.54% (Isobutene). R124 produces the highest net power output for both cases, while isobutene delivers the highest exergetic efficiency. Clearly, the selection of net power output and EPC as objectives can be more attractive for ORC configurations, due to the full utilization of the possible heat in the exhaust gas and to the low EPC for all working fluids. Comparisons between these configurations using case 2 are provided in the next subsection.

Table 4-9 Results of optimization for the ideal solutions for ORC with IHE (Works in kW, efficiencies in %, EPC $/kWh, temperature in °C, pressure in bar).

Fluid	Objective function	T_{eva}	$PPTD_{eva}$	$PPTD_{con}$	T_{sup}	P_{int}	T_{out}	W_{net}	η_{ex}	EPC
R152a	Case 1	99.85	6.01	6.27	20	13.30	82	92.24	51.39	0.132
	Case 2	100.67	6.86	10.00	19.05	12.27	82	92.16	50.26	0.126
Cyclopropane	Case 1	112.37	5.03	7.80	18.20	13.79	93.91	84.20	53.76	0.133
	Case 2	99.02	5.00	10.00	17.02	12.78	82	91.27	49.81	0.127
Dimethyl-ether	Case 1	113.29	5.02	8.02	19.68	12.00	95.15	82.96	53.85	0.133
	Case 2	103.07	5.00	10.00	12.40	9.93	82	92.38	50.40	0.126
Propyne	Case 1	114.49	5.03	8.24	19.69	12.48	99.37	78.92	54.54	0.135
	Case 2	97.50	5.02	10.00	20	9.73	82	90.97	49.61	0.126
R600a	Case 1	117.02	5.03	6.75	0.18	7.26	89.03	88.69	53.47	0.132
	Case 2	104.42	6.23	10.00	3.64	6.87	82	91.25	49.76	0.126
Butene	Case 1	116.13	5.03	5.98	2.17	7.06	99.60	77.14	54.17	0.139
	Case 2	100.26	5.79	10.00	8.28	4.97	82	89.87	49.01	0.125
R600	Case 1	117.73	5.08	6.18	4.84	6.25	103.09	72.27	53.84	0.141
	Case 2	101.50	5.38	10.00	1.08	4.61	82	91.06	49.66	0.124
R124	Case 1	110.01	5.27	6.04	8.55	8.51	82	94.96	53.05	0.131
	Case 2	110.06	6.08	10.00	5.88	8.56	82	94.69	51.65	0.126
R236ea	Case 1	115.84	5.03	5.58	0.34	4.91	89.64	87.31	53.45	0.132
	Case 2	106.13	6.27	10.00	3.34	4.20	82	91.14	49.70	0.124
Isobutene	Case 1	120.63	5.06	5.19	8.53	8.06	106.80	68.19	54.69	0.148
	Case 2	99.76	5.06	10.00	9.80	5.87	82	90.25	49.22	0.125
R1234zez	Case 1	115.71	5.06	5.99	8.26	4.61	101.65	75.17	54.63	0.138
	Case 2	99.51	5.03	10.00	2.63	3.66	82	91.57	49.94	0.124
R245fa	Case 1	114.79	5.07	5.46	0.23	4.05	97.47	79.39	54.12	0.136
	Case 2	102.15	5.22	10.00	3.05	2.99	82	91.47	49.88	0.123

The net power output under the optimized conditions is shown in **Figure 4.5**. As seen from **Figure 4.5**, the ORC with IHE and the basic ORC have the highest and the lowest values of the net power output, respectively. By comparing the different configurations, it can be observed that the ORC-IHE exhibits the highest net power output for all dry and isentropic fluids. With respect to dry and isentropic fluids, ORC with IHE exhibits approximately 0.4-5% and 2.53-8.78 % higher net power output compared to regenerative ORC and basic ORC, respectively. In contrast to dry and isentropic fluids, regenerative ORC with wet fluids exhibits higher net power output as shown in **Figure 4.5** except for cyclopropane. The growth in net power output for wet fluids is associated with the higher mass flows in the system compared to other configurations. The largest net power output 96.3kW is obtained for ORC-IHE with R236ea. While the lowest net power output 85.59kW is obtained for basic-ORC with R152a as working fluid.

The EPC under the optimized conditions is presented in **Figure 4.6**. Throughout all three configurations, the basic-ORC exhibits the lowest EPC, followed by the regenerative configuration, while the ORC-IHE has the highest EPC. Moreover, the results reveal that the EPC is strongly affected by the cycle configuration, regardless of the working fluid type. The EPC of ORC-IHE ranges from 0.147 to 0.157$/kWh which is apparently higher than that of basic ORC and regenerative ORC ranging from 0.116 to 0.123$/kWh for different working fluids. It can be seen that ORC-IHE is 21–23% and regenerative ORC is about 5% higher EPC than that of basic ORC. For basic ORC using different working fluids, the lowest EPC 0.116$/kWh for R1234zez, and the highest net power output 90.51kW for dimethyl ether are obtained. R236ea was the best performance fluid in terms of the net power output while

cyclopropane, R1234zez and R245fa had the lowest EPC when considering ORC-IHE. On the other hand, wet fluids achieve relatively high performance for regenerative ORC, which makes them an attractive alternative for this configuration.

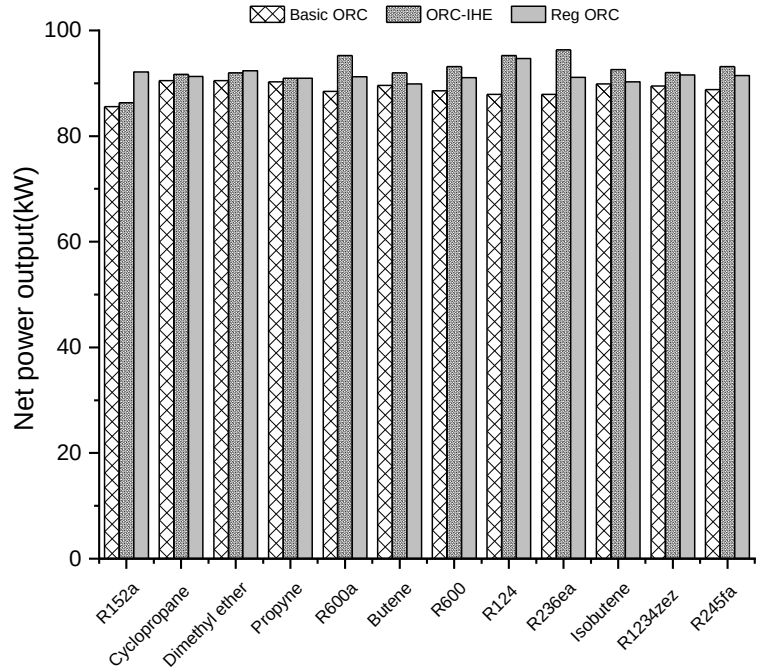

Figure 4.5 *Optimal net power output for the optimized configurations.*

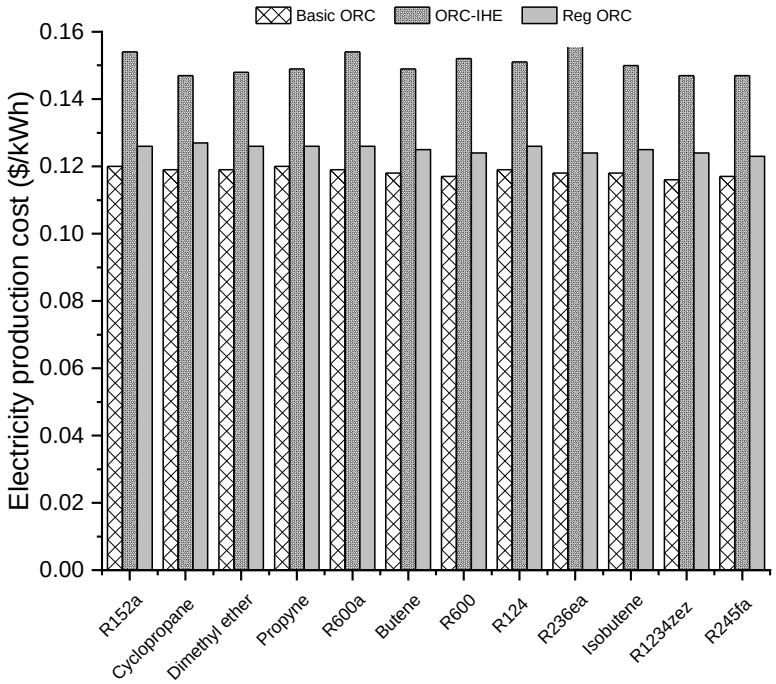

Figure 4.6 *optimal EPC for the optimized configurations.*

Figure 4.7 shows the evaporator temperature to inlet heat source temperature ratio for each one of the different simulated working fluids and cycle configurations, as a function of the critical temperature. As shown in **Figure 4.7**, the working fluids reaching the optimal

performance are those that present a T_{eva}/T_{hot} ratio between 0.68-0.75, 0.66-0.73 and 0.64-0.73 for basic-ORC, ORC-IHE and regenerative ORC, respectively. It is possible to note that for the different configurations considered, almost the same tendency is obtained with the T_{eva}/T_{hot} ratio. For ORC with IHE and regenerative ORC, working fluids with a T_{eva}/T_{hot} equal to 0.73 present a high net power output. This result can be explained by considering that all these fluids have a similar evaporation temperature and therefore a similar average temperature of heat input. For basic ORC, wet fluids (cyclopropane, dimethyl ether, propyne) exhibit the highest net power output, and this even exceeds that of dry and isentropic fluids.

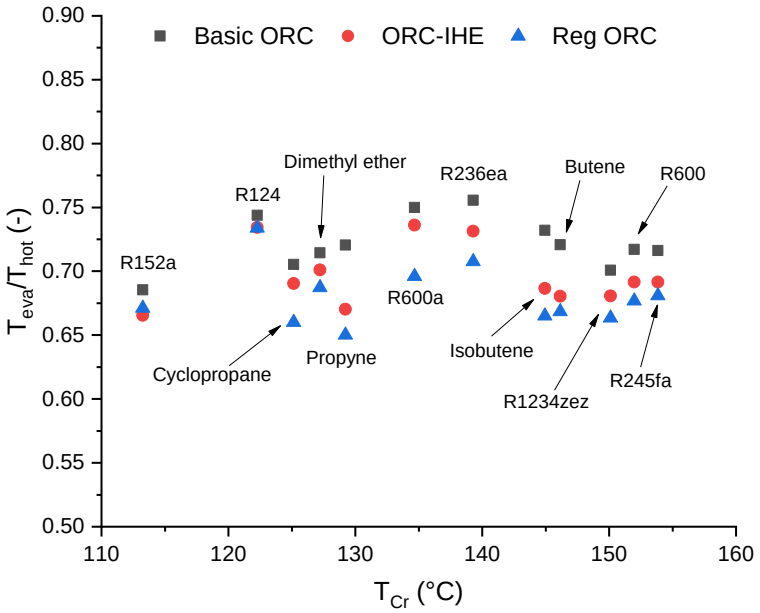

Figure 4.7 *optimal Teva/Thot with critical temperature in different ORC configurations.*

Figures 4.8-4.10 shows the contribution of each equipment in the total destroyed exergy, in the studied configurations. For each configuration two selected working fluid are presented, for the other working fluids their results are given in the appendix. It is observed that highest exergy destruction in evaporator followed by the expander. The major part of the exergy destruction has been developed in evaporator and expander due to larger temperature difference in heat addition and expansion processes. The integration of regenerative tank and reduces the exergy destruction rate of wet fluids. Whereas the addition of IHE improves the performance of dry and isentropic fluids.

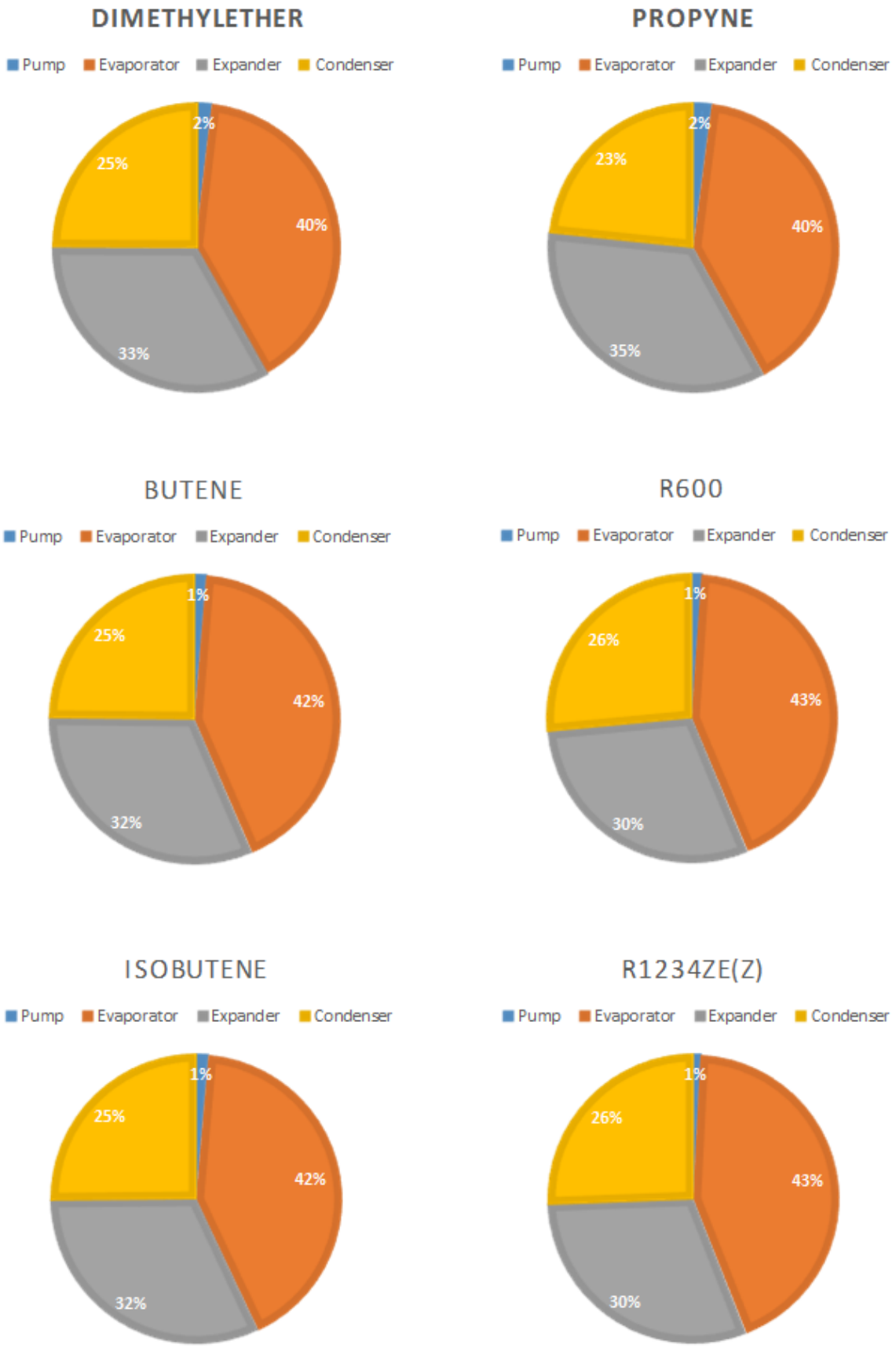

Figure 4.8 *Percentage of the exergy destruction in the basic ORC components.*

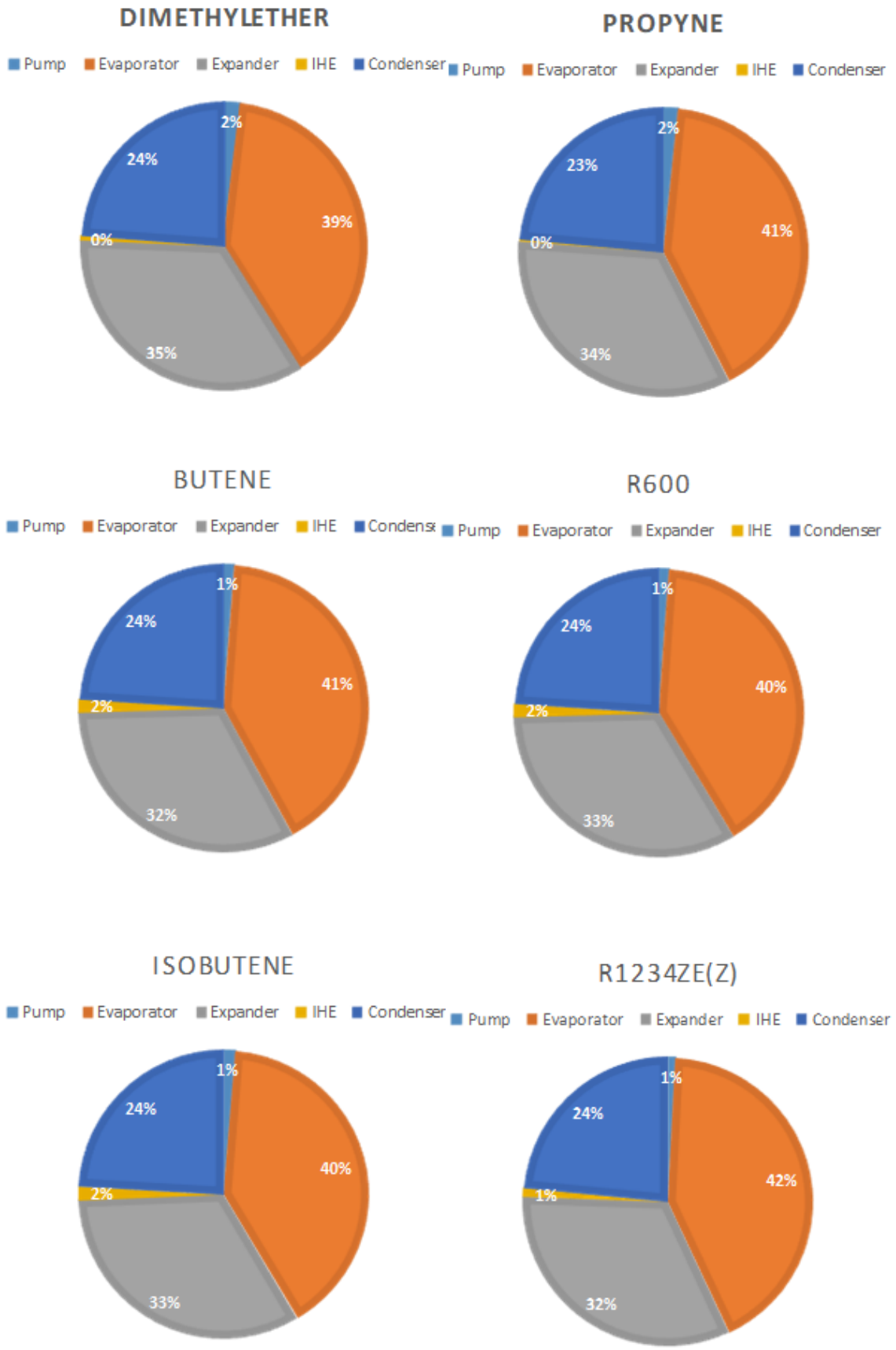

Figure 4.9 *Percentage of the exergy destruction in the ORC-IHE components.*

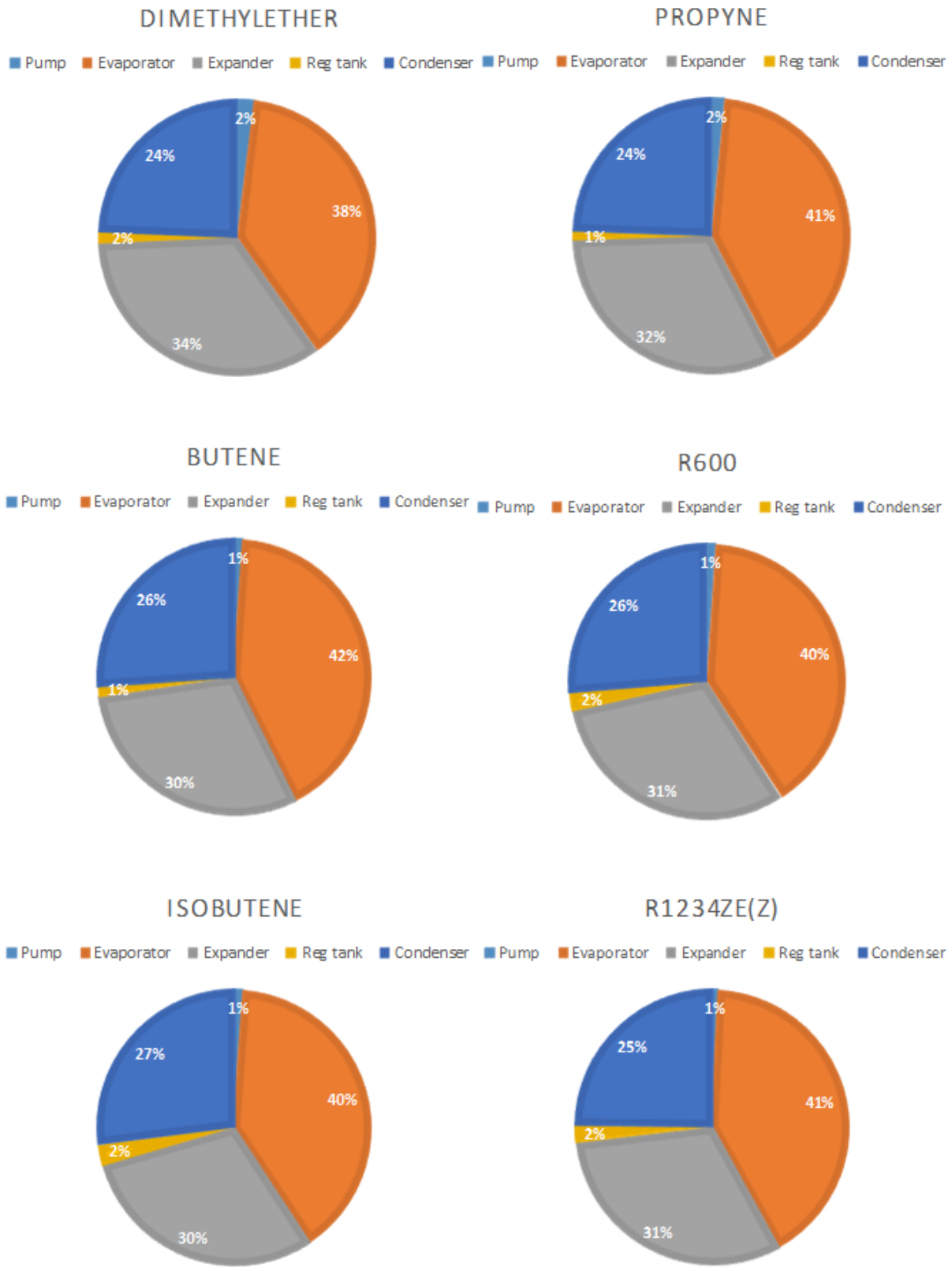

Figure 4.10 *Percentage of the exergy destruction in the regenerative ORC components.*

4.4. Conclusions

This study presented the multi-objective optimization of different ORC configurations and for different working fluid categories. The proposed optimization is conducted for two-cases; the first is the combination of exergy efficiency and EPC, the second is the combination of net output power and EPC. Twelve premium fluids were very carefully selected as working fluids after careful consideration of up-to-date literature, including dry, isentropic and wet fluids, for the selected configurations were investigated. The evaporation temperature, PPTD in the evaporator and condenser, superheat degree, IHE effectiveness and intermediate pressure were used as decision variables. The Pareto frontier of each case and (working fluid type-cycle configuration) is generated by applying the NSGA-II to the optimization problem and the best solution in the Pareto curve is selected by the TOPSIS method. The main conclusions are the following:

- According to the optimization results, the selection of net power output and EPC as objectives can be more attractive for ORC configurations, due to the full utilization of the possible heat in the exhaust gas and to the low EPC for all working fluids.
- Comparing the cycle configurations, ORC with IHE exhibits approximately 0.4-5% and 2.53-8.78 % higher net power output compared to regenerative ORC and basic ORC, respectively.
- For different ORC configurations, the basic ORC has the lowest EPC followed by the regenerative configuration, while the ORC-IHE has the highest EPC; the EPC is highly affected by the cycle configuration, regardless of the working fluid type.
- Wet fluids have better overall performance when operating in regenerative ORC configuration.
- It is found that, the working fluids that reach the optimal performance are those that have an optimal evaporation temperature to inlet temperature of the heat source ratio between 0.68-0.75, 0.66-0.73 and 0.64-0.73 for basic ORC, ORC with IHE and regenerative ORC, respectively.

Conclusion and future work

Currently, the recovery and conversion of low grade waste heat into electricity is attracting a lot of attention to improve the energy efficiency of industrial processes. In practice, a large amount of energy input is often wasted in the form of low or medium waste heat that cannot be economically converted into electricity by the conventional Rankine cycle but by an Organic Rankine Cycle (ORC). The recovery of this waste heat not only improves the energy efficiency of industrial processes, but also decreases the thermal pollution caused by the direct release of this heat into the environment. Starting from this context, the present implemented the thermo-economic modelling and optimization to recover industrial waste heat sources at low temperature using the ORC cycle.

Firstly, a bibliographical research on ORCs was carried out. For that, the operating principle and the evolution of the development of ORCs as well as the scientific knowledge of several configurations of the ORC cycle were presented. Actually, the subcritical ORC cycle is the most used configuration for waste heat recovery in industrial processes thanks to its simplicity, safety and stability of operation.

Regarding the evaluation of the thermodynamic performance of the ORC systems, energy and exergy analysis methods were used in this thesis. A comparison of the different configuration of the reheat ORCs considering exergy efficiency and total thermal conductance value as objective functions and evaporation pressure, reheat pressure, superheating degree, PPTD and IHE effectiveness as decision variables.

The parametric study indicates that for each working fluid there is an optimal evaporation pressure, which simultaneously maximizes and minimizes the exergy efficiency and total UA value, respectively. The increase of reheat pressure increases the exergy efficiency, total UA value and power output. Wet fluids produce more power output compared to dry and isentropic fluids. In the case of wet fluids, superheat has a positive impact on exergy efficiency, however, for dry and isentropic fluids the increase of superheat degree decreases the power output.

Considering the optimization outcomes, there is an optimal reheat pressure which maximizes the exergy efficiency and minimizes the total UA value, the reheat pressure to evaporation pressure ratio ranges are 0.27–0.48 and 0.45–0.54 for ORC with and without IHE, respectively. The optimum superheat degree approaches its upper bound for wet fluids. The gain in exergy efficiency of the ORC-IHE using R236ea and R245fa is 23.7% and 20.2% compared to the ORC without IHE. This confirms that the integration of IHE is more effective for dry and isentropic fluids compared to wet fluids. The results revealed that R236ea and propyne are the best working fluids for the ORC with and without IHE, respectively. The outlet temperatures of the hot gas in ORC with IHE was higher than those of basic that it can be further utilized e.g. combined heat and power applications.

In general, the feasibility of a waste heat recovery project can only be confirmed after its economic evaluation. A cost correlation for each component of an ORC system is used leading to the possibility to perform thermo-economic optimizations. Based on the thermo-economic optimizations, the selection of net power output and EPC as objectives can be more attractive for ORC configurations, due to the full utilization of the possible heat in the exhaust gas and to the low Electricity Production Cost (EPC) for all working fluids. Comparing the

cycle configurations, ORC with IHE exhibits approximately 0.4-5% and 2.53-8.78% higher net power output compared to regenerative ORC and basic ORC, respectively. For different ORC configurations, the basic ORC has the lowest EPC followed by the regenerative configuration, while the ORC-IHE has the highest EPC; the EPC is highly affected by the cycle configuration, regardless of the working fluid type. Wet fluids have better overall performance when operating in regenerative ORC configuration. It is found that, the working fluids that reach the optimal performance are those that have an optimal evaporation temperature to inlet temperature of the heat source ratio between 0.68-0.75, 0.66-0.73 and 0.64-0.73 for basic ORC, ORC with IHE and regenerative ORC, respectively.

Future work

Heat exchangers design: the integration of the code with simplified routines will allow achieving a higher level of detail removing some fixed assumptions at the basis of the present approach. Pressure drops and heat transfer coefficients won't be consider constant anymore and they will be linked to fluid properties.

Develop an integrated, accurate and flexible thermo-economic design and optimization methodology for ORC systems for a wide range of temperatures and heat source capacities.

The application of double stage ORCs can lead to substantial performance improvement compared to the basic cycle. However, the thermo-economic optimization of these configurations is a prerequisite for the complete evaluation of their cost competitiveness.

The experimental testing of the ORC will be crucial in demonstrating the technical feasibility, indicate potential performance improvement modifications (cycle configuration, working fluid mixture).

References

[1] International Energy Agency. World Energy Outlook 2021. OECD; 2021. https://doi.org/10.1787/14fcb638-en.

[2] Huijbregts MAJ, Rombouts LJA, Hellweg S, Frischknecht R, Hendriks AJ, van de Meent D, et al. Is Cumulative Fossil Energy Demand a Useful Indicator for the Environmental Performance of Products? Environ Sci Technol 2006;40:641–8. https://doi.org/10.1021/es051689g.

[3] Lamb WF, Wiedmann T, Pongratz J, Andrew R, Crippa M, Olivier JGJ, et al. A review of trends and drivers of greenhouse gas emissions by sector from 1990 to 2018. Environ Res Lett 2021;16:073005. https://doi.org/10.1088/1748-9326/abee4e.

[4] Kannan N, Vakeesan D. Solar energy for future world: - A review. Renewable and Sustainable Energy Reviews 2016;62:1092–105. https://doi.org/10.1016/j.rser.2016.05.022.

[5] Shoaib M, Siddiqui I, Rehman S, Khan S, Alhems LM. Assessment of wind energy potential using wind energy conversion system. Journal of Cleaner Production 2019;216:346–60. https://doi.org/10.1016/j.jclepro.2019.01.128.

[6] Moreira JR. Global Biomass Energy Potential. Mitig Adapt Strat Glob Change 2006;11:313–42. https://doi.org/10.1007/s11027-005-9003-8.

[7] Rubio-Maya C, Ambríz Díaz VM, Pastor Martínez E, Belman-Flores JM. Cascade utilization of low and medium enthalpy geothermal resources − A review. Renewable and Sustainable Energy Reviews 2015;52:689–716. https://doi.org/10.1016/j.rser.2015.07.162.

[8] Market Report Series: Energy Efficiency 2018. Paris: 2018.

[9] Heating – Analysis. IEA n.d. https://www.iea.org/reports/heating (accessed March 27, 2022).

[10] Clean and efficient heat for industry – Analysis. IEA n.d. https://www.iea.org/commentaries/clean-and-efficient-heat-for-industry (accessed March 27, 2022).

[11] Elsaid K, Taha Sayed E, Yousef BAA, Kamal Hussien Rabaia M, Ali Abdelkareem M, Olabi AG. Recent progress on the utilization of waste heat for desalination: A review. Energy Conversion and Management 2020;221:113105. https://doi.org/10.1016/j.enconman.2020.113105.

[12] Key Visualizations | Climate Watch n.d. https://www.climatewatchdata.org/ (accessed March 27, 2022).

[13] Wolf V, Bertrand A, Leyer S. Analysis of the thermodynamic performance of transcritical CO2 power cycle configurations for low grade waste heat recovery. Energy Reports 2022;8:4196–208. https://doi.org/10.1016/j.egyr.2022.03.040.

[14] Forman C, Muritala IK, Pardemann R, Meyer B. Estimating the global waste heat potential. Renewable and Sustainable Energy Reviews 2016;57:1568–79. https://doi.org/10.1016/j.rser.2015.12.192.

[15] Johnson I, Choate WT, Davidson A. Waste heat recovery. Technology and opportunities in US industry. BCS, Inc., Laurel, MD (United States); 2008.

[16] Brückner S, Liu S, Miró L, Radspieler M, Cabeza LF, Lävemann E. Industrial waste heat recovery technologies: An economic analysis of heat transformation technologies. Applied Energy 2015;151:157–67. https://doi.org/10.1016/j.apenergy.2015.01.147.

[17] Benedetti M, Dadi D, Giordano L, Introna V, Lapenna PE, Santolamazza A. Design of a Database of Case Studies and Technologies to Increase the Diffusion of Low-Temperature Waste Heat Recovery in the Industrial Sector. Sustainability 2021;13:5223. https://doi.org/10.3390/su13095223.

[18] Wu W, Wang B, Shi W, Li X. Absorption heating technologies: A review and perspective. Applied Energy 2014;130:51–71. https://doi.org/10.1016/j.apenergy.2014.05.027.

[19] Chen H, Goswami DY, Stefanakos EK. A review of thermodynamic cycles and working fluids for the conversion of low-grade heat. Renewable and Sustainable Energy Reviews 2010;14:3059–67. https://doi.org/10.1016/j.rser.2010.07.006.

[20] Hung T-C, Shai TY, Wang SK. A review of organic Rankine cycles (ORCs) for the recovery of low-grade waste heat. Energy 1997;22:661–7.

[21] F. Tchanche B, Pétrissans M, Papadakis G. Heat resources and organic Rankine cycle machines. Renewable and Sustainable Energy Reviews 2014;39:1185–99. https://doi.org/10.1016/j.rser.2014.07.139.

[22] Invernizzi CM. Closed power cycles. Lecture Notes in Energy 2013;11.

[23] Dincer I, Demir ME. 4.8 Steam and Organic Rankine Cycles. In: Dincer I, editor. Comprehensive Energy Systems, Oxford: Elsevier; 2018, p. 264–311. https://doi.org/10.1016/B978-0-12-809597-3.00410-7.

[24] Bahrampoury R, Behbahaninia A. Thermodynamic optimization and thermoeconomic analysis of four double pressure Kalina cycles driven from Kalina cycle system 11. Energy Conversion and Management 2017;152:110–23. https://doi.org/10.1016/j.enconman.2017.09.046.

[25] Leibowitz H, Mirolli M. First Kalina combined-cycle plant tested successfully. Power Engineering 1997;101:44–8.

[26] Zhang X, He M, Zhang Y. A review of research on the Kalina cycle. Renewable and Sustainable Energy Reviews 2012;16:5309–18. https://doi.org/10.1016/j.rser.2012.05.040.

[27] Bell LE. Cooling, Heating, Generating Power, and Recovering Waste Heat with Thermoelectric Systems. Science 2008;321:1457–61. https://doi.org/10.1126/science.1158899.

[28] Rowe DM, editor. CRC handbook of thermoelectrics. Boca Raton, FL: CRC Press; 1995.

[29] Vining CB. An inconvenient truth about thermoelectrics. Nature Mater 2009;8:83–5. https://doi.org/10.1038/nmat2361.

[30] Jouhara H, Żabnieńska-Góra A, Khordehgah N, Doraghi Q, Ahmad L, Norman L, et al. Thermoelectric generator (TEG) technologies and applications. International Journal of Thermofluids 2021;9:100063. https://doi.org/10.1016/j.ijft.2021.100063.

[31] Chen J, Li K, Liu C, Li M, Lv Y, Jia L, et al. Enhanced Efficiency of Thermoelectric Generator by Optimizing Mechanical and Electrical Structures. Energies 2017;10:1329. https://doi.org/10.3390/en10091329.

[32] Gambier P, Anton SR, Kong N, Erturk A, Inman DJ. Piezoelectric, solar and thermal energy harvesting for hybrid low-power generator systems with thin-film batteries. Meas Sci Technol 2012;23:015101. https://doi.org/10.1088/0957-0233/23/1/015101.

[33] Smoker J, Nouh M, Aldraihem O, Baz A. Energy harvesting from a standing wave thermoacoustic-piezoelectric resonator. Journal of Applied Physics 2012;111:104901. https://doi.org/10.1063/1.4712630.

[34] Peng Y, Choo KD, Oh S, Lee I, Jang T, Kim Y, et al. An Efficient Piezoelectric Energy Harvesting Interface Circuit Using a Sense-and-Set Rectifier. IEEE J Solid-State Circuits 2019;54:3348–61. https://doi.org/10.1109/JSSC.2019.2945262.

[35] Sun X. An Overview on Piezoelectric Power Generation System for Electricity Generation. JPEE 2017;05:11–8. https://doi.org/10.4236/jpee.2017.52002.

[36] Abdul Khalid KA, Leong TJ, Mohamed K. Review on Thermionic Energy Converters. IEEE Trans Electron Devices 2016;63:2231–41. https://doi.org/10.1109/TED.2016.2556751.

[37] Jouhara H, Khordehgah N, Almahmoud S, Delpech B, Chauhan A, Tassou SA. Waste heat recovery technologies and applications. Thermal Science and Engineering Progress 2018;6:268–89. https://doi.org/10.1016/j.tsep.2018.04.017.

[38] Zywica G, Kaczmarczyk TZ, Ihnatowicz E. A review of expanders for power generation in small-scale organic Rankine cycle systems: Performance and operational aspects. Proceedings of the Institution of Mechanical Engineers, Part A: Journal of Power and Energy 2016;230:669–84. https://doi.org/10.1177/0957650916661465.

[39] Yari M. Exergetic analysis of various types of geothermal power plants. Renewable Energy 2010;35:112–21. https://doi.org/10.1016/j.renene.2009.07.023.

[40] Tchanche BF, Papadakis G, Lambrinos G, Frangoudakis A. Fluid selection for a low-temperature solar organic Rankine cycle. Applied Thermal Engineering 2009;29:2468–76. https://doi.org/10.1016/j.applthermaleng.2008.12.025.

[41] Hung T-C, Shai TY, Wang SK. A review of organic Rankine cycles (ORCs) for the recovery of low-grade waste heat. Energy 1997;22:661–7.

[42] Drescher U, Brüggemann D. Fluid selection for the Organic Rankine Cycle (ORC) in biomass power and heat plants. Applied Thermal Engineering 2007;27:223–8. https://doi.org/10.1016/j.applthermaleng.2006.04.024.

[43] Bianchi M, De Pascale A. Bottoming cycles for electric energy generation: Parametric investigation of available and innovative solutions for the exploitation of low and medium temperature heat sources. Applied Energy 2011;88:1500–9. https://doi.org/10.1016/j.apenergy.2010.11.013.

[44] Le VL. Étude de la faisabilité des cycles sous-critiques et supercritiques de Rankine pour la valorisation de rejets thermiques. Université de Lorraine, 2014.

[45] Ether Engines. n.d. http://douglas-self.com/MUSEUM/POWER/ether/ether.htm (accessed February 14, 2022).

[46] Carnot S. Réflexions sur la puissance motrice du feu. Vrin; 1978.

[47] Galloway E. History and progress of the steam engine: with a practical investigation of its structure and application. Thomas Kelly; 1832.

[48] Macchi E, Astolfi M. Organic rankine cycle (ORC) power systems: technologies and applications. Woodhead Publishing; 2016.

[49] Colonna P, Casati E, Trapp C, Mathijssen T, Larjola J, Turunen-Saaresti T, et al. Organic Rankine cycle power systems: from the concept to current technology, applications, and an outlook to the future. Journal of Engineering for Gas Turbines and Power 2015;137.

[50] Spencer LC. A comprehensive review of small solar-powered heat engines: Part I. A history of solar-powered devices up to 1950. Solar Energy 1989;43:191–6.

[51] Spencer LC. A comprehensive review of small solar-powered heat engines: Part II. Research since 1950—“conventional” engines up to 100 kW. Solar Energy 1989;43:197–210.

[52] El-Wakil MM. Powerplant technology 1984.

[53] Guo T, Wang HX, Zhang SJ. Fluids and parameters optimization for a novel cogeneration system driven by low-temperature geothermal sources. Energy 2011;36:2639–49. https://doi.org/10.1016/j.energy.2011.02.005.

[54] Vélez F, Segovia JJ, Martín MC, Antolín G, Chejne F, Quijano A. A technical, economical and market review of organic Rankine cycles for the conversion of low-grade heat for power generation. Renewable and Sustainable Energy Reviews 2012;16:4175–89. https://doi.org/10.1016/j.rser.2012.03.022.

[55] Shengjun Z, Huaixin W, Tao G. Performance comparison and parametric optimization of subcritical Organic Rankine Cycle (ORC) and transcritical power cycle system for low-temperature geothermal power generation. Applied Energy 2011;88:2740–54. https://doi.org/10.1016/j.apenergy.2011.02.034.

[56] Vaja I, Gambarotta A. Internal Combustion Engine (ICE) bottoming with Organic Rankine Cycles (ORCs). Energy 2010;35:1084–93. https://doi.org/10.1016/j.energy.2009.06.001.

[57] Uehara H, Ikegami Y. Optimization of a Closed-Cycle OTEC System. Journal of Solar Energy Engineering 1990;112:247–56. https://doi.org/10.1115/1.2929931.

[58] Soltani M, M. Kashkooli F, Dehghani-Sanij AR, Kazemi AR, Bordbar N, Farshchi MJ, et al. A comprehensive study of geothermal heating and cooling systems. Sustainable Cities and Society 2019;44:793–818. https://doi.org/10.1016/j.scs.2018.09.036.

[59] Eugster WJ. Road and bridge heating using geothermal energy. Overview and examples. Proceedings European geothermal congress, vol. 2007, 2007.

[60] Barbier E. Geothermal energy technology and current status: an overview. Renewable and Sustainable Energy Reviews 2002;6:3–65. https://doi.org/10.1016/S1364-0321(02)00002-3.

[61] Quoilin S, Broek MVD, Declaye S, Dewallef P, Lemort V. Techno-economic survey of Organic Rankine Cycle (ORC) systems. Renewable and Sustainable Energy Reviews 2013;22:168–86. https://doi.org/10.1016/j.rser.2013.01.028.

[62] Wieland C, Dawo F, Schifflechner C, Astolfi M. Market report on Organic Rankine Cycle power systems: recent developments and outlook. Proceedings of the 6th International Seminar on ORC Power Systems, 2021.

[63] Rahbar K, Mahmoud S, Al-Dadah RK, Moazami N, Mirhadizadeh SA. Review of organic Rankine cycle for small-scale applications. Energy Conversion and Management 2017;134:135–55. https://doi.org/10.1016/j.enconman.2016.12.023.

[64] Breeze PA. Power generation technologies. Third edition. Kidlington, Oxford, United Kingdom ; Cambridge, MA, United States: Newnes, an imprint of Elsevier; 2019.

[65] Quoilin S, Orosz M, Hemond H, Lemort V. Performance and design optimization of a low-cost solar organic Rankine cycle for remote power generation. Solar Energy 2011;85:955–66. https://doi.org/10.1016/j.solener.2011.02.010.

[66] Elsaid K, Taha Sayed E, Yousef BAA, Kamal Hussien Rabaia M, Ali Abdelkareem M, Olabi AG. Recent progress on the utilization of waste heat for desalination: A review. Energy Conversion and Management 2020;221:113105. https://doi.org/10.1016/j.enconman.2020.113105.

[67] Sikarwar BS, Sundén B, Wang Q, editors. Advances in Fluid and Thermal Engineering: Select Proceedings of FLAME 2020. Singapore: Springer Singapore; 2021. https://doi.org/10.1007/978-981-16-0159-0.

[68] Fierro JJ, Escudero-Atehortua A, Nieto-Londoño C, Giraldo M, Jouhara H, Wrobel LC. Evaluation of waste heat recovery technologies for the cement industry. International Journal of Thermofluids 2020;7–8:100040. https://doi.org/10.1016/j.ijft.2020.100040.

[69] Moreira LF, Arrieta FRP. Thermal and economic assessment of organic Rankine cycles for waste heat recovery in cement plants. Renewable and Sustainable Energy Reviews 2019;114:109315. https://doi.org/10.1016/j.rser.2019.109315.

[70] Ma G, Cai J, Zeng W, Dong H. Analytical Research on Waste Heat Recovery and Utilization of China's Iron & Steel Industry. Energy Procedia 2012;14:1022–8. https://doi.org/10.1016/j.egypro.2011.12.1049.

[71] Zhang L, Wu L, Zhang X, Ju G. Comparison and Optimization of Mid-low Temperature Cogeneration Systems for Flue Gas in Iron and Steel Plants. J Iron Steel Res Int 2013;20:33–40. https://doi.org/10.1016/S1006-706X(13)60193-4.

[72] Tian H, Shu G, Wei H, Liang X, Liu L. Fluids and parameters optimization for the organic Rankine cycles (ORCs) used in exhaust heat recovery of Internal Combustion Engine (ICE). Energy 2012;47:125–36. https://doi.org/10.1016/j.energy.2012.09.021.

[73] Astolfi M. An innovative approach for the techno-economic optimization of organic rankine cycles 2014.

[74] Pili R, García Martínez L, Wieland C, Spliethoff H. Techno-economic potential of waste heat recovery from German energy-intensive industry with Organic Rankine Cycle technology. Renewable and Sustainable Energy Reviews 2020;134:110324. https://doi.org/10.1016/j.rser.2020.110324.

[75] Bombarda P, Invernizzi C, Gaia M. Performance Analysis of OTEC Plants With Multilevel Organic Rankine Cycle and Solar Hybridization. Journal of Engineering for Gas Turbines and Power 2013;135:042302. https://doi.org/10.1115/1.4007729.

[76] Pereira JS, Ribeiro JB, Mendes R, Vaz GC, André JC. ORC based micro-cogeneration systems for residential application – A state of the art review and current challenges. Renewable and Sustainable Energy Reviews 2018;92:728–43. https://doi.org/10.1016/j.rser.2018.04.039.

[77] Lion S, Michos CN, Vlaskos I, Rouaud C, Taccani R. A review of waste heat recovery and Organic Rankine Cycles (ORC) in on-off highway vehicle Heavy Duty Diesel Engine applications. Renewable and Sustainable Energy Reviews 2017;79:691–708. https://doi.org/10.1016/j.rser.2017.05.082.

[78] Bao J, Zhao L. A review of working fluid and expander selections for organic Rankine cycle. Renewable and Sustainable Energy Reviews 2013;24:325–42. https://doi.org/10.1016/j.rser.2013.03.040.

[79] Rohsenow WM, Hartnett JP, Ganic EN. Handbook of heat transfer applications 1985.

[80] Meyer D, Wong CS, Engle F, Krumdieck S. Design and build of a 1 kilowatt organic Rankine cycle power generator 2013.

[81] Peters MS, Timmerhaus KD, West RE. Plant design and economics for chemical engineers. 5th ed. New York: McGraw-Hill; 2003.

[82] Kakac S, Liu H, Pramuanjaroenkij A. Heat exchangers: selection, rating, and thermal design. CRC press; 2002.

[83] Georges E, Declaye S, Dumont O, Quoilin S, Lemort V. Design of a small-scale organic Rankine cycle engine used in a solar power plant. Int J Low-Carbon Tech 2013;8:i34–41. https://doi.org/10.1093/ijlct/ctt030.

[84] Quoilin S, Lemort V, Lebrun J. Experimental study and modeling of an Organic Rankine Cycle using scroll expander. Applied Energy 2010;87:1260–8. https://doi.org/10.1016/j.apenergy.2009.06.026.

[85] Walraven D, Laenen B, D'haeseleer W. Optimum configuration of shell-and-tube heat exchangers for the use in low-temperature organic Rankine cycles. Energy Conversion and Management 2014;83:177–87. https://doi.org/10.1016/j.enconman.2014.03.066.

[86] Li J, Yang Z, Hu S, Yang F, Duan Y. Effects of shell-and-tube heat exchanger arranged forms on the thermo-economic performance of organic Rankine cycle systems using hydrocarbons. Energy Conversion and Management 2020;203:112248.

[87] Hou TK, Kazi SN, Mahat AB, Teng CB, Al-Shamma'a A, Shaw A. Industrial Heat Exchanger: Operation and Maintenance to Minimize Fouling and Corrosion. Heat Exchangers–Advanced Features and Applications 2017.

[88] Qiu G, Liu H, Riffat S. Expanders for micro-CHP systems with organic Rankine cycle. Applied Thermal Engineering 2011;31:3301–7. https://doi.org/10.1016/j.applthermaleng.2011.06.008.

[89] Persson JG. Performance mapping vs design parameters for screw compressors and other displacement compressor types. VDI Berichte 1990;859.

[90] Chys M, van den Broek M, Vanslambrouck B, De Paepe M. Potential of zeotropic mixtures as working fluids in organic Rankine cycles. Energy 2012;44:623–32. https://doi.org/10.1016/j.energy.2012.05.030.

[91] Quoilin S, Declaye S, Lemort V. Expansion machine and fluid selection for the organic Rankine cycle. Proceedings of the 7th International Conference on Heat Transfer, Fluid Mechanics and Thermodynamics, Antalya, Turkey, 2010, p. 19–21.

[92] Çengel YA, Boles MA. Thermodynamics: an engineering approach. Eighth edition. New York: McGraw-Hill Education; 2015.

[93] Schuster A, Karellas S, Aumann R. Efficiency optimization potential in supercritical Organic Rankine Cycles. Energy 2010;35:1033–9. https://doi.org/10.1016/j.energy.2009.06.019.

[94] Gao H, Liu C, He C, Xu X, Wu S, Li Y. Performance Analysis and Working Fluid Selection of a Supercritical Organic Rankine Cycle for Low Grade Waste Heat Recovery. Energies 2012;5:3233–47. https://doi.org/10.3390/en5093233.

[95] Xu H, Gao N, Zhu T. Investigation on the fluid selection and evaporation parametric optimization for sub- and supercritical organic Rankine cycle. Energy 2016;96:59–68. https://doi.org/10.1016/j.energy.2015.12.040.

[96] Moloney F, Almatrafi E, Goswami DY. Working fluid parametric analysis for recuperative supercritical organic Rankine cycles for medium geothermal reservoir temperatures. Renewable Energy 2020;147:2874–81. https://doi.org/10.1016/j.renene.2018.09.003.

[97] Cayer E, Galanis N, Nesreddine H. Parametric study and optimization of a transcritical power cycle using a low temperature source. Applied Energy 2010;87:1349–57. https://doi.org/10.1016/j.apenergy.2009.08.031.

[98] Dai B, Li M, Ma Y. Thermodynamic analysis of carbon dioxide blends with low GWP (global warming potential) working fluids-based transcritical Rankine cycles for low-grade heat energy recovery. Energy 2014;64:942–52. https://doi.org/10.1016/j.energy.2013.11.019.

[99] Braimakis K, Preißinger M, Brüggemann D, Karellas S, Panopoulos K. Low grade waste heat recovery with subcritical and supercritical Organic Rankine Cycle based on natural refrigerants and their binary mixtures. Energy 2015;88:80–92. https://doi.org/10.1016/j.energy.2015.03.092.

[100] Kosmadakis G, Manolakos D, Papadakis G. Experimental investigation of a low-temperature organic Rankine cycle (ORC) engine under variable heat input operating at both subcritical and supercritical conditions. Applied Thermal Engineering 2016;92:1–7. https://doi.org/10.1016/j.applthermaleng.2015.09.082.

[101] Das D, Kazim M, Sadr R, Pate M. Optimal hydrocarbon based working fluid selection for a simple supercritical Organic Rankine Cycle. Energy Conversion and Management 2021;243:114424. https://doi.org/10.1016/j.enconman.2021.114424.

[102] Guzović Z, Rašković P, Blatarić Z. The comparision of a basic and a dual-pressure ORC (Organic Rankine Cycle): Geothermal Power Plant Velika Ciglena case study. Energy 2014;76:175–86. https://doi.org/10.1016/j.energy.2014.06.005.

[103] Li J, Ge Z, Duan Y, Yang Z, Liu Q. Parametric optimization and thermodynamic performance comparison of single-pressure and dual-pressure evaporation organic Rankine cycles. Applied Energy 2018;217:409–21. https://doi.org/10.1016/j.apenergy.2018.02.096.

[104] Feng H, Wu Z, Chen L, Ge Y. Constructal thermodynamic optimization for dual-pressure organic Rankine cycle in waste heat utilization system. Energy Conversion and Management 2021;227:113585. https://doi.org/10.1016/j.enconman.2020.113585.

[105] Yari M, Mehr AS, Zare V, Mahmoudi SMS, Rosen MA. Exergoeconomic comparison of TLC (trilateral Rankine cycle), ORC (organic Rankine cycle) and Kalina cycle using a low grade heat source. Energy 2015;83:712–22. https://doi.org/10.1016/j.energy.2015.02.080.

[106] DiPippo R. Ideal thermal efficiency for geothermal binary plants. Geothermics 2007;36:276–85. https://doi.org/10.1016/j.geothermics.2007.03.002.

[107] Ho T, Mao SS, Greif R. Comparison of the Organic Flash Cycle (OFC) to other advanced vapor cycles for intermediate and high temperature waste heat reclamation and solar thermal energy. Energy 2012;42:213–23. https://doi.org/10.1016/j.energy.2012.03.067.

[108] Schuster A, Karellas S, Kakaras E, Spliethoff H. Energetic and economic investigation of Organic Rankine Cycle applications. Applied Thermal Engineering 2009;29:1809–17.

[109] Stoppato A. Energetic and economic investigation of the operation management of an Organic Rankine Cycle cogeneration plant. Energy 2012;41:3–9.

[110] Quoilin S, Declaye S, Tchanche BF, Lemort V. Thermo-economic optimization of waste heat recovery Organic Rankine Cycles. Applied Thermal Engineering 2011;31:2885–93.

[111] Chen H, Goswami DY, Rahman MM, Stefanakos EK. Energetic and exergetic analysis of CO2- and R32-based transcritical Rankine cycles for low-grade heat conversion. Applied Energy 2011;88:2802–8.

[112] Hung TC, Wang SK, Kuo CH, Pei BS, Tsai KF. A study of organic working fluids on system efficiency of an ORC using low-grade energy sources. Energy 2010;35:1403–11.

[113] Badr O, Probert SD, O'callaghan PW. Selecting a working fluid for a Rankine-cycle engine. Applied Energy 1985;21:1–42.

[114] Lakew AA, Bolland O. Working fluids for low-temperature heat source. Applied Thermal Engineering 2010;30:1262–8.

[115] Mikielewicz D, Mikielewicz J. A thermodynamic criterion for selection of working fluid for subcritical and supercritical domestic micro CHP. Applied Thermal Engineering 2010;30:2357–62.

[116] Bahadormanesh N, Rahat S, Yarali M. Constrained multi-objective optimization of radial expanders in organic Rankine cycles by firefly algorithm. Energy Conversion and Management 2017;148:1179–93. https://doi.org/10.1016/j.enconman.2017.06.070.

[117] Rayegan R, Tao YX. A procedure to select working fluids for Solar Organic Rankine Cycles (ORCs). Renewable Energy 2011;36:659–70. https://doi.org/10.1016/j.renene.2010.07.010.

[118] He C, Liu C, Gao H, Xie H, Li Y, Wu S, et al. The optimal evaporation temperature and working fluids for subcritical organic Rankine cycle. Energy 2012;38:136–43. https://doi.org/10.1016/j.energy.2011.12.022.

[119] Xi H, Li M-J, Xu C, He Y-L. Parametric optimization of regenerative organic Rankine cycle (ORC) for low grade waste heat recovery using genetic algorithm. Energy 2013;58:473–82. https://doi.org/10.1016/j.energy.2013.06.039.

[120] Long R, Bao YJ, Huang XM, Liu W. Exergy analysis and working fluid selection of organic Rankine cycle for low grade waste heat recovery. Energy 2014;73:475–83. https://doi.org/10.1016/j.energy.2014.06.040.

[121] Zhai H, Shi L, An Q. Influence of working fluid properties on system performance and screen evaluation indicators for geothermal ORC (organic Rankine cycle) system. Energy 2014;74:2–11. https://doi.org/10.1016/j.energy.2013.12.030.

[122] Astolfi M, Romano MC, Bombarda P, Macchi E. Binary ORC (organic Rankine cycles) power plants for the exploitation of medium–low temperature geothermal sources – Part A: Thermodynamic optimization. Energy 2014;66:423–34. https://doi.org/10.1016/j.energy.2013.11.056.

[123] Yang M-H, Yeh R-H. Thermo-economic optimization of an organic Rankine cycle system for large marine diesel engine waste heat recovery. Energy 2015;82:256–68.

[124] Imran M, Usman M, Park B-S, Yang Y. Comparative assessment of Organic Rankine Cycle integration for low temperature geothermal heat source applications. Energy 2016;102:473–90. https://doi.org/10.1016/j.energy.2016.02.119.

[125] Wang YZ, Zhao J, Wang Y, An QS. Multi-objective optimization and grey relational analysis on configurations of organic Rankine cycle. Applied Thermal Engineering 2017;114:1355–63. https://doi.org/10.1016/j.applthermaleng.2016.10.075.

[126] Bekiloğlu HE, Bedir H, Anlaş G. Multi-objective optimization of ORC parameters and selection of working fluid using preliminary radial inflow turbine design. Energy Conversion and Management 2019;183:833–47. https://doi.org/10.1016/j.enconman.2018.12.039.

[127] Li P, Mei Z, Han Z, Jia X, Zhu L, Wang S. Multi-objective optimization and improved analysis of an organic Rankine cycle coupled with the dynamic turbine efficiency model. Applied Thermal Engineering 2019;150:912–22. https://doi.org/10.1016/j.applthermaleng.2019.01.058.

[128] Altun AF, Kilic M. Thermodynamic performance evaluation of a geothermal ORC power plant. Renewable Energy 2020;148:261–74. https://doi.org/10.1016/j.renene.2019.12.034.

[129] Algieri A, Morrone P. Comparative energetic analysis of high-temperature subcritical and transcritical Organic Rankine Cycle (ORC). A biomass application in the Sibari district. Applied Thermal Engineering 2012;36:236–44. https://doi.org/10.1016/j.applthermaleng.2011.12.021.

[130] Feng Y, Zhang Y, Li B, Yang J, Shi Y. Sensitivity analysis and thermoeconomic comparison of ORCs (organic Rankine cycles) for low temperature waste heat recovery. Energy 2015;82:664–77. https://doi.org/10.1016/j.energy.2015.01.075.

[131] Wang ZQ, Zhou NJ, Guo J, Wang XY. Fluid selection and parametric optimization of organic Rankine cycle using low temperature waste heat. Energy 2012;40:107–15. https://doi.org/10.1016/j.energy.2012.02.022.

[132] Wang D, Ling X, Peng H, Liu L, Tao L. Efficiency and optimal performance evaluation of organic Rankine cycle for low grade waste heat power generation. Energy 2013;50:343–52. https://doi.org/10.1016/j.energy.2012.11.010.

[133] Xu J, Yu C. Critical temperature criterion for selection of working fluids for subcritical pressure Organic Rankine cycles. Energy 2014;74:719–33. https://doi.org/10.1016/j.energy.2014.07.038.

[134] Darvish K, Ehyaei M, Atabi F, Rosen M. Selection of Optimum Working Fluid for Organic Rankine Cycles by Exergy and Exergy-Economic Analyses. Sustainability 2015;7:15362–83. https://doi.org/10.3390/su71115362.

[135] Xu P, Lu J, Li T, Zhu J. Thermodynamic optimization and fluid selection of organic Rankine cycle driven by a latent heat source. J Cent South Univ 2017;24:2829–41. https://doi.org/10.1007/s11771-017-3698-z.

[136] Zhu Y, Li W, Sun G, Li H. Thermo-economic analysis based on objective functions of an organic Rankine cycle for waste heat recovery from marine diesel engine. Energy 2018;158:343–56. https://doi.org/10.1016/j.energy.2018.06.047.

[137] Uusitalo A, Honkatukia J, Turunen-Saaresti T, Grönman A. Thermodynamic evaluation on the effect of working fluid type and fluids critical properties on design and performance of Organic Rankine Cycles. Journal of Cleaner Production 2018;188:253–63. https://doi.org/10.1016/j.jclepro.2018.03.228.

[138] Meinel D, Wieland C, Spliethoff H. Effect and comparison of different working fluids on a two-stage organic rankine cycle (ORC) concept. Applied Thermal Engineering 2014;63:246–53. https://doi.org/10.1016/j.applthermaleng.2013.11.016.

[139] Safarian S, Aramoun F. Energy and exergy assessments of modified Organic Rankine Cycles (ORCs). Energy Reports 2015;1:1–7. https://doi.org/10.1016/j.egyr.2014.10.003.

[140] Li G. Organic Rankine cycle performance evaluation and thermoeconomic assessment with various applications part I: Energy and exergy performance evaluation. Renewable and Sustainable Energy Reviews 2016;53:477–99. https://doi.org/10.1016/j.rser.2015.08.066.

[141] Zhang C, Liu C, Xu X, Li Q, Wang S, Chen X. Effects of superheat and internal heat exchanger on thermo-economic performance of organic Rankine cycle based on fluid type and heat sources. Energy 2018;159:482–95. https://doi.org/10.1016/j.energy.2018.06.177.

[142] Kezrane C, Laouid YA, Lasbet Y, Habib SH. Comparison of different Organic Rankine Cycle for power generation using waste heat. EJEE 2018;20:151–69. https://doi.org/10.3166/ejee.20.151-169.

[143] Valencia G, Fontalvo A, Cárdenas Y, Duarte J, Isaza C. Energy and Exergy Analysis of Different Exhaust Waste Heat Recovery Systems for Natural Gas Engine Based on ORC. Energies 2019;12:2378. https://doi.org/10.3390/en12122378.

[144] Wang J, Yan Z, Wang M, Ma S, Dai Y. Thermodynamic analysis and optimization of an (organic Rankine cycle) ORC using low grade heat source. Energy 2013;49:356–65. https://doi.org/10.1016/j.energy.2012.11.009.

[145] Xi H, Li M-J, Xu C, He Y-L. Parametric optimization of regenerative organic Rankine cycle (ORC) for low grade waste heat recovery using genetic algorithm. Energy 2013;58:473–82. https://doi.org/10.1016/j.energy.2013.06.039.

[146] Imran M, Park BS, Kim HJ, Lee DH, Usman M, Heo M. Thermo-economic optimization of Regenerative Organic Rankine Cycle for waste heat recovery applications. Energy Conversion and Management 2014;87:107–18. https://doi.org/10.1016/j.enconman.2014.06.091.

[147] Yang F, Zhang H, Song S, Bei C, Wang H, Wang E. Thermoeconomic multi-objective optimization of an organic Rankine cycle for exhaust waste heat recovery of a diesel engine. Energy 2015;93:2208–28. https://doi.org/10.1016/j.energy.2015.10.117.

[148] Feng Y, Zhang Y, Li B, Yang J, Shi Y. Sensitivity analysis and thermoeconomic comparison of ORCs (organic Rankine cycles) for low temperature waste heat recovery. Energy 2015;82:664–77. https://doi.org/10.1016/j.energy.2015.01.075.

[149] Gotelip Correa Veloso T, Sotomonte CAR, Coronado CJR, Nascimento MAR. Multi-objective optimization and exergetic analysis of a low-grade waste heat recovery ORC application on a Brazilian FPSO. Energy Conversion and Management 2018;174:537–51. https://doi.org/10.1016/j.enconman.2018.08.042.

[150] Laouid YAA, Kezrane C, Lasbet Y, Pesyridis A. Towards improvement of waste heat recovery systems: A multi-objective optimization of different organic Rankine cycle configurations. International Journal of Thermofluids 2021;11:100100. https://doi.org/10.1016/j.ijft.2021.100100.

[151] Xi H, Li M-J, He Y-L, Tao W-Q. A graphical criterion for working fluid selection and thermodynamic system comparison in waste heat recovery. Applied Thermal Engineering 2015;89:772–82. https://doi.org/10.1016/j.applthermaleng.2015.06.050.

[152] Meng D, Liu Q, Ji Z. Performance analyses of regenerative organic flash cycles for geothermal power generation. Energy Conversion and Management 2020;224:113396.

[153] Sun J, Liu Q, Duan Y. Effects of evaporator pinch point temperature difference on thermo-economic performance of geothermal organic Rankine cycle systems. Geothermics 2018;75:249–58. https://doi.org/10.1016/j.geothermics.2018.06.001.

[154] Liu Q, Shen A, Duan Y. Parametric optimization and performance analyses of geothermal organic Rankine cycles using R600a/R601a mixtures as working fluids. Applied Energy 2015;148:410–20. https://doi.org/10.1016/j.apenergy.2015.03.093.

[155] Zhang X, Wu L, Wang X, Ju G. Comparative study of waste heat steam SRC, ORC and S-ORC power generation systems in medium-low temperature. Applied Thermal Engineering 2016;106:1427–39. https://doi.org/10.1016/j.applthermaleng.2016.06.108.

[156] Papadopoulos AI, Stijepovic M, Linke P. On the systematic design and selection of optimal working fluids for Organic Rankine Cycles. Applied Thermal Engineering 2010;30:760–9. https://doi.org/10.1016/j.applthermaleng.2009.12.006.

[157] Saleh B, Koglbauer G, Wendland M, Fischer J. Working fluids for low-temperature organic Rankine cycles. Energy 2007;32:1210–21. https://doi.org/10.1016/j.energy.2006.07.001.

[158] Javanshir A, Sarunac N. Thermodynamic analysis of a simple Organic Rankine Cycle. Energy 2017;118:85–96. https://doi.org/10.1016/j.energy.2016.12.019.

[159] Li P, Han Z, Jia X, Mei Z, Han X, Wang Z. Comparative analysis of an organic Rankine cycle with different turbine efficiency models based on multi-objective optimization. Energy Conversion and Management 2019;185:130–42. https://doi.org/10.1016/j.enconman.2019.01.117.

[160] Mikielewicz D, Wajs J, Ziółkowski P, Mikielewicz J. Utilisation of waste heat from the power plant by use of the ORC aided with bleed steam and extra source of heat. Energy 2016;97:11–9. https://doi.org/10.1016/j.energy.2015.12.106.

[161] Van Erdeweghe S, Van Bael J, Laenen B, D'haeseleer W. Design and off-design optimization procedure for low-temperature geothermal organic Rankine cycles. Applied Energy 2019;242:716–31. https://doi.org/10.1016/j.apenergy.2019.03.142.

[162] Dai Y, Wang J, Gao L. Parametric optimization and comparative study of organic Rankine cycle (ORC) for low grade waste heat recovery. Energy Conversion and Management 2009;50:576–82. https://doi.org/10.1016/j.enconman.2008.10.018.

[163] Zalzala AM, Fleming PJ, Fleming P. Genetic algorithms in engineering systems. vol. 55. Iet; 1997.

[164] Deb K. Introduction to genetic algorithms for engineering optimization. New optimization techniques in engineering, Springer; 2004, p. 13–51.

[165] Deb K, Agrawal S, Pratap A, Meyarivan T. A fast elitist non-dominated sorting genetic algorithm for multi-objective optimization: NSGA-II. International conference on parallel problem solving from nature, Springer; 2000, p. 849–58.

[166] Deb K, Pratap A, Agarwal S, Meyarivan T. A fast and elitist multiobjective genetic algorithm: NSGA-II. IEEE Trans Evol Computat 2002;6:182–97. https://doi.org/10.1109/4235.996017.

[167] Li S, Kang L, Zhao X-M. A Survey on Evolutionary Algorithm Based Hybrid Intelligence in Bioinformatics. BioMed Research International 2014;2014:1–8. https://doi.org/10.1155/2014/362738.

[168] Loni R, Najafi G, Bellos E, Rajaee F, Said Z, Mazlan M. A review of industrial waste heat recovery system for power generation with Organic Rankine Cycle: Recent challenges and future outlook. Journal of Cleaner Production 2021;287:125070. https://doi.org/10.1016/j.jclepro.2020.125070.

[169] Fang Y, Yang F, Zhang H. Comparative analysis and multi-objective optimization of organic Rankine cycle (ORC) using pure working fluids and their zeotropic mixtures for diesel engine waste heat recovery. Applied Thermal Engineering 2019;157:113704. https://doi.org/10.1016/j.applthermaleng.2019.04.114.

[170] Hwang C-L, Yoon K. Multiple Attribute Decision Making: Methods and Applications A State-of-the-Art Survey. Berlin Heidelberg: Springer-Verlag; 1981. https://doi.org/10.1007/978-3-642-48318-9.

[171] Krohling RA, Pacheco AG. A-TOPSIS–an approach based on TOPSIS for ranking evolutionary algorithms. Procedia Computer Science 2015;55:308–17.

[172] Laouid YAA, Kezrane C, Lasbet Y, Nord LO. WET WORKING FLUIDS FOR REGENERATIVE ORC WITH VARYING HEAT SOURCE TEMPERATURE 2019:5.

[173] Zhang T, Liu L, Hao J, Zhu T, Cui G. Correlation analysis based multi-parameter optimization of the organic Rankine cycle for medium- and high-temperature waste heat recovery. Applied Thermal Engineering 2021;188:116626. https://doi.org/10.1016/j.applthermaleng.2021.116626.

[174] Fallah M, Ghiasi RA, Mokarram NH. A comprehensive comparison among different types of geothermal plants from exergy and thermoeconomic points of view. Thermal Science and Engineering Progress 2018;5:15–24. https://doi.org/10.1016/j.tsep.2017.10.017.

[175] Xinxin Z, Congtian Z, Maogang H, Jingfu W. Selection and Evaluation of Dry and Isentropic Organic Working Fluids Used in Organic Rankine Cycle Based on the Turning Point on Their Saturated Vapor Curves. J Therm Sci 2019:16.

[176] Chen G, An Q, Wang Y, Zhao J, Chang N, Alvi J. Performance prediction and working fluids selection for organic Rankine cycle under reduced temperature. Applied Thermal Engineering 2019;153:95–103. https://doi.org/10.1016/j.applthermaleng.2019.02.011.

[177] Amiri Rad E, Mohammadi S, Tayyeban E. Simultaneous optimization of working fluid and boiler pressure in an organic Rankine cycle for different heat source temperatures. Energy 2020;194:116856. https://doi.org/10.1016/j.energy.2019.116856.

[178] Köse Ö, Koç Y, Yağlı H. Performance improvement of the bottoming steam Rankine cycle (SRC) and organic Rankine cycle (ORC) systems for a triple combined system using gas turbine (GT) as topping cycle. Energy Conversion and Management 2020;211:112745. https://doi.org/10.1016/j.enconman.2020.112745.

[179] Ye Z, Yang J, Shi J, Chen J. Thermo-economic and environmental analysis of various low-GWP refrigerants in Organic Rankine cycle system. Energy 2020;199:117344. https://doi.org/10.1016/j.energy.2020.117344.

[180] Wang S, Liu C, Li Q, Liu L, Huo E, Zhang C. Selection principle of working fluid for organic Rankine cycle based on environmental benefits and economic performance. Applied Thermal Engineering 2020;178:115598. https://doi.org/10.1016/j.applthermaleng.2020.115598.

[181] Yang J, Gao L, Ye Z, Hwang Y, Chen J. Binary-objective optimization of latest low-GWP alternatives to R245fa for organic Rankine cycle application. Energy 2021;217:119336. https://doi.org/10.1016/j.energy.2020.119336.

[182] Alshammari F, Elashmawy M, Bechir Ben Hamida M. Effects of working fluid type on powertrain performance and turbine design using experimental data of a 7.25ℓ heavy-duty diesel engine. Energy Conversion and Management 2021;231:113828. https://doi.org/10.1016/j.enconman.2021.113828.

[183] Bina SM, Jalilinasrabady S, Fujii H. Thermo-economic evaluation of various bottoming ORCs for geothermal power plant, determination of optimum cycle for Sabalan power plant exhaust. Geothermics 2017;70:181–91.

[184] Liu X, Wei M, Yang L, Wang X. Thermo-economic analysis and optimization selection of ORC system configurations for low temperature binary-cycle geothermal plant. Applied Thermal Engineering 2017;125:153–64. https://doi.org/10.1016/j.applthermaleng.2017.07.016.

[185] Braimakis K, Karellas S. Energetic optimization of regenerative Organic Rankine Cycle (ORC) configurations. Energy Conversion and Management 2018;159:353–70. https://doi.org/10.1016/j.enconman.2017.12.093.

[186] Gholizadeh T. Thermodynamic and thermoeconomic analysis of basic and modified power generation systems fueled by biogas. Energy Conversion and Management 2019:13.

[187] Jiménez-Arreola M, Wieland C, Romagnoli A. Direct vs indirect evaporation in Organic Rankine Cycle (ORC) systems: A comparison of the dynamic behavior for waste heat recovery of engine exhaust. Applied Energy 2019;242:439–52. https://doi.org/10.1016/j.apenergy.2019.03.011.

[188] Bademlioglu AH, Canbolat AS, Kaynakli O. Multi-objective optimization of parameters affecting Organic Rankine Cycle performance characteristics with Taguchi-Grey Relational Analysis. Renewable and Sustainable Energy Reviews 2020;117:109483. https://doi.org/10.1016/j.rser.2019.109483.

[189] Turgut MS, Turgut OE. Multi-objective optimization of the basic and single-stage Organic Rankine Cycles utilizing a low-grade heat source. Heat Mass Transfer 2019;55:353–74. https://doi.org/10.1007/s00231-018-2425-0.

[190] Hu S, Li J, Yang F, Yang Z, Duan Y. Multi-objective optimization of organic Rankine cycle using hydrofluorolefins (HFOs) based on different target preferences. Energy 2020;203:117848. https://doi.org/10.1016/j.energy.2020.117848.

[191] Wang L, Bu X, Li H. Multi-objective optimization and off-design evaluation of organic rankine cycle (ORC) for low-grade waste heat recovery. Energy 2020;203:117809. https://doi.org/10.1016/j.energy.2020.117809.

[192] Herrera-Orozco I, Valencia-Ochoa G, Duarte-Forero J. Exergo-environmental assessment and multi-objective optimization of waste heat recovery systems based on Organic Rankine cycle configurations. Journal of Cleaner Production 2021;288:125679. https://doi.org/10.1016/j.jclepro.2020.125679.

[193] Peris B, Navarro-Esbrí J, Molés F, Mota-Babiloni A. Experimental study of an ORC (organic Rankine cycle) for low grade waste heat recovery in a ceramic industry. Energy 2015;85:534–42. https://doi.org/10.1016/j.energy.2015.03.065.

[194] Li Y-R, Du M-T, Wu C-M, Wu S-Y, Liu C, Xu J-L. Economical evaluation and optimization of subcritical organic Rankine cycle based on temperature matching analysis. Energy 2014;68:238–47. https://doi.org/10.1016/j.energy.2014.02.038.

[195] Bell IH, Wronski J, Quoilin S, Lemort V. Pure and Pseudo-pure Fluid Thermophysical Property Evaluation and the Open-Source Thermophysical Property Library CoolProp. Ind Eng Chem Res 2014;53:2498–508. https://doi.org/10.1021/ie4033999.

[196] Gimelli A, Luongo A, Muccillo M. Efficiency and cost optimization of a regenerative Organic Rankine Cycle power plant through the multi-objective approach. Applied Thermal Engineering 2017;114:601–10. https://doi.org/10.1016/j.applthermaleng.2016.12.009.

[197] Cayer E, Galanis N, Nesreddine H. Parametric study and optimization of a transcritical power cycle using a low temperature source. Applied Energy 2010;87:1349–57. https://doi.org/10.1016/j.apenergy.2009.08.031.

[198] Turton R, editor. Analysis, synthesis, and design of chemical processes. 5th edition. Boston: Prentice Hall; 2018.

[199] Schuster A, Karellas S, Aumann R. Efficiency optimization potential in supercritical Organic Rankine Cycles. Energy 2010;35:1033–9. https://doi.org/10.1016/j.energy.2009.06.019.

[200] Zare V. A comparative exergoeconomic analysis of different ORC configurations for binary geothermal power plants. Energy Conversion and Management 2015;105:127–38. https://doi.org/10.1016/j.enconman.2015.07.073.

[201] Sadreddini A, Ashjari MA, Fani M, Mohammadi A. Thermodynamic analysis of a new cascade ORC and transcritical CO2 cycle to recover energy from medium temperature heat source and liquefied natural gas. Energy Conversion and Management 2018;167:9–20. https://doi.org/10.1016/j.enconman.2018.04.093.

[202] Abbas WKA, Linnemann M, Baumhögger E, Vrabec J. Experimental study of two cascaded organic Rankine cycles with varying working fluids. Energy Conversion and Management 2021;230:113818. https://doi.org/10.1016/j.enconman.2020.113818.

[203] Li L, Tao L, Liu Q. Experimental analysis of organic Rankine cycle power generation system with radial inflow turbine and R245fa. Advances in Mechanical Engineering 2020;12:168781402092166. https://doi.org/10.1177/1687814020921663.

[204] Lin C-H, Hsu P-P, He Y-L, Shuai Y, Hung T-C, Feng Y-Q, et al. Investigations on experimental performance and system behavior of 10 kW organic Rankine cycle using scroll-type expander for low-grade heat source. Energy 2019;177:94–105. https://doi.org/10.1016/j.energy.2019.04.015.

[205] Hu S, Li J, Yang F, Yang Z, Duan Y. Multi-objective optimization of organic Rankine cycle using hydrofluorolefins (HFOs) based on different target preferences. Energy 2020;203:117848. https://doi.org/10.1016/j.energy.2020.117848.

[206] Song J, Loo P, Teo J, Markides CN. Thermo-economic optimization of organic Rankine cycle (ORC) systems for geothermal power generation: A comparative study of system configurations n.d.:30. https://doi.org/10.3389/fenrg.2020.00006.

[207] Özahi E, Tozlu A, Abuşoğlu A. Thermoeconomic multi-objective optimization of an organic Rankine cycle (ORC) adapted to an existing solid waste power plant. Energy Conversion and Management 2018;168:308–19. https://doi.org/10.1016/j.enconman.2018.04.103.

[208] Yang A, Su Y, Shen W, Chien I-L, Ren J. Multi-objective optimization of organic Rankine cycle system for the waste heat recovery in the heat pump assisted reactive dividing wall column. Energy Conversion and Management 2019;199:112041. https://doi.org/10.1016/j.enconman.2019.112041.

[209] Aziz F, Mudasar R, Kim M-H. Exergetic and heat load optimization of high temperature organic Rankine cycle. Energy Conversion and Management 2018;171:48–58. https://doi.org/10.1016/j.enconman.2018.05.094.

[210] Wang M, Jing R, Zhang H, Meng C, Li N, Zhao Y. An innovative Organic Rankine Cycle (ORC) based Ocean Thermal Energy Conversion (OTEC) system with performance simulation and multi-objective optimization. Applied Thermal Engineering 2018;145:743–54. https://doi.org/10.1016/j.applthermaleng.2018.09.075.

[211] Zhang X, Bai H, Zhao X, Diabat A, Zhang J, Yuan H, et al. Multi-objective optimisation and fast decision-making method for working fluid selection in organic Rankine cycle with low-temperature waste heat source in industry. Energy Conversion and Management 2018;172:200–11. https://doi.org/10.1016/j.enconman.2018.07.021.

[212] Hu K, Zhu J, Zhang W, Liu K, Lu X. Effects of evaporator superheat on system operation stability of an organic Rankine cycle. Applied Thermal Engineering 2017;111:793–801. https://doi.org/10.1016/j.applthermaleng.2016.09.177.

[213] Peris B, Navarro-Esbrí J, Mateu-Royo C, Mota-Babiloni A, Molés F, Gutiérrez-Trashorras AJ, et al. Thermo-economic optimization of small-scale Organic Rankine Cycle: A case study for low-grade industrial waste heat recovery. Energy 2020;213:118898. https://doi.org/10.1016/j.energy.2020.118898.

Appendix

Appendix A: working fluid properties

Table 1 Classification of working fluids according to their composition.

Chemical name	Alternative name	Class	ODP	GWP
Methane	R50	Alkane	n.a.	21.0
Ethane	R170	Alkane	n.a.	5.5
Propane	R290	Alkane	n.a.	3.3
n-Butane	R600	Alkane	n.a.	4.0
2-Methylpropane	Isobutane - R600a	Alkane	n.a.	n.a.
Pentane	R601	Alkane	n.a.	n.a.
2-Methylbutane	Isopentane-R601a	Alkane	n.a.	n.a.
2,2-Dimethylpropane	Neopentane	Alkane	n.a.	n.a.
Hexane	-	Alkane	n.a.	n.a.
2-Methylpentane	Isohexane	Alkane	n.a.	n.a.
Heptane	-	Alkane	n.a.	n.a.
Octane	-	Alkane	n.a.	n.a.
Nonane	-	Alkane	n.a.	n.a.
Decane	-	Alkane	n.a.	n.a.
Dodecane	-	Alkane	n.a.	n.a.
Ethene	Ethylene - R1150	Alkene	n.a.	3.7
Propene	Propylene - R1270	Alkene	n.a.	1.8
1-Butene	Butene	Alkene	n.a.	n.a.
Cis-2-butene	Cis-butene	Alkene	n.a.	n.a.
Trans-2-butene	Trans-butene	Alkene	n.a.	n.a.
2-Methyl-1-propene	Isobutene	Alkene	n.a.	n.a.
Propyne	-	Alkyne	n.a.	n.a.
Cyclopropane	-	Cycloalkane	n.a.	n.a.
Cyclopentane	-	Cycloalkane	n.a.	n.a.
Cyclohexane	-	Cycloalkane	n.a.	n.a.
Methylcyclohexane	-	Cycloalkane	n.a.	n.a.
n-Propylcyclohexane	-	Cycloalkane	n.a.	n.a.
Benzene	-	Aromatic	n.a.	n.a.
Methylbenzene	Toluene	Aromatic	n.a.	2.7
Trichlorofluoromethane	R11	CFC	1.000	4750.0
Dichlorodifluoromethane	R12	CFC	1.000	10890.0
Chlorotrifluoromethane	R13	CFC	1.000	14420.0
1,1,2-Trichloro-1,2,2-trifluoroethane	R113	CFC	0.800	6130.0
1,2-Dichloro-1,1,2,2-tetrafluoroethane	R114	CFC	1.000	10040.0
Chloropentafluoroethane	R115	CFC	0.600	7370.0
Dichlorofluoromethane	R21	HCFC	0.040	151.0
Chlorodifluoromethane	R22	HCFC	0.055	1810.0
2,2-Dichloro-1,1,1-trifluoroethane	R123	HCFC	0.020	77.0
1-Chloro-1,2,2,2-tetrafluoroethane	R124	HCFC	0.022	609.0
1,1-Dichloro-1-fluoroethane	R141b	HCFC	0.110	725.0
1-Chloro-1,1-difluoroethane	R142b	HCFC	0.065	2310.0
Trifluoromethane	R23	HFC	0.000	14760.0
Difluoromethane	R32	HFC	0.000	675.0
Fluoromethane	R41	HFC	0.000	92.0
Pentafluoroethane	R125	HFC	0.000	3500.0
1,1,1,2-Tetrafluoroethane	R134a	HFC	0.000	1430.0
1,1,1-Trifluoroethane	R143a	HFC	0.000	4470.0
1,1-Difluoroethane	R152a	HFC	0.000	124.0
Fluoroethane	R161	HFC	0.000	12.0

1,1,1,2,3,3,3-Heptafluoropropane	R227ea	HFC	0.000	3220.0
1,1,1,2,3,3-Hexafluoropropane	R236ea	HFC	0.000	1370.0
1,1,1,3,3,3-Hexafluoropropane	R236fa	HFC	0.000	9810.0
1,1,2,2,3-Pentafluoropropane	R245ca	HFC	0.000	693.0
1,1,1,3,3-Pentafluoropropane	R245fa	HFC	0.000	1030.0
1,1,1,3,3-Pentafluorobutane	R365mfc	HFC	0.000	794.0
2,3,3,3-Tetrafluoroprop-1-ene	R1234yf	HFO	0.000	4.0
Trans-1,3,3,3-tetrafluoropropene	R1234ze	HFO	0.000	6.0
Tetrafluoromethane	Perfluoromethane - R14	PFC	0.000	7390.0
Hexafluoroethane	Perfluoroethane - R116	PFC	0.000	12200.0
Octafluoropropane	Perfluoropropane - R218	PFC	0.000	8830.0
Octafluorocyclobutane	Perfluorocyclobutane - RC318	PFC	0.000	10030.0
Decafluorobutane	Perfluorobutane	PFC	0.000	8860.0
Dodecafluoropentane	Perfluoropentane	PFC	0.000	9160.0
Hexamethyldisiloxane	MM	Linear Siloxane	n.a.	n.a.
Octamethyltrisiloxane	MDM	Linear Siloxane	n.a.	n.a.
Decamethyltetrasiloxane	MD2M	Linear Siloxane	n.a.	n.a.
Dodecamethylpentasiloxane	MD3M	Linear Siloxane	n.a.	n.a.
Tetradecamethylhexasiloxane	MD4M	Linear Siloxane	n.a.	n.a.
Octamethylcyclotetrasiloxane	D4	Cyclid siloxane	n.a.	n.a.
Decamethylcyclopentasiloxane	D5	Cyclid siloxane	n.a.	n.a.
Dodecamethylcyclohexasiloxane	D6	Cyclid siloxane	n.a.	n.a.
Propanone	Acetone	Ketone	n.a.	0.5
Ethyl alcohol	Ethanol	Alcohol	n.a.	n.a.
Methanol	Methanol	Alcohol	n.a.	2.8
Dimethyl ester carbonic acid	Dimethyl carbonate	Carbonate ester	n.a.	n.a.
Trifluoroiodomethane	-	Haloalkane	n.a.	n.a.
Methoxymethane	Dimethylether	Ether	n.a.	n.a.
Ammonia	R717	Inorganic	0.000	0.0
Carbon dioxide	R744	Inorganic	0.000	1.0
Water	R718	Inorganic	0.000	0.0

Appendix B: the exergy destruction for different fluids and configurations

Basic ORC

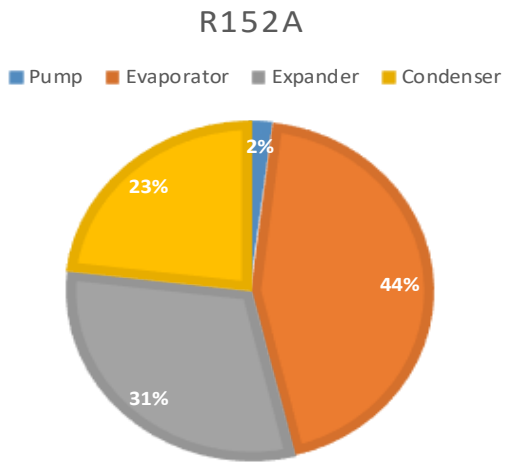

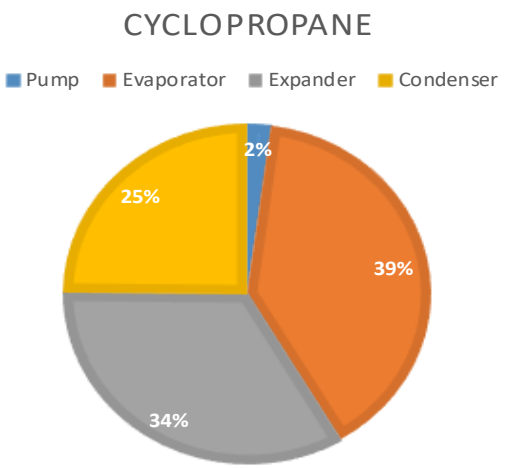

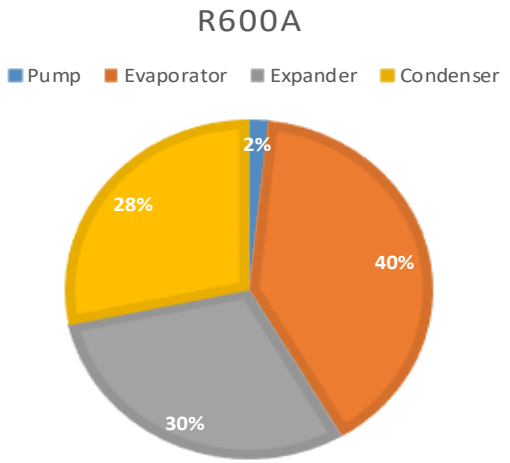

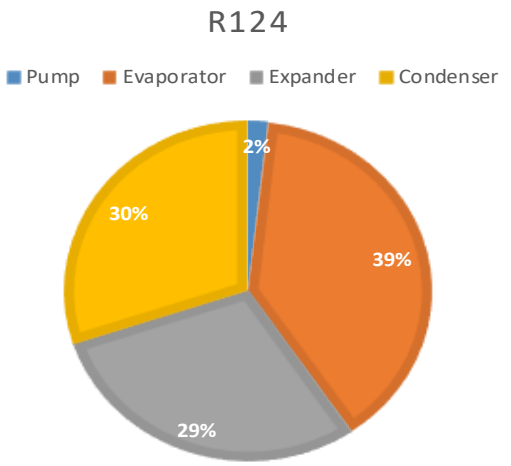

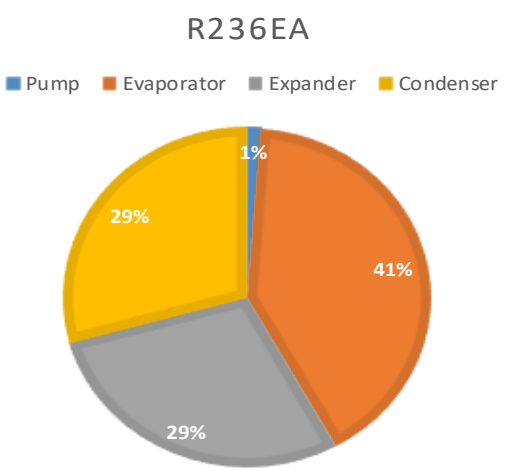

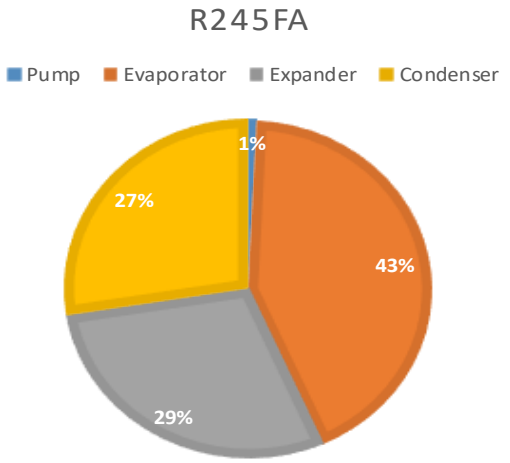

ORC with IHE

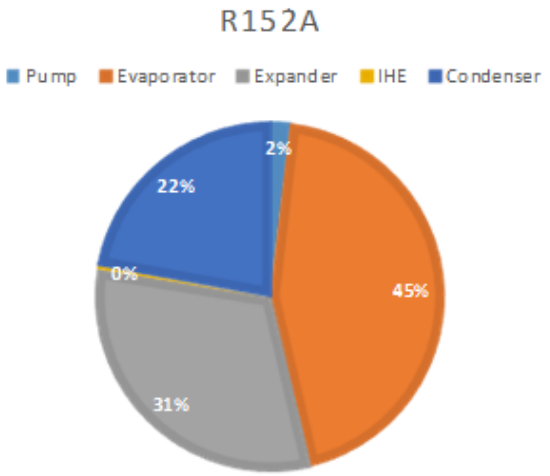
R152A
Pump
Evaporator
Expander
IHE
Condenser
2%
45%
31%
0%
22%

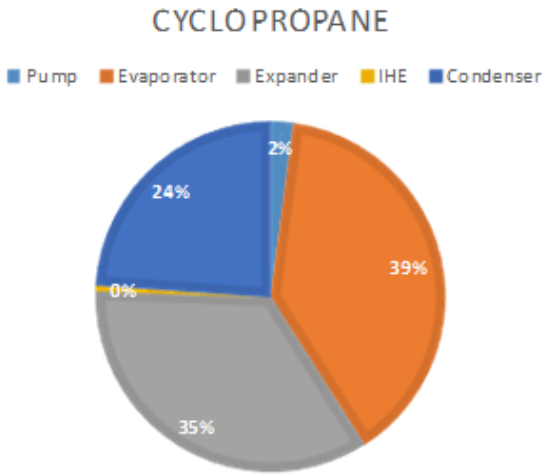
CYCLOPROPANE
Pump
Evaporator
Expander
IHE
Condenser
2%
39%
35%
0%
24%

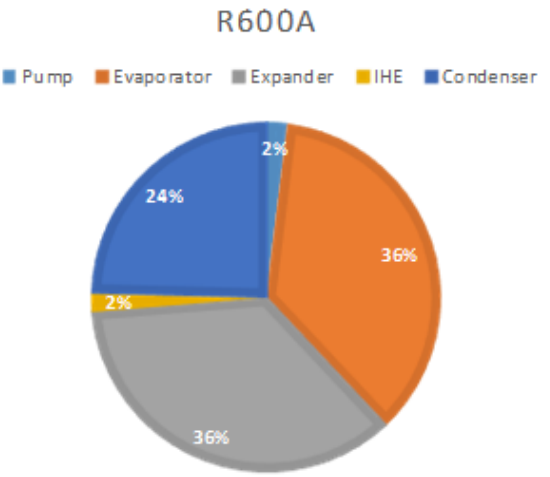
R600A
Pump
Evaporator
Expander
IHE
Condenser
2%
36%
36%
2%
24%

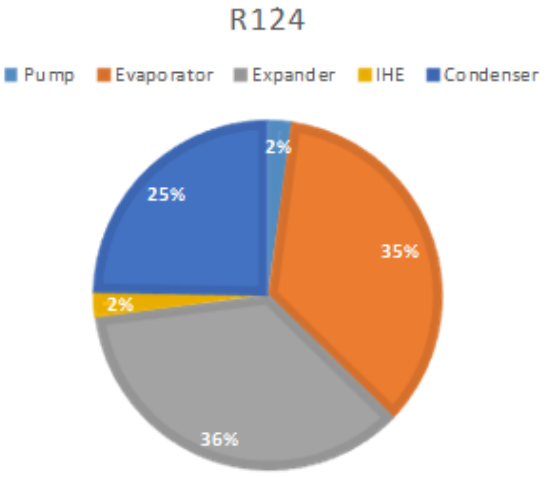
R124
Pump
Evaporator
Expander
IHE
Condenser
2%
35%
36%
2%
25%

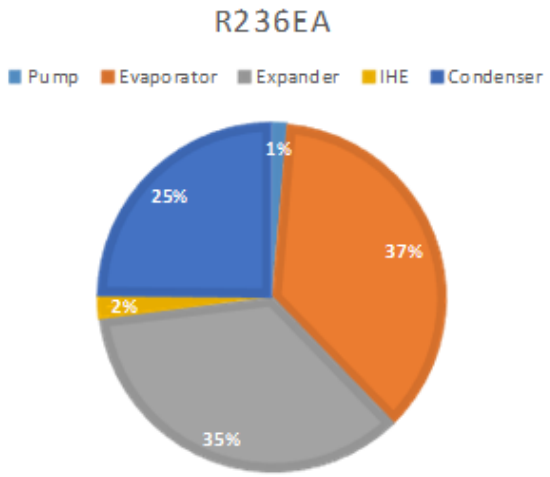
R236EA
Pump
Evaporator
Expander
IHE
Condenser
1%
37%
35%
2%
25%

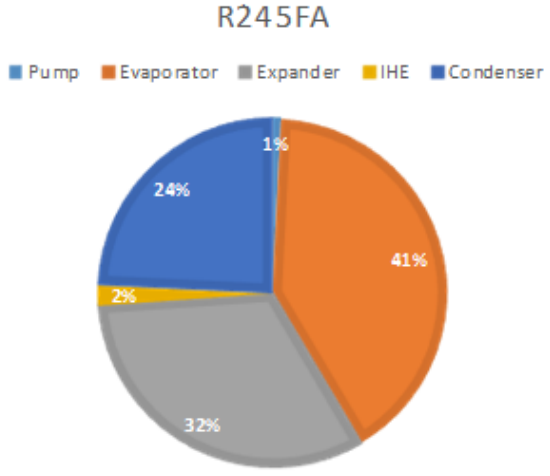
R245FA
Pump
Evaporator
Expander
IHE
Condenser
1%
41%
32%
2%
24%

Regenerative ORC